# University of Stavanger

Faculty of Science and Technology

MASTER'S THESIS

Study program/Specialization: Petroleum Engineering / Drilling Technology	Spring semester, 2020 Open
Writer: Yahya Ibrahin Hassan Mohamud	*Yahya Mohamud* ………………………………………… (Writer's signature)

Faculty supervisor: Mesfin Belayneh

Thesis title: **ROP Modelling, Analysis and Optimization Study Based on Morvin Field 6506/11 Drilling Data.**

Credits (ECTS): 30

| Key words:
  • ROP
  • Modelling
  • Drilling Optimization
  • Morvin Field
  • Multiple Regression
  • MSE
  • D-exponent
  • Warren
  • Bourgoyne & Young | Pages: 139 + enclosure: 33

Stavanger, 06.07.2019 |

University of Stavanger
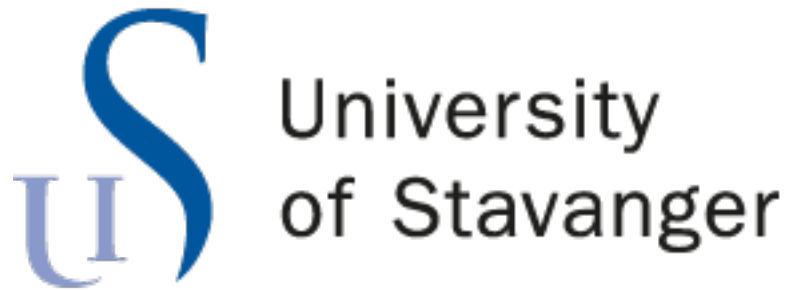
Faculty of Science and Technology

Department of Energy and Petroleum Engineering

Master's Thesis

ROP Modelling, Analysis and Optimization Study Based on Morvin Field 6506/11 Drilling Data

---

Yahya I. Hassan Mohamud

July 6, 2020

Abstract

During the planning phase, the drilling rate of penetration (ROP) optimization simulation studies are performed in order to increase ROP, reduce the drilling time - and bit wear. Optimizing ROP is important to improve the overall drilling performance and reduce operational costs.

This thesis presents the ROP modelling based on the drilling data obtained from Morvin Field 6506/11 in the Norwegian Sea. The models used for the assessment were Multiple regression, MSE, D-exp, Warren and Bourgoyne & Young models. The modelling approaches were based on the entire well data, hole sections and geological groups. Furthermore, the models were tested on its own, nearby and far-away wells. Finally, modelling and drilling ahead ROP predictions on its own well were also tested.

Results show that the model predictions are good enough when applying on the wells they are derived from. The degree of the prediction reduces when applying on far away wells. It was also found out that the modelling and application on the drilling ahead approach works well. From the evaluation, it was observed that using 90 % of the data for the modelling predicts the 10 % of the drilling ahead quite well. Out of the considered modelling scenarios, modelling based on the geological groups provided the best results.

Moreover, in this thesis, the Bourgoyne & Young model was modified to include more drilling parameters. The modelling and application results showed better prediction.

Acknowledgements

Contents

List of Figures

List of Tables

Nomenclature

α Cutter siderake angle

ΔP_B Pressure loss across drill bit

γ_f Fluid specific gravity

log   Logarithm

μ Bit specific coefficient of sliding friction or Viscosity

ρ Density

σ_c Uniaxial compressive strength

θ Cutter backrake angle

A Cross-sectional area

A_m Matrix strength constant

A_n Cross-sectional area of nozzles

A_v Ratio of jet velocity to return velocity

C_b Drill bit cost

C_d Drilling cost or Drag coefficient

C_m Drilling motor cost

C_r Rig cost

D_b Bit diameter

D_c Cutter diameter

D_n Nozzle diameter

D_{exp} D-exponent

E Exponent for rotary speed

F Thrust force

F_j Jet impact force

F_{jm} Modified jet impact force

ft feet

g_p Pore pressure gradient

R_0 Rate of penetration without overbalance

t_c Connection time

t_d Drilling time

t_t Tripping time

v_f Return fluid velocity

v_n Nozzle velocity

W/d_{bt} Threshold value

W_f Bit wear

hr   Hour

in   Inch

kpsi   Kilo-pound

lb   Pound

lbf   Pound-force

N   Rotary speed (RPM)

psi   Pounds per square inch

q   Flow rate

R   Rate of penetration

S   Compressive Strength

T   Torque

Abbreviations

B&Y	*Bourgoyne and Young*	**Mod.**	*Modelled*
Coeff. constant	*Coefficient constant*	**MSE**	*Mechanical Specific Energy*
D-exp	*Drillabillity exponent*	**Multiple reg.**	*Multiple regression*
DSP	*Digital Signal Processing*	**MW**	*Mud Weight*
ECD	*Equivalent Circulation Density*	**NCS**	*Norwegian Continental Shelf*
EFF	*Bit efficiency*	**NPT**	*Non-Productive Time*
Eq.	*Equation*	**OP**	*Observation point*
Filt.	*Filtered*	**ROP**	*Rate of Penetration*
Flow	*Flow rate*	**RPM**	*Revolutions Per Minute*
FP	*Formation Pressure*	**T**	*Torque*
Geo. groups	*Geological groups*	**TVD**	*True Vertical Depth*
Gr.	*Group*	**UCS**	*Uniaxial Compressive Strength*
MAPE	*Mean Absolute Percentage Error*	**USD**	*US Dollar*
MD	*Measured Depth*	**WOB**	*Weight On Bit*

1. Introduction

1.1 Background

Worldwide energy demand has rapidly increased since the "oil boom" in the late 1970s. Both the demand and consumption are increasing in line with increasing industrialization and growing population. After the "oil boom", the petroleum demand was mainly associated with discovering new hydrocarbon reserves [1].

Since most of the resources are in the reservoirs, it is important to develop new methods and technologies to exploit more out of the existing reservoirs. Despite the drilling rate per day increasing due to technological development, the non-productive time associated with the problem accounts for higher and increase in drilling budget. There is also invisible non-productive time associated for instance with vibrations, which reduce the drilling rate and damage of the drill bit, which again reduces the drilling rate.

One of the methods to deal with this issue is by performing an appropriate design during planning phase. For instance, selecting the right bit and use vibration control equipment as part of the drilling system. Moreover, performing rate of penetration (ROP) optimization simulation with the objective of increasing ROP and reducing bit wear will reduce the drilling time and undesired tripping operation associated with bit damage. For this, it is important to use a good ROP model that simulates the process well. In the literature study, there are several models available. These are derived based on physics and empirical-based equations. The research question addressed is, which model is good enough to model the field ROP?

This thesis therefore deals with the assessment of five ROP models used for application and investigation of how to optimize parameters in order to improve drilling speed and reduce drilling time. For the modelling and testing, a total of four well's drilling data obtained from Morvin field block 6506/11 were used.

1.2 Problem Formulation

In literature, there are several ROP models used to predict the penetration rate. However, each model have their own weaknesses and strengths. In this thesis, Final Well Reports which are available from the North Sea will be used to model drilling a well. The issues to be addressed are:

- How good enough are the ROP models to predict the field ROP?

- How good is the multiple regression model compared with the literature models?

- How can the modelling techniques be applied in real-time drilling operations?

- What are the limitation and application range of the models?

- How can we optimize drilling parameters to improve ROP and reduced drilling time as drilling goes on?

- How dependent is multiple regression modelling technique on drilling parameters?

1.3 Objective

The main objective of this thesis work is to answer the research questions stated in chapter 1.2. For this, the Morvin field data obtained from the Norwegian continental shelf (NCS) will be used. The activities are:

- Review ROP models.

- Modelling of ROP based on Morvin field drilling data.

- Test the models on its own well, nearby and far-away wells.

- Finally, propose the best modelling approach for field application.

1.4 Research Methods

The research approaches designed in this thesis consists of three main parts. The first is the review of the ROP models, from which modelling workflows have been developed. The second part deals with the application of the workflow to model ROP based on field drilling data. The third part deals with the testing and modelling of the ROP models. The models will be tested on its own well, nearby and far-away wells. The objective here is to investigate the applications and limitations of the models. Figure 1.1 shows the chart of the research methods used in this thesis.
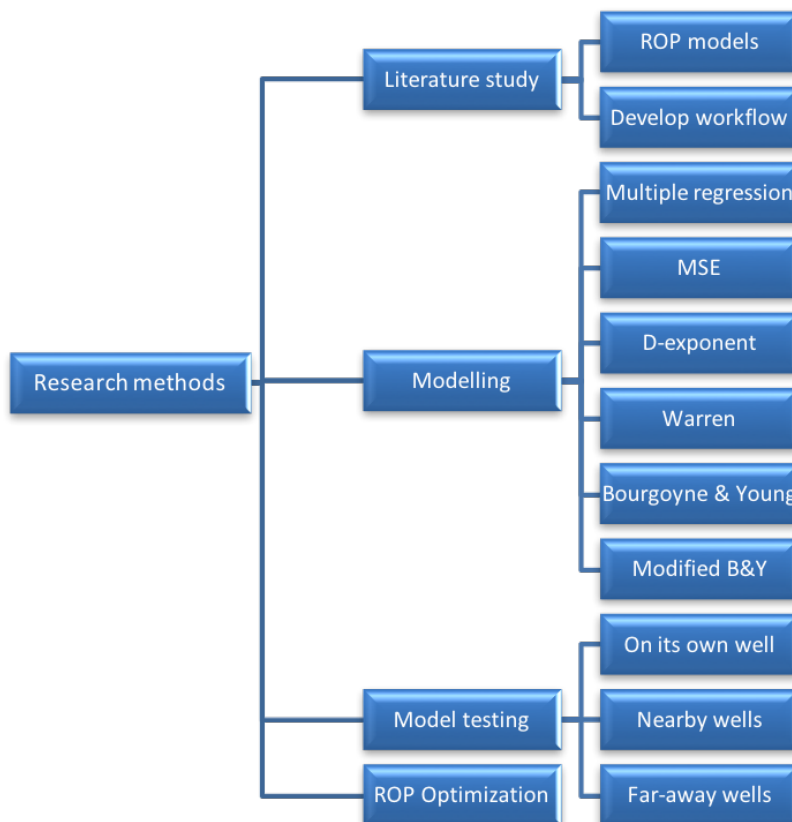
Figure 1.1: Summary of the research program.

2. Literature Review

2.1 Drill Bits

Drill bits are in the tip of the drill string, below the drill collar and drill string. The functionality of the bit is to crush the rock formation by implementing axial- and rotational forces, WOB and torque. The drill bit usually consists of 2-3 cones depending on the formation. The cones are made of hard material such as tungsten carbide, steel and natural diamond. The cones also have hard teeth to cut and gauge the rocks. The rock cuttings are circulated to the surface by circulating fluid in order to attack the new surface of rock. [2]

Figure 2.1 shows the combination of the two cutting actions, cutting- and indentation that the drill bit proposes to penetrate through the formation. Indentation is described as the action where WOB is applied to the drill bit, and it pushes into the formation. By this, action the bit gets a grip on the rock to make it break. In cutting action, lateral movement is implemented sideways on the drill bit to break and crush the rock [3]. Drill bits are a fundamental part of the drilling system and there is a wide range of drill bits. Therefore, selecting the right bit is important for efficient drilling and reduce undesired drilling cost [4].
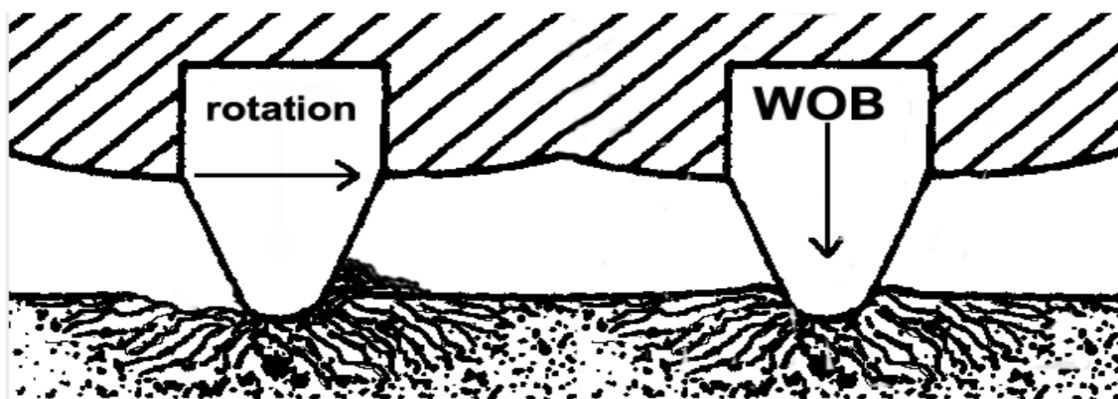
Figure 2.1: Drill bits using both indentation and cutting actions [5]

2.1.1   Roller Cone Bits

Roller cone bits are the most common drill bits used. Roller cones are divided into milled-tooth and insert-tooth bits. The bit has a large variety when it comes to teeth and bearing design, meaning they are applicable for a wide range of formations. Long and widely spaced teeth combined with large offset are used for soft formations. As the formation hardness increases the tooth length and offset is reduced. Selecting the right bit is important due to reducing the non-productive time (NPT) and maintaining the desired ROP rate.

The design of Roller cone bits are made up of steel, which makes it sufficiently resistant to hardenability, machinability, yield strength and heat treatment. The main focus when designing the bits are material selection, hole deviation, rotary speed, mechanical requirements, hydraulic requirements and geometry- and cutting shapes [6].

The selection of bit design also depends on the condition of the environment it will operate in and how it will function. The external factors affecting the drill bit are WOB, rotary speed and hydraulics, it is also crucial to consider the contribution of conditions as formation hardness, depth, drilling fluids and hole deviation when designing and a selecting drill bit. In Figure 2.2 an illustration of a Roller cone bit and its features is presented [7].
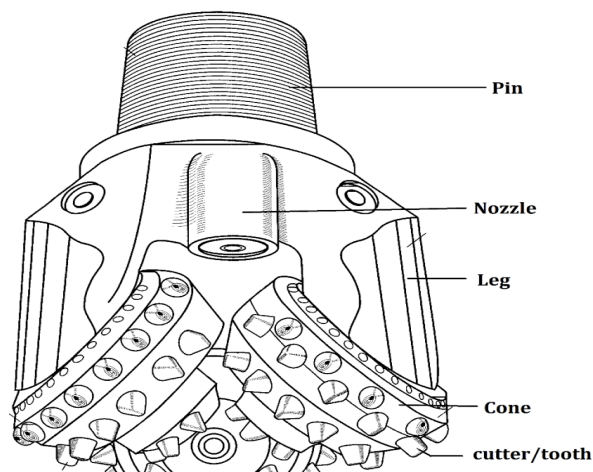
Figure 2.2: Illustration of Roller cone bit [7].

Milled-tooth bit consist of three cones, which are equal in size. The cones are seated on shafts which are mounted on the legs of the bit body. The bearings allow the cones free rotation, offset increase cutting action and the nozzles cleans the bit and wellbore. Both tooth and bearing design vary greatly for Roller cone bits, meaning they are applicable for several different formations ranging from soft to hard.

Insert-tooth bits are best suited for hard and abrasive formations. The insert-tooth bit is made up of tungsten carbide inserts, where the teeth are integrated part of the cone body. Furthermore, the bit functionality is the same as for the milled-tooth bit.

Table 2.1: Relationship between Roller cone bit features [8].

Formation Characteristics	Soft	Medium	High
Insert/Tooth Spacing	Wide	Relatively Wide	Close
Insert/Tooth Properties	Long & Sharp	Shorter & Stubbier	Short & Rounded
Penetration and Cuttings Generator	-	Relatively High	Relatively Low
Cleaning Flow Rate Requirements	-	Relatively High	Relatively Low

2.1.2   Fixed Cutter Bits

Fixed cutter bits are divided into Polycrystalline Diamond Compact (PDC) and Natural-Diamond bits. What distinguishes Roller cone from Fixed Cutter bits is that Fixed Cutter doesn't have any moving parts which makes it suitable when drilling small holes. The cutters are integrated into the body of the bit. Therefore, unlikely compared to Roller cone bit PDC bit shears the rock instead of crushing it. High RPM and low WOB are applied because of dragging and scraping [6].

PDC bits are the most used bits in this category as the rock formation in this bit is sheared instead of crushed. There is required less energy, which means less WOB is applied, however, higher RPM is enforced. The PDC is designed by coining a layer of numerous small polycrystalline artificial diamonds to a cemented tungsten carbide under high pressure and temperature. By composing the diamonds in the layers in a random orientation, wear resistance and high strength are obtained [6]. Figure 2.3 shows an illustration of a typical PDC bit.
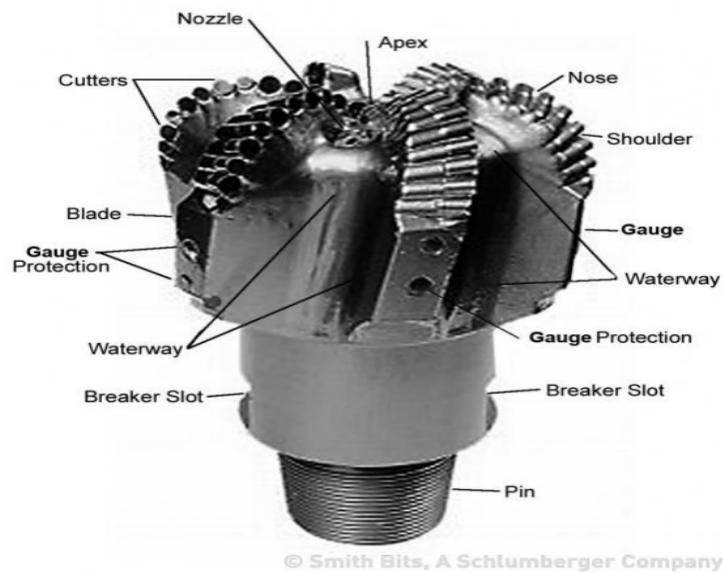
Figure 2.3: Illustration of PDC bit [9].

Diamond bits are the other Fixed Cutter bits available. Diamond bits are used in hard abrasive formations as diamond is the hardest material to be found. Furthermore, when using Diamond bits, we drill with high RPM, therefore the grains between the rock cementation is broken. Fine cuttings are obtained by using low volumes per rotation, however, to obtain the desired ROP we must drill with high ROP. Diamond bits are mostly used for its resistance against wear and its hardness. However, this kind of bit is sensitive when it comes to vibrations and shock in the wellbore. Sufficient circulation is important to avoid overheating and cuttings agglomerating on the bit. The diamonds in the bit are held in place partial encapsulation in the matrix body [6].

2.1.3 Bit Optimization

The selection of drill bit is evaluated to be the most important criteria deciding the drilling rate. Over the years studies of drill bits have been presented in order to develop and improve them as drill bit efficiency and cost is a major factor in the cost of drilling a well. The equation for calculating the drilling cost is as following [10] [11]:

$$C_d = \frac{C_r(t_c + t_d + t_t) + C_m t_d + C_b}{\Delta D} \qquad (2.1)$$

Where, C_d, C_r, C_m and C_b are the cost of drilling, rig, drilling motor and drill bit given in [USD/ft]. Moreover, t_c, t_d and t_t are connection-, drilling- and trip time, respectively in [hr], while ΔD is drilled depth in [ft].

Drill bit design and type are directly linked to the cost of drilling a well. Therefore this is crucial as optimization of the bit will cause lower drilling time and additionally lead to a higher penetration rate and reduce the number of trips to change the bit due to wear [12].

Choosing the right drill bit in a given formation is a combination of several operational factors such as the formation characteristics, rule of thumb and mathematical models [10]. The drill bit selection depends upon drilling operational factors including diameter, WOB, wear and drilling fluid [13].

2.2 Factors Affecting ROP

Rate of Penetration (ROP) is controlled by several factors, such as rock, mechanical and fluid properties. The cost per foot drilled in a well is directly related to the factors affecting the ROP. In general, the factors affecting ROP can be divided into two groups, controllable and uncontrollable variables. The controllable variables are defined as dependent on the drilling condition and they should be controlled to obtain the required speed to break and crush the rock formation and avoid problems that occur in the drilling phase. The uncontrolled variables are mostly associated with the formation characteristics and are independent of the drilling operation [14] [15].

2.2.1 Bit Type

The choice of the type of drill bit is strongly related to the rate of penetration. Studies have shown that the highest initial ROP is when Roller cone bits with long teeth and large cone-offset angle are applied, despite being most applicable in soft formations [16].

While on Fixed Cutter bits the ROP depends on the number of blades and bottom-cutting angles to achieve wedging-type rock failure. In recent years, both PDC and Diamond bits have been developed with certain features to achieve a higher rate of ROP such as hydraulic-design to avoid bit bailing, mechanical-design and steel-bodied bits [6].

2.2.2   Formation Characteristics

The formation properties affecting the penetration rate the most are yield point and ultimate strength of the formation. Hence, in permeable rocks, the drilling fluids tend to migrate through the rock decreasing the differential pressure as it causes pressure from beneath the rock on the drill bit. The penetration rate is also a function of the mineral composition of the rock. Hard and abrasive containing rocks may lead to rapid dulling of the cutting elements, while rock with soft minerals may cause the bit to ball up. This leading to an inefficient drilling operation [6].

2.2.3   Drilling Fluid Properties

The drilling fluid properties are a major influence on ROP. The penetration rate is function of several drilling fluid parameters such as fluid viscosity, density, size, and content of solid and chemical composition. Increasing fluid viscosity, density and solid content lead to a lower rate of penetration.

Overbalance is caused by pressure differences between the well pressure and hydrostatic pressure of formation fluid. Bourgoyne & Young (1974) showed the effect of overbalance on ROP on a semi-log plot. Figure 2.4 shows that the penetration rate decreases with increased overbalance [6].

$$\log \frac{R}{R_0} = -0.052 m D (g_p - \rho_f) \tag{2.2}$$

Where, R is the ROP. R_0 is ROP without overbalance. m is the slope of the line. D is the depth (TVD). g_p is pore pressure gradient and g_f is ECD.

2.2.4   Operating Conditions

Several studies have been done in order to show the impact of WOB and RPM on the penetration rate. Bourgoyne & Young (1991) developed a model to show the impact of WOB on ROP experimentally. The formulation required that all the drilling parameters should be held as constants.

Figure 2.4 clarifies that no penetration is achieved before the threshold formation is exceeded (Point a). For low WOB values the ROP increases linearly (Point b). Point b is also where the bit transforms from scraping/grinding to shearing the rock, as the WOB increases the correlation between WOB and ROP still increase linearly, however, the slope is steeper. This indicates that drilling operation is more efficient (Point c). When the WOB exceeds a certain limit (Point C), an increase in WOB leads to a small change in ROP (Point d). Finally, in the last segment high bit-weight may cause a decrease in penetration rate because of bit foundering which is caused by poor hole-cleaning due to large amounts of cuttings (Point e).
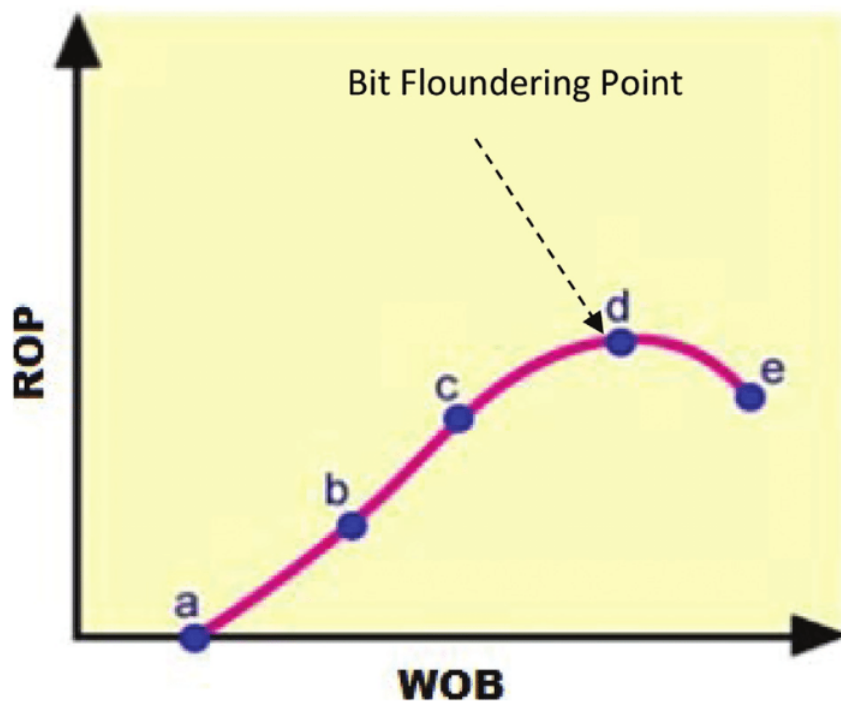
Figure 2.4: Relation between WOB and ROP [17].

In 1962 Maurer derived an equation to show the relationship between rotational speed and penetration rate, where all the drilling parameters were treated as constant. At low RPM the ROP increases linearly, however, for larger rates the cuttings generated causes inefficient drilling operation. The equation formulated for Roller cone bits by Maurer were built on the following assumptions: The crater volume is proportional to the square of the depth of cutter penetration and the depth of cutter penetration is inversely proportional to the formation strength.

$$ROP = \frac{K}{S^2} \left[\frac{W}{D_b} - \left(\frac{W}{d_b} \right)_t \right]^2 \cdot N \tag{2.3}$$

Where, S is the compressive strength of the rock. K is a constant and $(W/d_b)_t$ is the threshold value.

When Fixed Cutter bits are compared to Roller cone bits, they usually crave lower bit weight, but higher rotary speed in order to cut and crush the rocks efficiently and to achieve the desired torque. Insufficient WOB and RPM may lead to cutter wear, chipping of diamond and poor penetration rate.

2.2.5   Drill Bit Hydraulics

To optimize the desired potential rate of penetration, hydraulic horsepower (HHP) and jet impact force (Fj) are two important criteria used. Experimental studies have shown that an increase in the rotation of the drillstring causes a decrease in slip velocity and the drag coefficient, leading to a more efficient hole-cleaning [18].

One of the main objectives of the drilling fluids is to transport the rock-cuttings from wellbore to surface and the efficiency of this process depends on the properties and system of the drilling fluid. Poor hole-cleaning leads to a decrease in penetration rate. Moreover, as the rock is crushed by the bit the bit nozzles will provide the desired jet force to clean the wellbore. If the horsepower applied isn't enough the cuttings will accumulate in the well, meaning poor ROP [18].

The pressure loss across the drill bit may arise in a turbulent region and is a function of bit nozzles, hydraulic horsepower, jet impact force and flowrate. The equation for pressure loss across the bit is expressed in equation (2.4) [19] [6]:

$$\Delta P_B = \rho_{mud} \cdot \frac{q^2}{12032 C_d^2 A_n^2} \tag{2.4}$$

Where, ΔP_B is the pressure loss across the drill bit, ρ_{mud} is density of the drilling fluid, q is the flow rate, C_d is the drag coefficient and A_n is the cross-sectional area of the nozzles.

3. ROP Models

There are several ROP models documented in literature's. Prior to drilling ROP optimization simulation studies should be conducted in order to optimize drilling parameters with the objective of obtaining higher ROP, lower drilling time, reduce bit wear and hence, reduce undesired tripping operation due to bit damage. For this, the ROP predictive power of the models play a key role. The ROP models depend on operational parameters, hydraulics parameters, bit cutter parameters, and formation strength as well [15]. Table 3.1 shows the different models along with the parameters they are derived from.

Table 3.1: Overview of drilling variables for ROP Models.

ROP Model	Multiple Reg.	MSE	D-exponent	Bourgoyne & Young	Hareland & Ramperstad	Bingham	Warren
Operational Variables							
Weight on Bit, WOB	✓	✓	✓	✓	✓	✓	✓
Torque, T	✓	✓		✓			
Rotary Speed, RPM	✓	✓	✓	✓	✓	✓	✓
Flow Rate, q	✓			✓			
Well Depth, D				✓			
ECD			✓	✓			
Bit Wear, W_f				✓	✓		
Rock Properties							
Formation Pressure, FP	✓			✓			
UCS		✓			✓		
Compressive Strength, S							✓
Bit Properties							
Bit Diameter, D_b		✓	✓	✓	✓	✓	✓
Nozzle Diameter, D_n				✓			
PDC Design Properties							
Number of Cutters, N_c					✓		
Cutter Diameter, D_c					✓		
Cutter Siderake Angle, α					✓		
Cutter Backrake Angle, θ					✓		
Drilling Fluid Properties							
Mud Weight, MW	✓		✓	✓			
Viscosity, μ				✓			✓

3.1   MSE Model

The concept of Mechanical Specific Energy was first introduced by Teale in 1965. The use of MSE was introduced to evaluate the bit and to know when to replace it [20]. MSE is defined as the energy that is required to excavate one volume of rock from the formation. In other words, it is the definition of how much work is done per unit of volume, expressed as [21]:

$$MSE = \frac{Input\ Energy}{Output\ ROP} \qquad (3.1)$$

MSE is the sum of work done by rotational force (T) and axial force (WOB). By considering a drill string, the work done per minute can be expressed:

$$\frac{Work\ Done}{min} = ROP \cdot F + 2\pi NT \qquad (3.2)$$

Where, ROP is the rate of penetration. F is thrust force. Torque is given as T. N is rotary speed. Moreover, the relationship between the volume of rock cuttings carried out after drilling per unit time, V and ROP are given as:

$$\frac{V_{rock}}{min} = Area \cdot ROP \qquad (3.3)$$

By combining the equations above we achieve equation (3.4). Where WOB and torque are expressed as first and second terms, respectively.

$$MSE = \frac{F}{A} + \frac{2\pi}{A} \cdot \frac{N \cdot T}{ROP} \qquad (3.4)$$

MSE can also be expressed as:

$$MSE = \frac{480 \cdot T \cdot N}{D_b^2 \cdot ROP} + \frac{4 \cdot WOB}{D_b^2 \cdot \pi} \qquad (3.5)$$

Unconfined compressive strength (UCS) is the maximum axial load that can be applied to the rock before it breaks. Teale studied the relation between MSE and UCS and he noticed that there was a clear association between them. In a lab test, he derived that MSE was exactly to UCS. By further studying this relationship he discovered that MSE and UCS were numerically equal if the bit is efficient, and unequal when the energy in bit is lost. The drill bit efficiency, EFF_M, is assumed to be 30 % - 40 % [22]:

$$UCS = EFF_M \cdot MSE \tag{3.6}$$

Therefore equation (3.5) can in terms of considering bit efficiency and unconfined compressive strength be expressed:

$$UCS = EFF_M \cdot \left(\frac{480 \cdot T \cdot N}{D_b^2 \cdot ROP} + \frac{4 \cdot WOB}{D_b^2 \cdot \pi} \right) \tag{3.7}$$

The field data provided are in the form WOB, RPM and ROP, therefore friction factor needs to be introduced in order to present penetration rate, ROP. [23].

$$T = \frac{\mu \cdot D_b \cdot WOB}{36} \tag{3.8}$$

By substituting equation (3.8) into equation (3.7) and rearranging the equation with respect to ROP, we can finally express ROP as:

$$ROP = \frac{13.333N\mu}{D_b \left(\frac{UCS}{EFF_M WOB} - \frac{4}{\pi D_b^2} \right)} \tag{3.9}$$

3.2 D-exponent Model

When drilling in over-pressurized formations it's difficult to detect by using ROP models. This is due to ROP models being a function of several parameters including formation pressure such as WOB, rotary speed, drilling fluid, circulation rate and drill bit properties.

Therefore, the D-exponent model was initially developed with the intention of normalizing the ROP when drilling in over-pressurized zones by neglecting the contribution of the drilling parameters mentioned above. In 1964 Bingham derived an equation for normalizing ROP models by including a drillability exponent, D_{exp} [24] [25]:

$$ROP = A_M N^E \left(\frac{WOB}{D_b}\right)^{D_{exp}} \tag{3.10}$$

Where, A_M is the rock matrix strength and E is an exponent for the rotary speed. Furthermore, Jorden and Shirley [6] developed the model further my assuming that both the rock matrix strength and rotary speed exponents were constants equal to 1. By considering these assumptions, rearranging equation (3.10) with respect to D_{exp} and considering the mud contribution, then the following equation is obtained [25]:

$$D_{exp} = \frac{\log \frac{ROP}{60N}}{\log \frac{12WOB}{10^6 D_b}} \cdot \left(\frac{\rho_n}{\rho_a}\right) \tag{3.11}$$

Here ρ_n is the normal hydrostatic gradient and ρ_a is the equivalent circulation density (ECD). Equation (3.11) calibrates the correlation between the bit's capacity to drill trough a zone also known as drillability and the over-pressurized zones. Figure 3.1 shows how ROP decreases a function of depth while the D-exponent increases in the normal-pressured zone. In the over-pressured zone we observe that ROP increases and D-exponent decreases due to the formation rock becoming more porous and less dense [26] [24] [27].
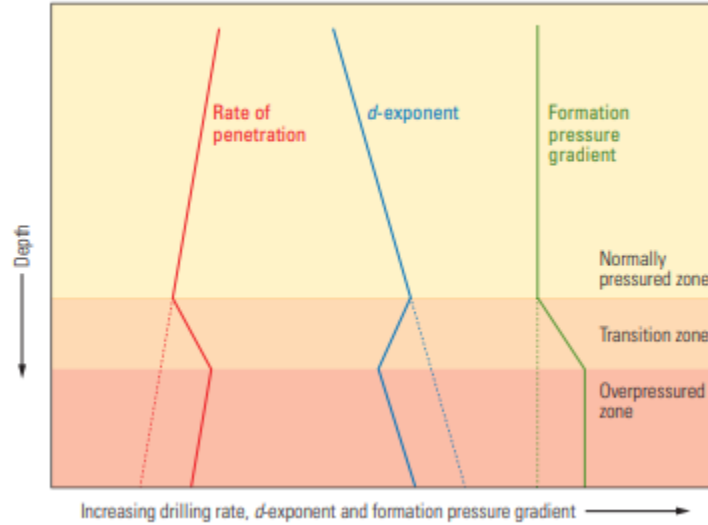
Figure 3.1: Overpressure effect on ROP and D-exponent [26].

3.3   Warren Model

In 1951 Warren proposed a ROP model for soft formation bits. The ROP model attained from Roller cone bits are either limited due to cutting-removal or cuttings-generation. Warren developed the ROP model from an experimental test in the laboratory under steady-state drilling condition. The model presented by Warren relates the mechanical factors ROP to WOB, RPM, bit strength, bit size and rock strength. The Warren model was improved and made more applicable in a larger scale of formations by combining the Warren model with more generalizing models taking the effects of mud properties, hydraulics, differential pressure etc. into account [28].

Developing a ROP model related to mechanical factors has been discussed and searched for several years. The initial model was assuming perfect hole condition, but the model was modified by Warren to make it more applicable and realistic in imperfect hole-cleaning conditions. Galle and Woods [29] proposed a model for soft formations. This model has regularly been used, however the model is limited when applied in practical situation as the assumption it is built on is disobeyed.

The Perfect-cleaning model was presented by Maurer [28]. This model takes the study of single tooth into account. However, the model is also limited when predicting ROP in soft formations as deviation occurs between the model and the experimental data. Cunningham proposed a model in recent years, but also this model lacked in the correlation to the experimental data [30].

3.3.1 Perfect-Cleaning Model

The Perfect-cleaning model was developed by Warren, but was later modified by Hareland. This model implies under the drilling process with tricone bits. The ROP model indicates that the rate where new cutting-chips are being formed is equal to the rate of cutting removal from the drill bit. Thus, this ROP model is being controlled by the rate of new chips being formed or the rate of cuttings removal. A combination of both processes is also a controlling factor. The Perfect-cleaning model calculates ROP from the mechanical factors using dimensional analysis and generalized response curves. The Perfect-cleaning model is viewed as the initial starting point for developing the Imperfect-cleaning model [31]:

$$ROP = (\frac{a \cdot S^2 \cdot D_b^3}{N^b \cdot WOB^2} + \frac{c}{N \cdot D_b})^{-1} \tag{3.12}$$

Where, "a" and "c" are bit constants. S is the confined rock strength. The first term in equation (3.12) explains the rate where the formation rock is cut into small chips by the drill bit. The second term modifies the predictions to account for the distribution of the applied WOB to more teeth, as the WOB is increased and the teeth penetrate deeper into the rock. Because of the first term being predominant for low ROP-values and the second term being predominant for high-ROP values, the ROP increase, as WOB increases to a certain point called inflection point. After this point, the ROP starts to increase at a decreasing rate [31].

3.3.2 Imperfect-Cleaning Model

In reality, the ROP model in most of the field cases is significantly affected by the rate where the rock cuttings are evacuated under the bit.

Equation (3.13) is not ideal for estimating field ROP without modification to account for imperfect cleaning, which is the case when dealing with reality. Hence, the ROP model is expressed as [6]:

$$ROP = (\frac{a \cdot S^2 \cdot D_b^3}{N \cdot WOB^2} + \frac{b}{N \cdot D_b} + \frac{c \cdot D_b \cdot \gamma_f \cdot \mu}{F_{jm}})^-1 \tag{3.13}$$

Where, the bit constant "b", has been included. γ_f and μ are the specific gravity and viscosity of the drilling fluid, respectively. Moreover, dimensional analysis is used to isolate a group of variables consisting of the modified jet impact force, F_{jm}:

$$F_{jm} = [1 - A_v^{-0.122}]F_j \tag{3.14}$$

Where, Av is the ratio of jet velocity to return velocity. Jet impact force is expressed as, F_j. A_v and F_j can mathematically be defined as:

$$A_v = \frac{v_n}{v_f} = \frac{0.15D_b^2}{3d_n^2} \tag{3.15}$$

$$F_j = 0.000516\rho q v_n \tag{3.16}$$

Whereas, v_n and v_f are the fluid velocities for the nozzles and the returned fluids. Furthermore, in Roller cone bits the ratio between the area available for fluid return and cross-sectional area is 15 %. The Roller cone bit has 3 jets. Moreover, ρ and q are respectively density and flow rate of the drilling fluid [30].

3.4   Bingham Model

In 1964 Bingham derived a relation between WOB, RPM, ROP and bit diameter. The model was unique because he added an empirical exponent to the relation which made the ROP model more applicable in a wide range of circumstances.

In fact, Murray and Cunningham (1955) were first in including an exponent depending on WOB in a ROP model, attributing the concept to H.B Woods. The Bingham model is defined as:

$$ROP = a \left(\frac{WOB}{D_b} \right)^b RPM \tag{3.17}$$

Where, "a" is drillability constant, "b" is an empirical WOB exponent. Both "a" and "b" are dimensionless constants for each formation. The model is viewed to be simple as it is most useful in low RPM and WOB values and therefore it doesn't take the depth into account. The Bingham is also limited as it doesn't consider changes in physical drilling conditions in different formation regions [15] [32].

3.5   Bourgoyne & Young Model

Bourgoyne & Young Model is viewed to be the most well-development ROP model to this day as it correlates for different eight parameters affecting the ROP. The Bourgoyne & Young Model was first derived for drilling with Roller cone bits, however, it is frequently used in drilling operations with PDC bits [33] [34] [35] [36].

$$ROP = f_1 \cdot f_2 \cdot f_3 \cdot f_4 \cdot f_5 \cdot f_6 \cdot f_7 \cdot f_8 \tag{3.18}$$

Where respectively the eight parameters affecting ROP are defined as:

- Strength of the formation (f_1)

- Normal compaction trend exponent (f_2)

- Undercompaction exponent (f_3)

- Differential pressure exponent (f_4)

- WOB exponent (f_5)

- Torque exponent (f_6)

- Tooth wear exponent (f_7)

- Hydraulic exponent (f_8)

A new modified model of the Bourgoyne & Young Model was presented. The formulation is simplified concerning the core real-time drilling optimization variables and well depth.

As a matter of fact, equation (3.18) doesn't take depth of the well into account. For this reason a modified Bourgoyne & Young model was introduced. The newly modified Bourgoyne & Young model includes the depth and real-time drilling optimization parameters [37]:

$$ROP = a_1 D^{a_2} WOB^{a_4} RPM^{a_6} q^{a_8} \tag{3.19}$$

To have a more precise description of the interaction of rock-bit, the force and moments are analyzed. This is more complicated in reality because of to compute failure criteria and stresses a full geometric description of contact points and deviation between the wellbore and bit is required [37].

4. Morvin Field and ROP Modelling Workflow Description

4.1 Overview of Morvin Field

Morvin is located in block 6506/11 in the Norwegian Sea approximately 15 km west of Åsgard Field, as shown in Figure 4.1. The field was discovered in 2001, however, the production started in 2010 with Equinor Energy AS being the operator with 64.0 % of the licensees. Vår Energi AS and PGNiG Upstream Norway AS have licensees at 30.0 % and 6.0 %, respectively [38].

Figure 4.1: Location of Morvin in Norwegian Sea [39].

Morvin Field is produced by pressure depletion and the major problem being drillability as the cost-benefit factor of drilling new wells is directly linked with well intervention operations to proceed production in already producing wells [38]. The field produces both gas and oil from the different formations which are of Jurassic sandstones. The Spekk Formation is said to have good reservoir properties, while the Garn and Ile Formations are relatively homo- and heterogeneous. Because of the position of the reservoirs lying in tilted and rotated fault block at the depth of around 4,500 m, there are some issues associated with high pressure and high temperature (HPHT) formations [38].

4.1.1 Welldata

The wells used for modelling and testing in this thesis are 6506/11-A-1, 6506/11-A-2, 6506/11-A-3 and 6506/11-A-4. The status of the wells and locations are shown in Table 4.1 and Figure 4.2, respectively.

The drilling data for Morvin field were provided by NPD, where they had to be filtered before being modelled. The filtration examples are illustrated in chapter 4.2.

Table 4.1: Overview of wellbore developments [38].

Wellbore	Entered date	Completed date	Purpose	Content
6506/11-A-1	24/11/2009	12/08/2010	Production	Oil, Gas and Condensate
6506/11-A-2	12/03/2010	13/05/2011	Production	Oil
6506/11-A-3	27/11/2009	17/02/2010	Production	Not Applicable
6506/11-A-4	22/10/2010	15/11/2010	Production	Oil

Figure 4.2: Map of study area. The wells used for modelling are in blue. [38].

4.1.2 Stratigraphic Correlation

In order to study the lateral geology in the wells considered for modelling, stratigraphic correlation is performed. The objective of stratigraphic correlation is to compare the lithostratigraphy groups of the different wells. The stratigraphic correlation is illustrated in Figure 4.3. It was constructed based on the geological information documented in "Final Well Report". The descriptions of the geological groups and formations within are summarized in the following.

Nordaland Group

Nordaland Group is the shallowest group in the field. However, according to the Final Well Report, it only occurs in well 6506-11-A-1. Nordaland Group consists of Kai and Naust Formations.

- Kai Formation is mainly of large claystones and fractions of limestone.

- Naust Formation consists of claystone with some traces of quartzitic grains intercalations.

Hordaland Group

Hordaland Group only cross the subsurface in well 6506/11-A-1, 6506/11-A-2 and 6506/11-A-3.

- The Hordaland Group consists of Brygge Formation which is dominated by claystone and fragments of limestone and siltstone.

Rogaland Group

Rogaland Group is to be found in all the wells with Tare and Tang Formations.

- Tare Formation is predominantly of claystone with fragments of limestone and siltstone.

- Tang Formation is on the other hand also predominantly of claystone with some traces of limestone.

Shetland Group

Shetland Group across the four wells. Shetland Group is formed by Springar, Nise and Kvitnos Formations.

- Springar Formation is dominated claystones. In well 6506/11-A-1, 6506/11-A-2 and 6506/11-A-3 limestone appear in thin layers. In well 6506/11-A-4 in addition to claystone, dolomitic limestones occur in thin layers.

- Nise Formation is also dominated by claystones, with stringers of limestone in well 6506/11-1, 6506/11-2 and 6506/11-3. In well 6506/11-4 the interval has stringers of dolomitic limestone in claystone interval.

- Kvitnos Formation consists of the same sedimentary rocks as Nise Formation with claystone and fragments of limestone and dolomitic limestone. However, in the lower part of the formation layers of sandstone tend to occur.

Cromer Knoll Group

Cromer Knoll Group is the second deepest for all the wells. This group is the most advanced groups. In well 6506/11-A-1 Lysning, Lange and Lyr Formations occur. In well 6506/11-A-2 the same formations for well 6506/11-A-1 occur as well, in addition to Albian Formation. Well 6506/11-A-3 being the shallowest well, only Lysning and Lange Formations occur. For well 6506/11-A-4 the formations are Lysning, Lange and Lyr Formations.

- Lysning Formation is mainly dominated by claystone with limestone bedding. Layers of sandstone may be present in the formation in addition.

- Lange Formation interval is mostly claystones with few limestone stringers. Also in this formation sandstones tend to be present in the final part of the formation. In well 6506/11-A-4 siltstone appear in the final depth.

- Albian Formation is dominated by claystone, with few sandstone and limestone stringers.

- Lyr Formation consists of claystone, stringers of either minor limestone or dolomite are also common.

Viking Group

Viking Group cross through well 6506/11-A-1, 6506/11-A-2 and 6506/11-A-4. In this group, the formations appear differently in the wells. For instance in well 6506/11-A-1 Spekk, Melke, Garn, Not, Ile and Ror Formations are the formations. The formations present in well 6506/11-A-2 are Spekk, Ile, Ror, Tofte (I-III), Lower Ror, Tilje (1-6) and Aare Formations. For well 6506/11-A-4 the formations that occur are Spekk, Melke, Garn, Not, Ile and Ror Formations.

- Spekk and Melke Formations are broadly of sandstone with increasing claystone with depth. Fractions of limestone stringers appear also.

- Garn Formation consists mostly of sandstone in kaolin matrix with some claystone. In the upper part of the formation an unexpected interval of claystone are present in addition to stringers of limestone.

- Not Formation is mostly of sandstone and claystone. The lower and middle part of the formation is of siltstone, small amount of limestone are present as well.

- Ile Formation consists of alternating sandstone and claystone. Minor limestone stringers are also to be found in this formation.

- Ror Formation also consists of alternating sandstone and claystone.

- Tofte Formation can be categorized into three, Tofte III, Tofte II and Tofte I. The top formation (Tofte III) consists of sandstone and claystone. In the middle and lower formations (Tofte II and Tofte I) limestone stringers are occurring.

- Lower Ror formation is a formation consisting of claystone and sandstone.

- Tilje Formation are divided into Tilje Formation 1 - 6. In the top formation, Tilje Formation 6 consists of sandstone and interbedded sandstone. Tilje Formation 5 consists of interbedded sandstone, claystone and siltstone. Tilje Formation 4 consists of sandstone and silty claystone. Tilje Formation 2 and 3 are of sandstone, siltstone and claystone. Tilje Formation 1 consists of sandstone with minor claystone and siltstone.

- Aare formation is primarily of sandstone, siltstone and claystone.
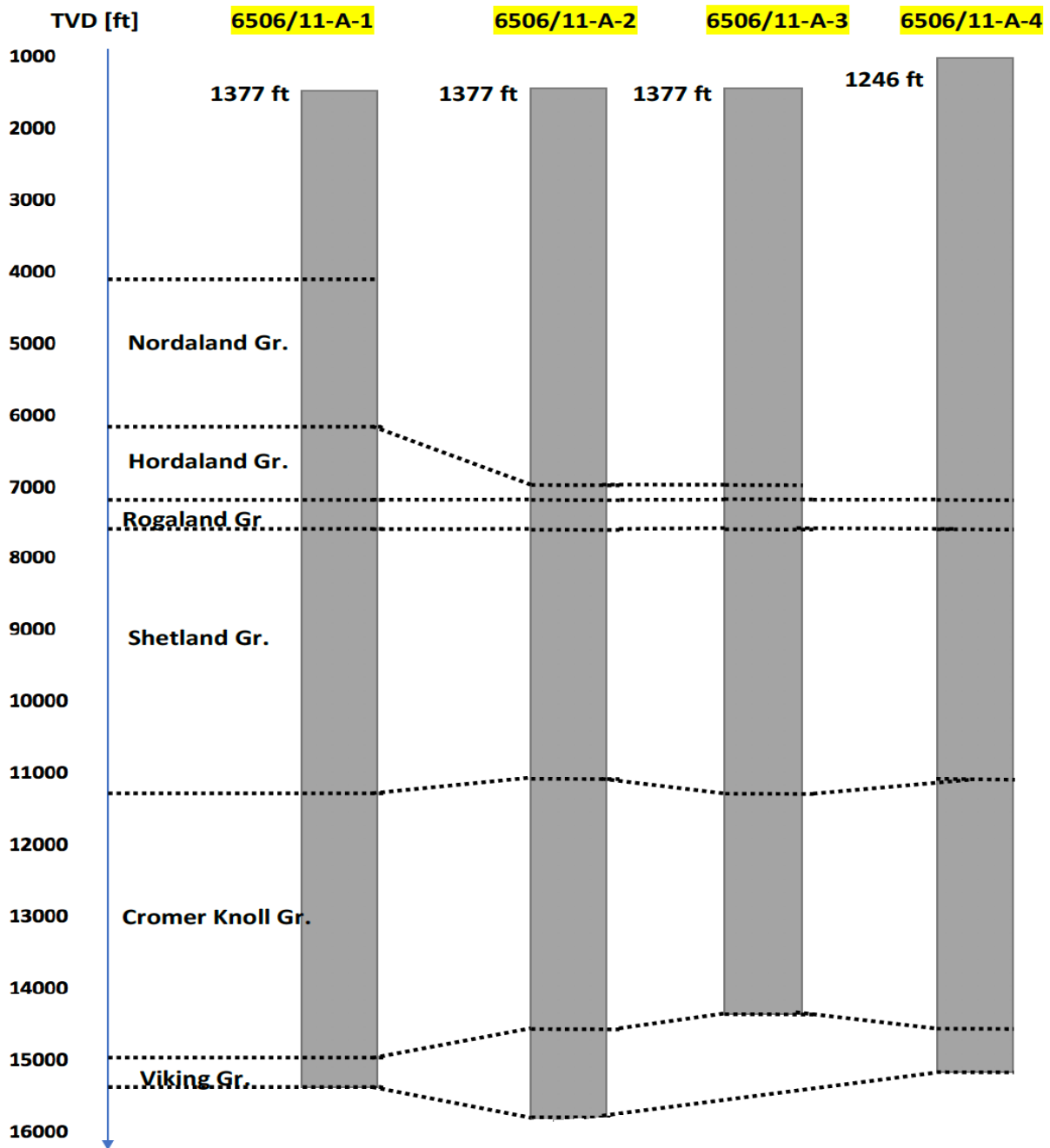
Figure 4.3: Stratigraphic correlation between the wells.

4.2   Data Filtration

4.2.1   Moving Average Filter

Moving average filter is a simple low pass FIR (Finite Impulse Response). However, it is one of the most effective and reliable when it comes to Digital Signal Processing (DSP). Moving average filter is used in cases to remove noise from signals. It smooths an array of sampled data or signals. In other words, it takes an average of a defined number of input point and produces a single output point, the higher filter length the smoother output. Moving average filter is said to have a superlative time response domain, however, the frequency domain is quite poor [40].

$$y_i = \frac{1}{N} \sum_{i=0}^{m-1} x_{N-i} \tag{4.1}$$

Where, y_i is the calculated signal outcome, N is the size of the sliding window. The smoothing of the signal strongly depends on the value of N, as larger sliding window leads to a smoother signal. However, in reality, if the window size is too large the signal will lose its sharpness. This phenomenon is illustrated in Figure 4.4

The Moving average filter was applied to the drilling data provided which were used to calculate ROP in order to reduce the contribution of unwanted signals and noises, this was done in Microsoft Excel. The window size used in this thesis were N=5. Thus, equation (4.1) can be transformed into equation (4.2) when dealing with ROP.

$$ROP_{Filtered} = \frac{1}{N} \sum_{i=0}^{m-1} ROP_{N-i} \tag{4.2}$$
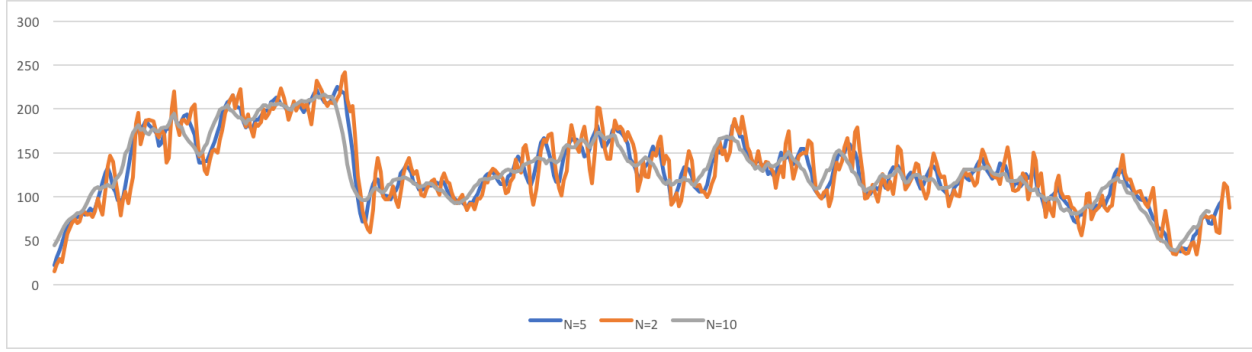
Figure 4.4: Illustration of moving average filter.

4.2.2 Exponential Smoothing

Exponential smoothing is a time series forecasting method for univariate data. This type of filter can be used to trend or extended data with a systematic trend. Compared to the Moving average filter where the previous data points are weighted equally, Exponential smoothing is used in exponential decreasing functions, as a function of time and is based on weighted averages. Exponential smoothing is a low pass filter, where it removes high-frequency noises in data. The equation for Exponential smoothing is shown below: [41]:

$$S_{t+1} = \alpha \cdot y_t + (1 - \alpha) \cdot S_t \qquad (4.3)$$

Where, S_{t+1} is the forecast value calculated. α is the smoothing factor [0-1]. S_t is the foregoing forecast and y_t is the foregoing value of the dataset being filtered.

Exponential smoothing was also tested in this thesis to the dataset provided. However, compared to Moving average this filter was mainly used to smooth the spikes and the result is shown in Figure 4.5. The smoothing factor was chosen to be α=0.85. When equation (4.3) is accounted for ROP it is expressed as:

$$ROP_{t+1}^{Filt} = \alpha \cdot ROP_t^{Filt} + (1 - \alpha) \cdot ROP_t^{Field} \qquad (4.4)$$
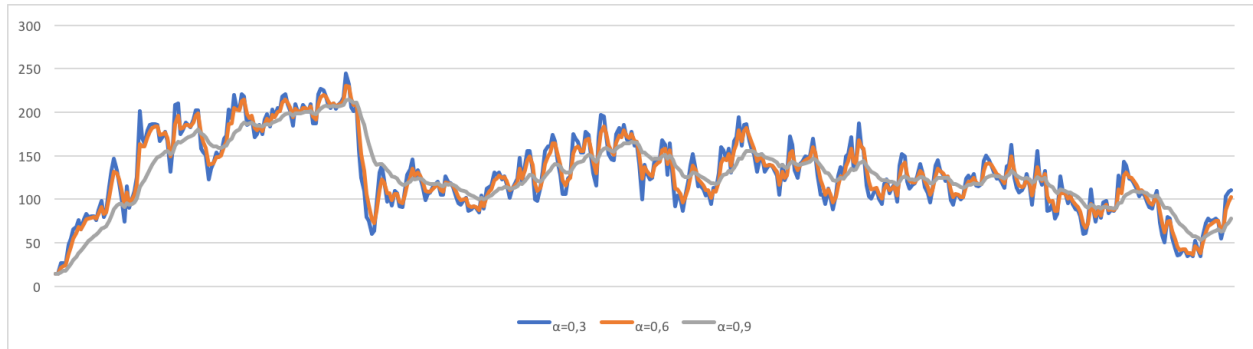
Figure 4.5: Illustration of exponential smoothing filter.

4.3 Modelling and Workflow Techniques

4.3.1 Multiple Regression Workflow

Multiple regression is a popular dataset-technique used in many fields. This method is applicable in datasets where there exists a correlation between the input variables within each other and with the dependent variables to a certain degree, assumed there is a linear relationship. The objective of Multiple regression is to study the relationship between the dependent variable and multiple independent variables. Initially in this method, one studies how strong the relationship between a single dependent variable and several input variables are. Later, it is possible to predict the contribution of each input variable and finally find the best-predicted equation [42] [43].

$$Y = \beta_0 + \beta_1 X_1 + \beta_2 X_2 + ... + \beta_k X_k \tag{4.5}$$

Where the dependent variable is given as Y and is the predicted value. Independent variables as X_1–X_k. β_1–β_k are the regression coefficients assigned to each independent variable and β_0 is the intersection point. Implementing equation (4.6) in terms of ROP and drilling parameters the equation can be written as.

$$ROP = \beta_0 + \beta_1 WOB + \beta_2 RPM + \beta_3 Torque + \beta_4 FP + \beta_5 MW + \beta_6 FlowRate \quad (4.6)$$

Equation (4.6) is based on several drilling data, where they make up the independent variable and ROP is Y-value predicted. Note that equation (4.6) is built on a few assumptions such as it doesn't take the well deviation into account. The depth of the well is only a reference and isn't considered in the analysis and the wells are correlated with respect to geological sections and modelled respectively.

The Multiple regression model is modelled in Microsoft Excel where each drilling data is provided to predict the rate of penetration. The regression coefficients are listed as constants as the independent variables in terms of drilling data are varying with the depth of the well. Initially, we start out the regression based modelling with the reference well. Furthermore, the coefficients are implemented in equation (4.6) to predict the ROP of the nearby and far-away wells. The workflow is presented in Figure 4.6:
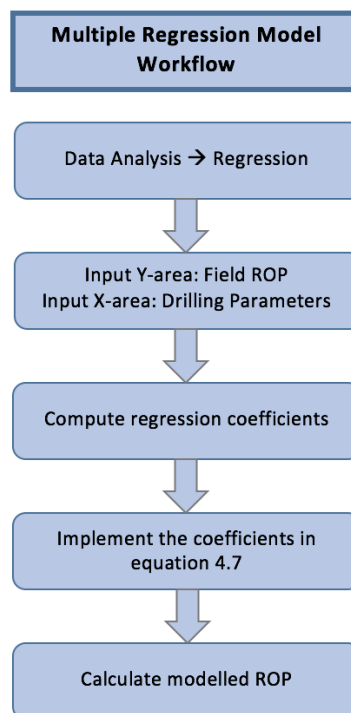
Figure 4.6: Multiple regression model workflow.

4.3.2 MSE Model Workflow

MSE is used to model ROP. As described in Chapter 3, MSE is the energy required to excavate one volume of rock from the formation. The procedure is that, first MSE values are calculated using equation (3.5) for reference well. The calculated MSE value is implemented into equation (4.7) to calculate ROP for the nearby and far-away wells. In this technique, it is assumed that the mechanical formation strength of the reference well, nearby and far-away wells are nearly equivalent. The MSE workflow is presented in Figure 4.7:
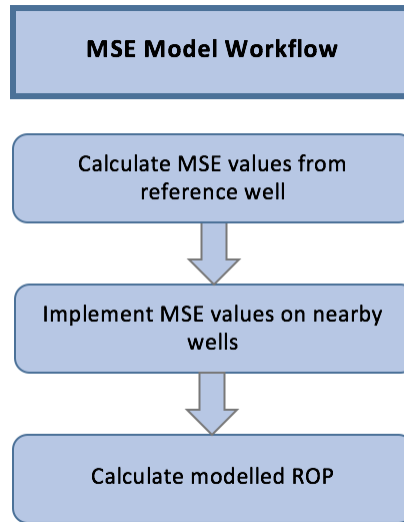
Figure 4.7: MSE model workflow.

The units for the parameters used for this ROP model are following: MSE in [Kpsi], WOB in [lbs], D_b in [in] and T in [lbf-ft].

$$MSE = \frac{480NT}{ROP \cdot 1000D_b^2} + \frac{4WOB}{\pi \cdot 1000D_b^2}$$

$$ROP = \frac{120NT}{250MSED_b^2 - \frac{WOB}{\pi}} \tag{4.7}$$

4.3.3 D-Exponent Model Workflow

The D-exponent model previously stated in Chapter 3 is a ROP model that is based on normalizing the drilling parameters for calculating ROP. Rehm et al. developed equation (3.11) that corrects for the contribution of ECD [27]. However, in this thesis due to lack of ECD values from the wells provided the last term ρ_n/ρ_a is neglected. The equation used in predicting the ROP in the D-exponent model is therefore equation (3.11) simplified to:

$$D_{exp} = \frac{\log \frac{ROP}{60N}}{\log \frac{12WOB}{10^6 D}} \tag{4.8}$$

By using equation (4.8) as a reference equation the D-exponent from the reference well is used to predict the modelled ROP for the next well by substituting it into equation (4.9), which is obtained by rearranging equation (4.8) with respect to ROP.

$$D_{exp} = \frac{\log \frac{ROP}{60N}}{\log \frac{12WOB}{10^6 D}}$$

$$\log \frac{ROP}{60N} = D_{exp} \cdot \log \frac{12WOB}{10^6 D_b}$$

$$ROP = 10^{D_{exp} \log \frac{12WOB}{10^6 D_b}} \cdot 60N \tag{4.9}$$

The units for the parameters in this model are ROP in [ft/hr], D_b in [in], WOB in [lbf] and RPM in [ft/min]. The workflow for D-exponent is presented in Figure 4.8
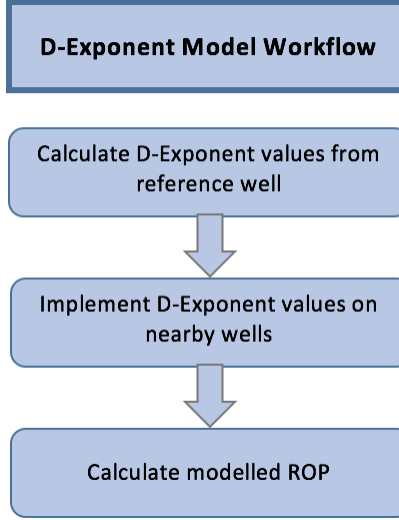
Figure 4.8: D-Exponent model workflow.

4.3.4 Warren Model Workflow

Warren model being introduced in Chapter 3.2 is a ROP for soft formation bits. This model relates the penetration rate to several factors such as rock strength, WOB, rotational speed, jet impact force and size- and type of the bit. When developing ROP for the Warren model the imperfect-cleaning model is used equation (3.13). Due to being more applicable as the ROP is significantly affected by the rate where the rock cuttings are evacuated under the bit.

In order to calculate the rock strength, which is not provided in the drilling data, we must assume the uniaxial compressive strength of the rock (UCS) is equal to 35 % of MSE, hence peak performance of drill bits is achieved when UCS is equal to 30-40 % of MSE. In order to calculate ROP by using imperfect cleaning model equation (3.13) must be rearranged:

$$ROP = \left(\frac{aS^2 D_b^3}{N \cdot WOB^2} + \frac{b}{N \cdot D_b} + \frac{cD_b\gamma_f\mu}{F_{jm}} \right)^{-1}$$

$$\frac{1}{ROP} = \frac{aS^2 D_b^3}{N \cdot WOB^2} + \frac{b}{N \cdot D_b} + \frac{cD_b\gamma_f\mu}{F_{jm}}$$

$$ROP = a\left(\frac{S^2 D_b^3 ROP}{N \cdot WOB^2}\right) + b\left(\frac{ROP}{N \cdot D_b}\right) + c\left(\frac{D_b \gamma_f \mu ROP}{F_{jm}}\right) \tag{4.10}$$

To be able to use equation (4.10), the equation must be expressed as a matrix with the three terms for the reference well $\left(\frac{S^2 D_b^3}{N \cdot WOB^2}\right)$, $\left(\frac{1}{N \cdot D_b}\right)$ and $\left(\frac{D_b \gamma_f \mu}{F_{jm}}\right)$. The equation be expressed as following matrix:

$$\begin{bmatrix} a \\ b \\ c \end{bmatrix} \begin{bmatrix} x_1 & y_1 & z_1 \\ x_2 & y_2 & z_2 \\ \vdots & \vdots & \vdots \\ x_n & y_n & z_n \end{bmatrix} = \begin{bmatrix} 1 \\ 1 \\ \vdots \\ 1 \end{bmatrix}$$

The terms are solved as matrix in MATLAB, generating "x", "y" and "z" values. Where, "x", "y" and "z" are respectively, the first, second and third terms. Furthermore, the matrix equation can now be solved in MATLAB to calculate "a", "b" and "c" coefficients. These values are now implemented into equation 4.10 for the next well and the following equation is obtained:

$$ROP = \frac{1}{a\left(\frac{S^2 D_b^3}{N \cdot WOB^2}\right) + b\left(\frac{1}{N \cdot D_b}\right) + c\left(\frac{D_b \gamma_f \mu}{F_{jm}}\right)} \tag{4.11}$$

The workflow for Warren model is presented in Figure 4.9.
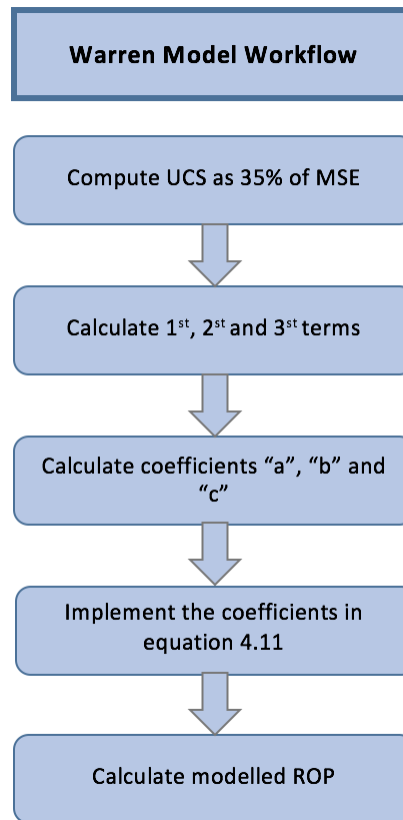
Figure 4.9: Warren model workflow.

4.3.5   Bourgoyne & Young Model Workflow

Bourgoyne & Young model equation is based on several drilling parameters. The ROP is modelled by combining the Bourgoyne & Young coefficients with the drilling parameters as presented in equation (4.12). In order to determine the coefficient values, regression analysis is performed. The steps to simplify equation 4.12 is converting the equation to logarithmic.

$$ROP = a_1 D^{a_2} WOB^{a_4} RPM^{a_6} q^{a_8} \tag{4.12}$$

$$\log(ROP) = \log(a_1 D^{a_2} WOB^{a_4} RPM^{a_6} q^{a_8})$$

$$log(ROP) = \log(a_1) + a_4 \log(D) + a_4 \log(WOB) + a_6 \log(RPM) + a_8 \log(q) \qquad (4.13)$$

The coefficients shown in equation (4.13) are derived by using the measured field data and regression technique. Figure 4.10 shows the process of computation. The coefficients are then implemented back into equation 4.10 where they are combined with the drilling parameters.
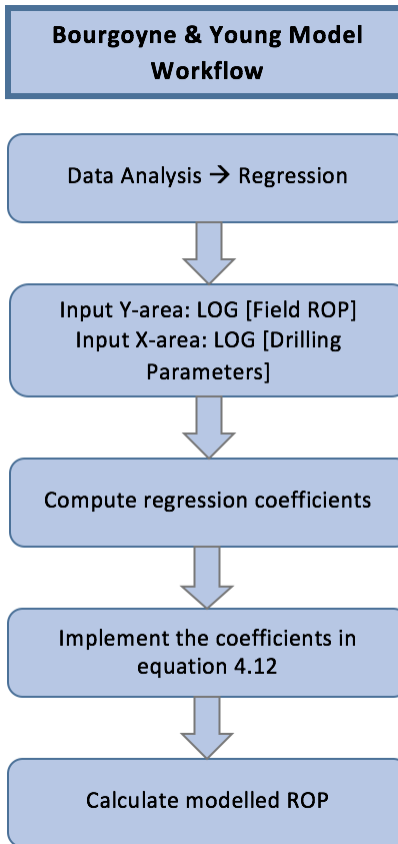
Figure 4.10: Bourgoyne & Young model workflow.

5.   Modelling and Results

During modelling, the workflows outlined in Chapter 4.3 are implemented. These are multiple regression (Figure 4.6), MSE (Figure 4.7), D-exponent (Figure 4.8), Warren (Figure 4.9) and Bourgoyne & Young (Figure 4.10) models. The modelling scenarios are based on entire well data, section by section, geology by geology after being correlated for, and drilling ahead approaches. To briefly describe the modelling hypothesis:

- **Entire well data**: This modelling approach uses the entire drilling data, which comprises of different geological groups.

- **Section by section**: The hole sections data associated with the 36" 26" 17.5 and 12.25" are used to develop models for each section. Here, each section may represent a single geology or a combination.

- **Lateral geological groups**: Using drilling reports, the geological sections of the drilled well are identified and correlated for, as shown in Figure 4.3 in chapter 4.1.2. Based on the geological group data, the ROP model was modelled and constants or coefficients are generated.

- **Drill ahead ROP prediction**: The main idea here is to develop a model in real-time and apply the model when planning to drill ahead. This method uses 90 % of the drilled well for modelling, but the coefficients/constants are applied for the whole section including the remaining 10 % data.

The ROP modelling is based on field drilling data, which comprises of field ROP, WOB, RPM, torque, drill bit size, mud weight, flow rate and pore pressure. Figure 5.1 shows the whole process of modelling, testing and reporting.
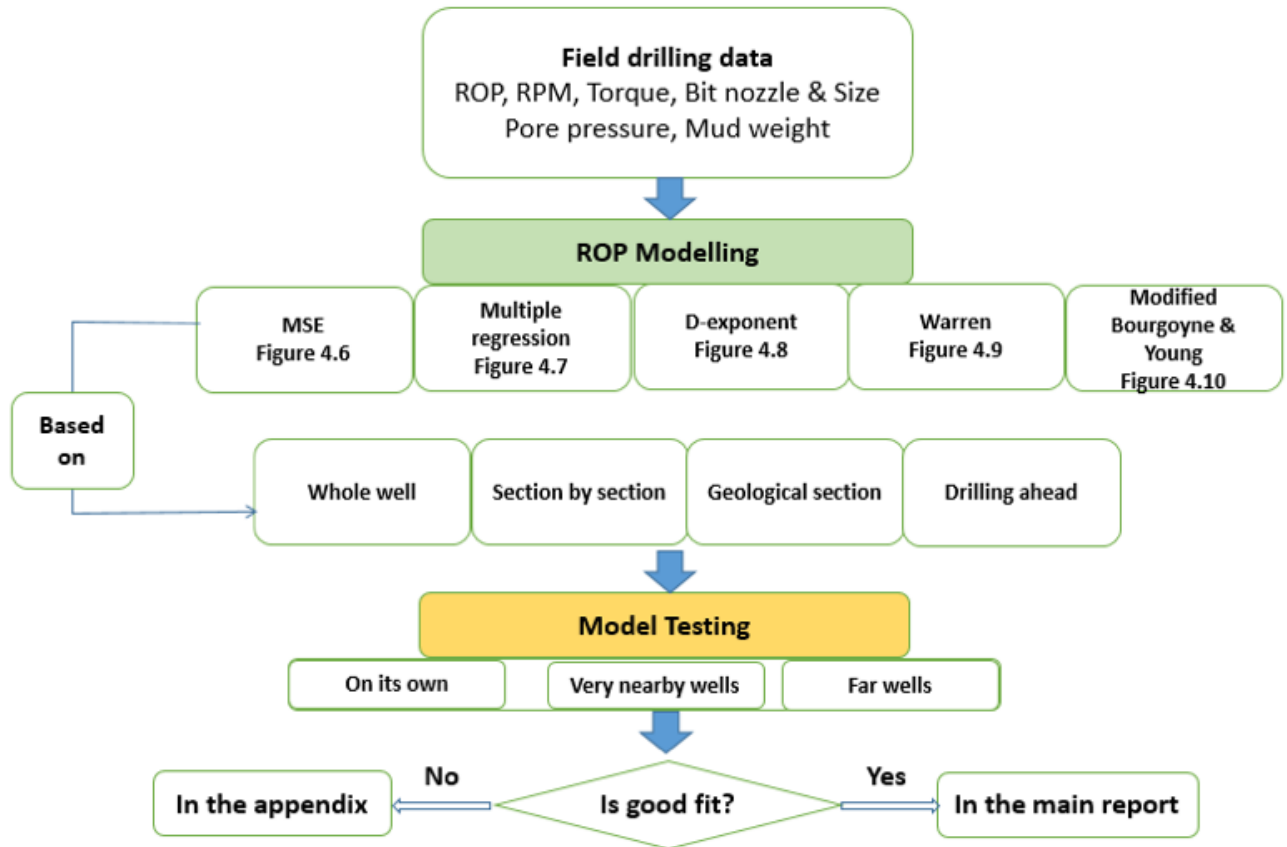
Figure 5.1: Summary of the modelling techniques, testing scenarios and reporting of results.

Modelling Testing

As illustrated in Figure 5.2, the models are tested on the considered wells. For instance, the model generated from well 6506/11-A-3 data will be tested on its own, nearby well (eg. well 6506/11-A-1) and far-away wells (6506/11-A-2 and 6506/11-A-4). The process is repeated for the other wells as well. The main idea here is to investigate the applicability and limitations of the models.
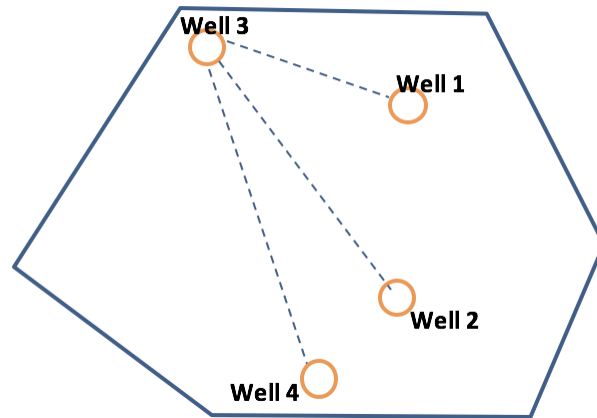
Figure 5.2: Illustration of well 6506/11-A-3 based model application on the nearby and far-away wells.

Criteria for reporting

It is well known that all modelling approaches will not give good results. The application of the models where it is applied for its own well or very close wells with similar geology, the applicability is higher. However, for the quality of the report, the criteria for pass or fail is introduced. If the testing result is good enough for most of the wells, it is reliable and reported in the main thesis. However, there are also cases when the testing results show huge discrepancy between the model and the measured, then it will be moved to Appendix. By studying the data, the poor results may be to modelling and the lateral geological variations. The possible reason for this could be because of poor quality of the measured input drilling data.

5.1 Multiple Regression Modelling

5.1.1 Investigating ROP Dependent Parameters

As reviewed in the theory part several parameters control the penetration rate. However, in this modelling part seven drilling parameters will be used for application. For instance, the Warren model comprises of three terms that control the ROP, with the first term dealing with indentation, the second part with the cutter and the third term with the effects of hydraulic.

The parameters affecting the ROP can be divided into drilling- and hydraulics parameters. Drilling parameters include WOB, torque and RPM. Drilling hydraulics related parameters are mud weight, formation pressure and flow rate. In order to study the effect of the drilling- and hydraulic parameters on ROP, field data from well 6506/11-A-2 in Morvin field are used to model the rate of penetration with Multiple regression model. The objective of this task is to verify the parameters ROP depends on. Initially the model consists of 6 parameters and is decreased with the step of one variable at the time. The quality of the modelled ROP is tested by considering the coefficient of determination (R^2) which is an element of [0,1]. $R^2 = 0$ means none of the parameters are function of ROP and if $R^2 = 1$ the parameters can predict the ROP without errors.

Table 5.1: Investigating ROP Dependent Parameters regression coefficient values.

Case	C_0	C_1	C_2	C_3	C_4	C_5	C_6	R^2
#1	-816.069	0.001	-0.007	0.089	0.297	59.737	94.868	0.728
#2	-696.206	-0.001	-0.003	0.125	0.256	62.499		0.714
#3	166.784	-0.004	0.002	0.525	-0.041			0.223
#4	124.628	-0.004	0.003	0.468				0.220

Case 1

Equation 5.1 is the model, which consists of seven parameters. The modelling result is shown in subfigure 5.3a and the coefficient values of the case are provided in Table 5.1. The model for case 1 is shown in equation (5.1)

$$ROP\left(\frac{ft}{h}\right) = C_0 + C_1 WOB + C_2 T + C_3 RPM + C_4 Flow + C_5 FP + C_6 MW \qquad (5.1)$$

The model fits relatively well with the measured ROP where, $R^2 = 0.777$. As shown in subfigure 5.3a, the correlation between the model and field data are good.

Case 2

By omitting mud weight, the second model uses six parameters. The coefficient values are shown in Table 5.1 and the result of the modelling is shown in subfigure 5.3b. The model fits with $R^2 = 0.749$, which is nearly similar to the seven-parameters model.

$$ROP\left(\frac{ft}{h}\right) = C_0 + C_1 WOB + C_2 T + C_3 RPM + C_4 Flow + C_5 FP \qquad (5.2)$$

Case 3

Furthermore, in the third model, the formation pressure is omitted. The model clearly shows that ROP strongly depends on formation pressure as $R^2 = 0.213$ and ROP modelled clearly deviates from the measured ROP. The modelling result is illustrated in subfigure 5.3c and the coefficient values are provided in Table 5.1.

$$ROP\left(\frac{ft}{h}\right) = C_0 + C_1 WOB + C_2 T + C_3 RPM + C_4 Flow \qquad (5.3)$$

Case 4

In the last model flow rate is removed and the only parameter left are WOB, T and RPM. The coefficient of determination is almost similar to case 3 being 0.212, indicating flow rate is a minor contribution on ROP. The modelling result is shown in subfigure 5.3d and the coefficient values in Table 5.1.

$$ROP\left(\frac{ft}{h}\right) = C_0 + C_1 WOB + C_2 T + C_3 RPM \qquad (5.4)$$

(a) Case 1

(b) Case 2

(c) Case 3

(d) Case 4
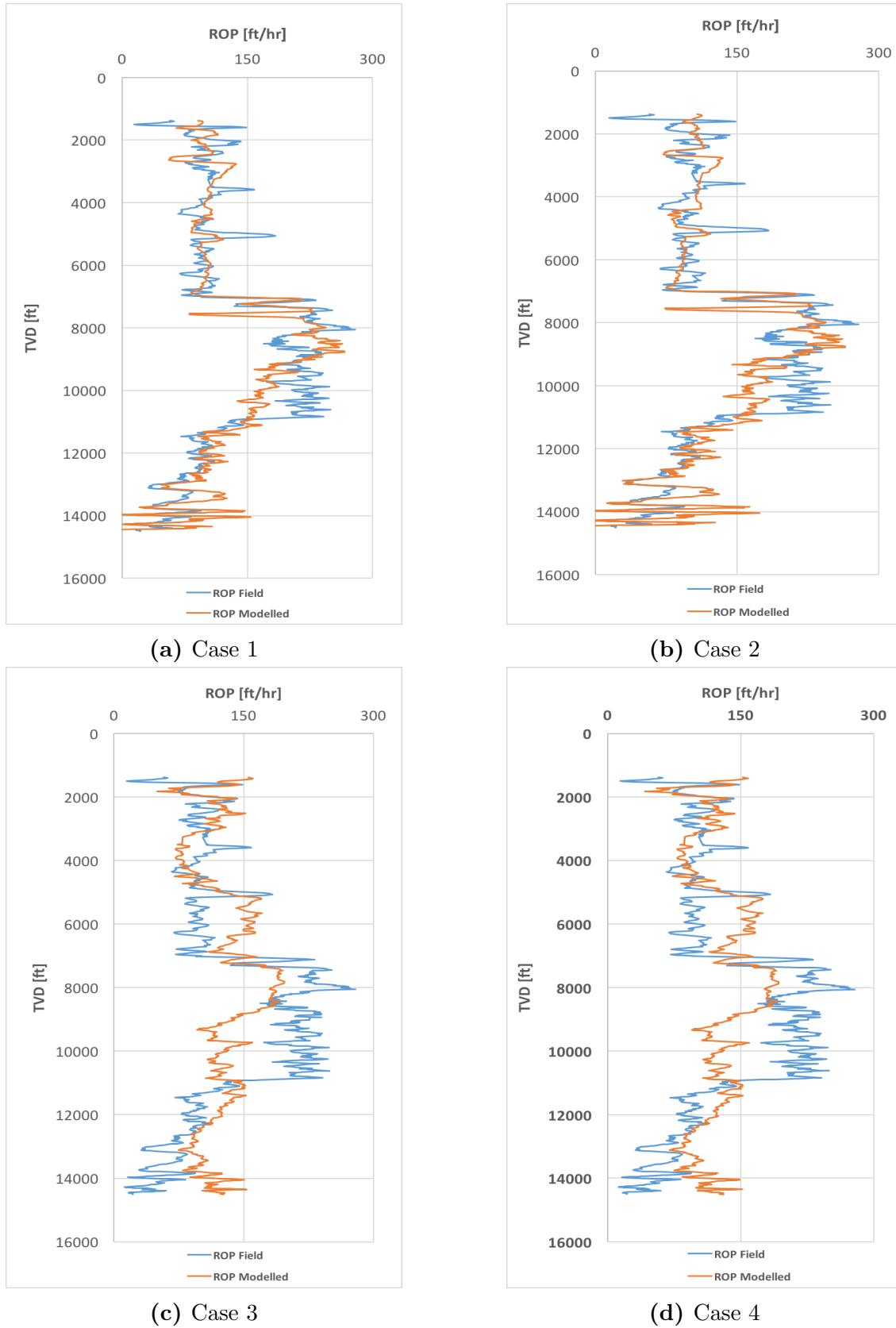
Figure 5.3: Investigating ROP Dependent Parameters modelling results.

From the modelling results, we observe that the first two cases show a good correlation with the measured ROP. Reducing the parameters in the last two cases showed that the discrepancy between the model and the measured data increases. Furthermore, we observe that when removing one parameter in each case, the correlation factor decreases. This indicates that the penetration rate depends on all the parameters as demonstrated in case 1.

5.1.2 Testing for its Own, Nearby and Far-Away Wells

The depth of the overburden except for well 6506/11-A-3 are all deeper than 8450 ft. Here, the total vertical depth until the top of the reservoir (i.e 8.5) hole sections data is considered for the modelling and application. Figure 5.4 shows the well depths.
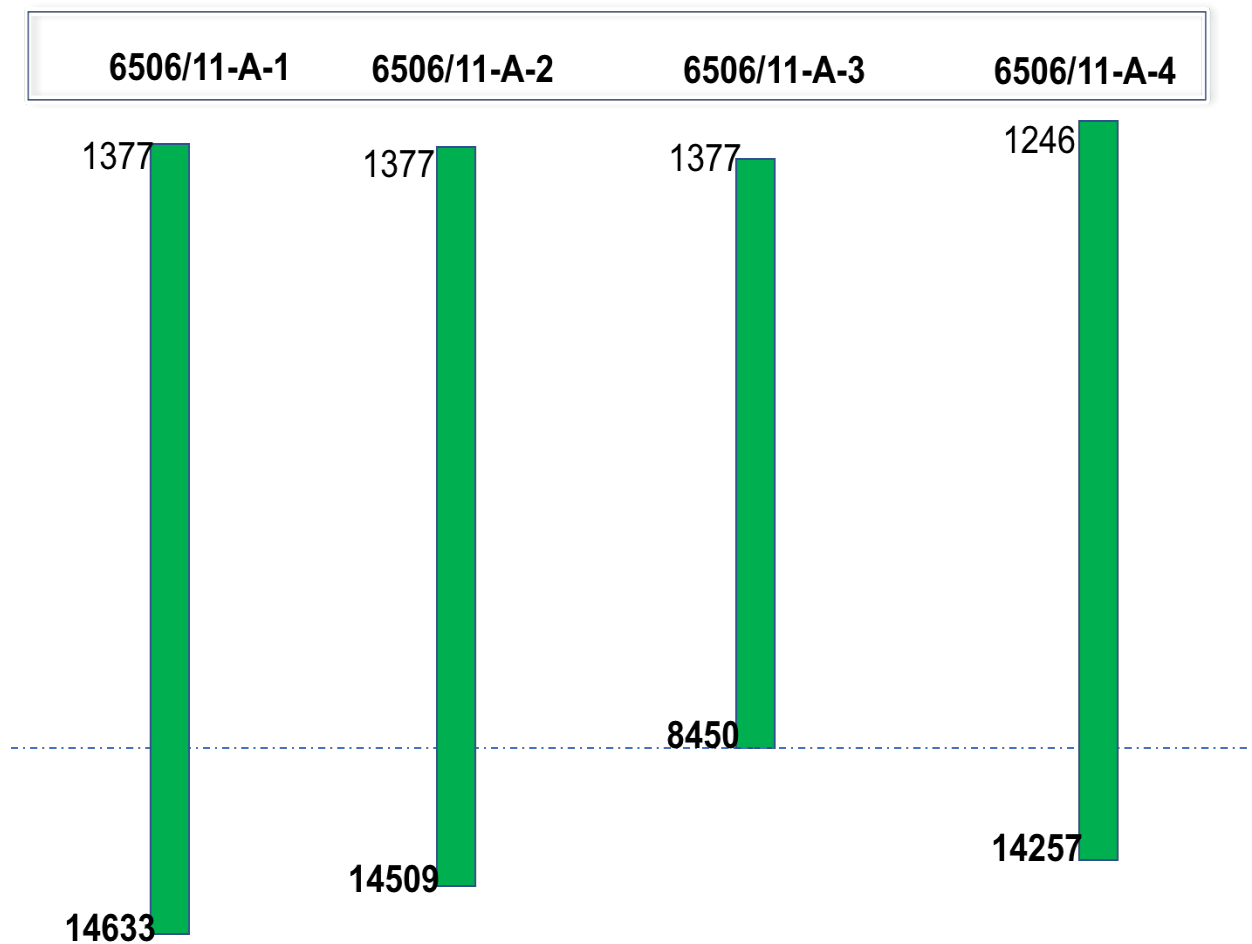
Figure 5.4: Sketch of entire wells.

In this section the wells 6506/11-A-1, 6506/11-A-2, 6506/11-A-3 and 6506/11-A-4 are modelled with coefficient values extracted from each of their well. The outcomes of the plots are presented in Figure 5.5. The modelled ROP is calculated using equation (5.5). The result coefficient values for the overburden sections are presented in Table 5.2 where ROP is plotted against true vertical depth (TVD).

$$ROP\left(\frac{ft}{h}\right) = C_0 + C_1 WOB + C_2 T + C_3 RPM + C_4 FP + C_5 Flow + C_6 MW \qquad (5.5)$$

Table 5.2: Multiple regression model - Regression coefficient values for entire well data.

Well	C_0	C_1	C_2	C_3	C_4	C_5	C_6	R^2
6506/11-A-2	43.254	-0.002	-0.012	0.460	8.585	-0.058	113.964	0.605
6506/11-A-2	-816.069	0.001	-0.007	0.089	59.737	0.297	94.868	0.728
6506/11-A-3	-211.664	-0.002	0.011	0.478	32.210	0.104	-141.171	0.553
6506/11-A-4	-168.627	-0.002	0.004	-0.102	0.890	0.154	83.256	0.434
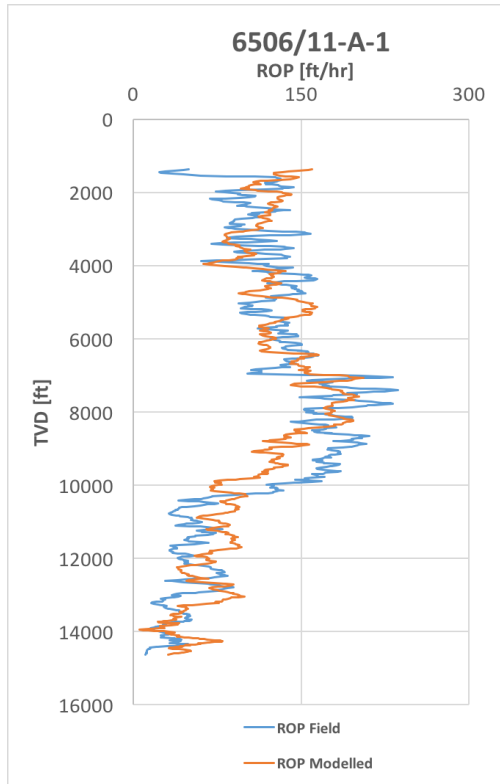
(a) 6506/11-A-1
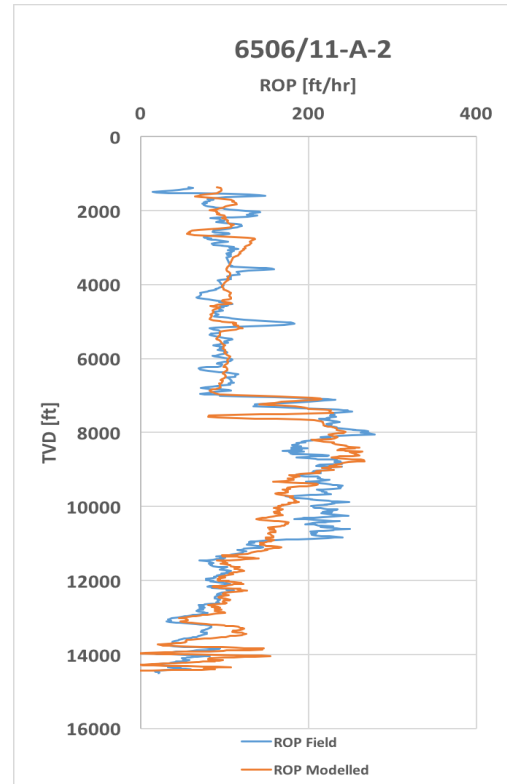
(b) 6506/11-A-2
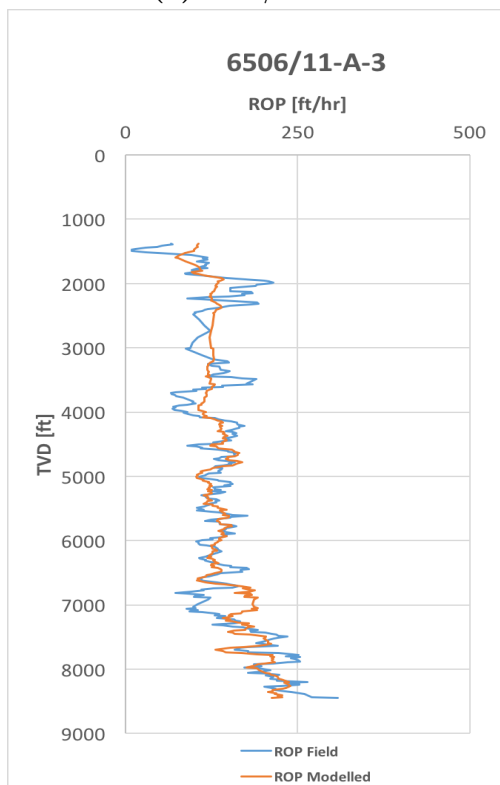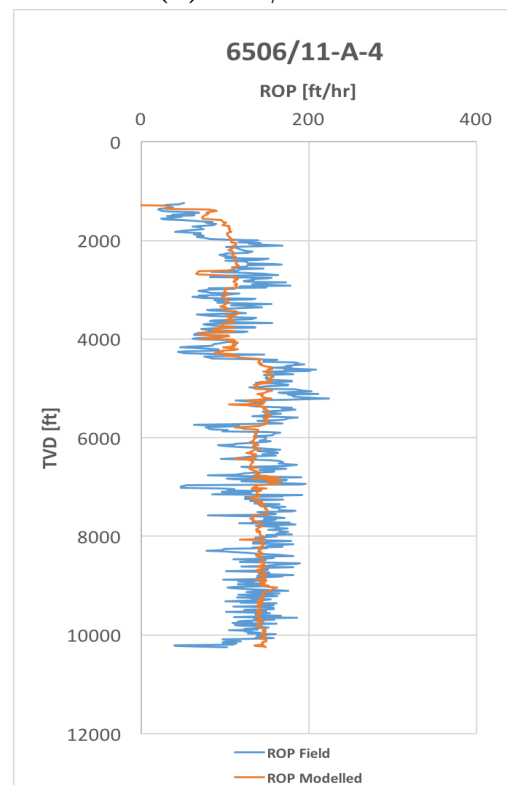
(c) 6506/11-A-3

(d) 6506/11-A-4

Figure 5.5: Multiple regression model - Using their own regression coeff. values.

Testing coefficients from nearby and far-away wells

The coefficients extracted from the wells are implemented in the nearby and far-away wells to the modelled ROP. The results are compared with the measured ROP of the wells in Figure 5.6 - 5.9.
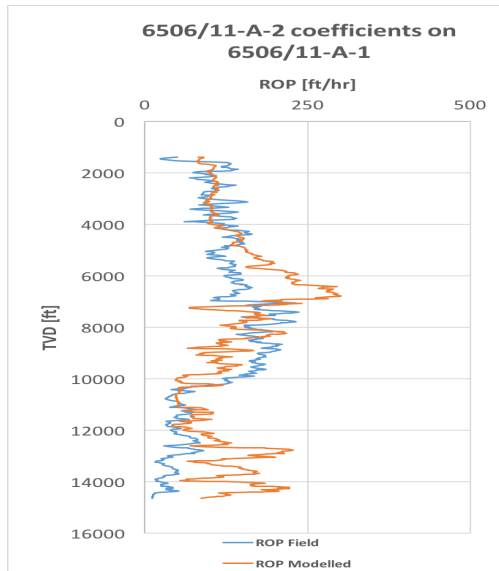
(a) using 6506/11-A-2 regression coefficient values
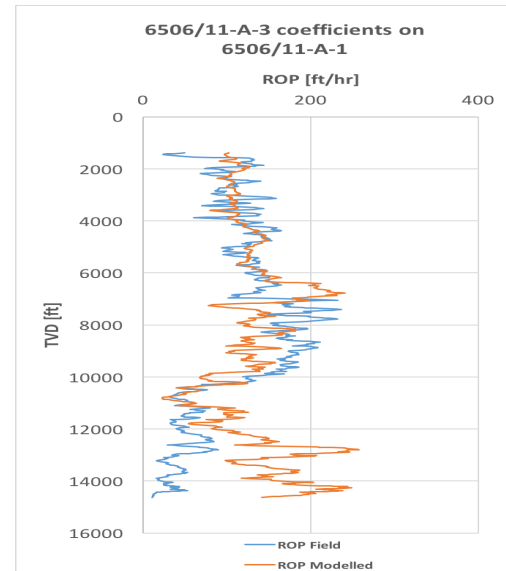
(b) using 6506/11-A-3 regression coefficient values
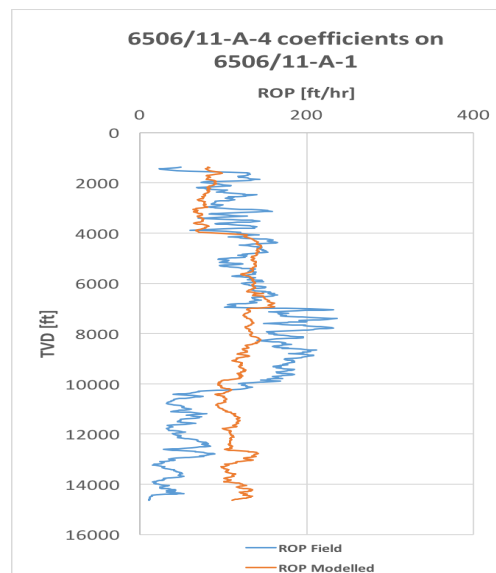
(c) using 6506/11-A-4 regression coefficient values

Figure 5.6: Multiple regression model - Nearby and far-away regression coeff. on 6506/11-A-1.
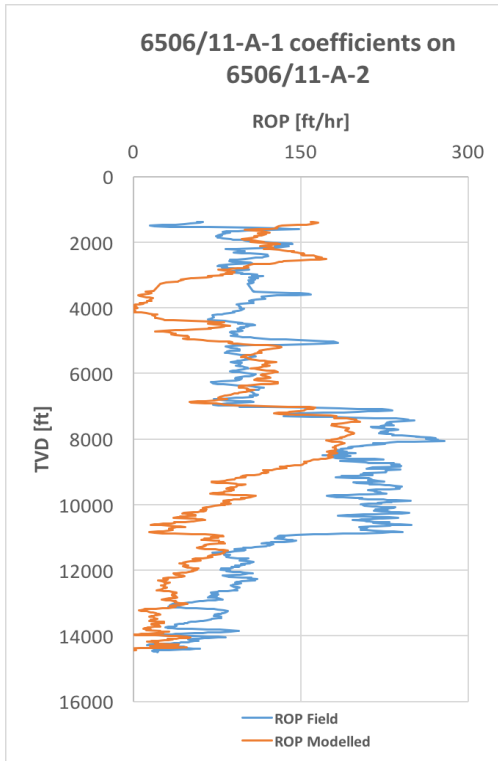
(a) using 6506/11-A-2 regression coefficient values
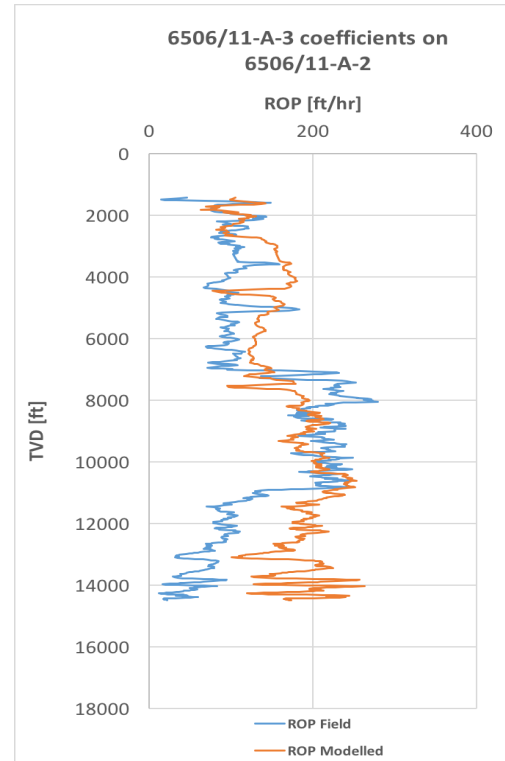
(b) using 6506/11-A-3 regression coefficient values
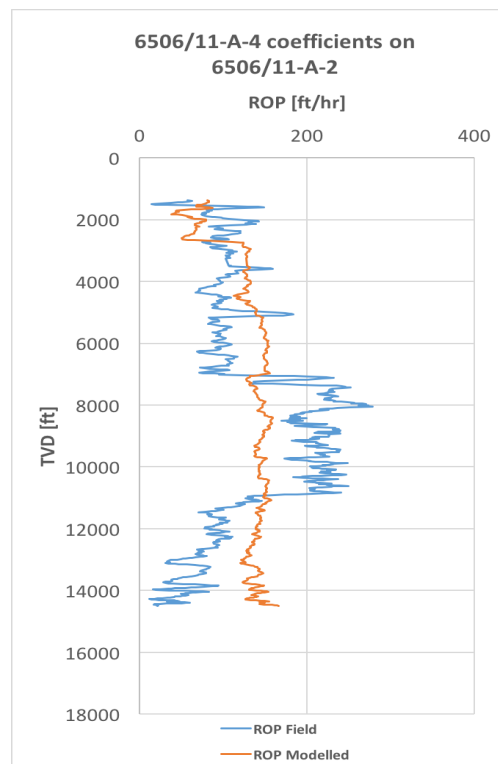
(c) using 6506/11-A-4 regression coefficient values

Figure 5.7: Multiple regression model - Nearby and far-away regression coeff. on 6506/11-A-2.
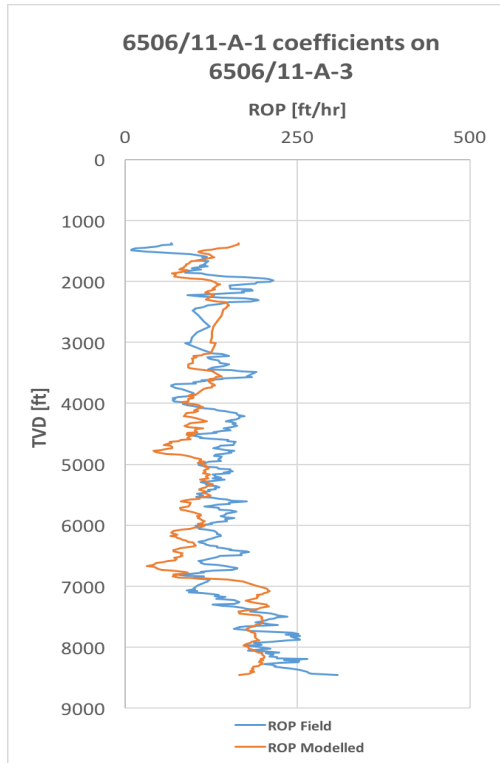
49

(a) using 6506/11-A-1 regression coefficient values
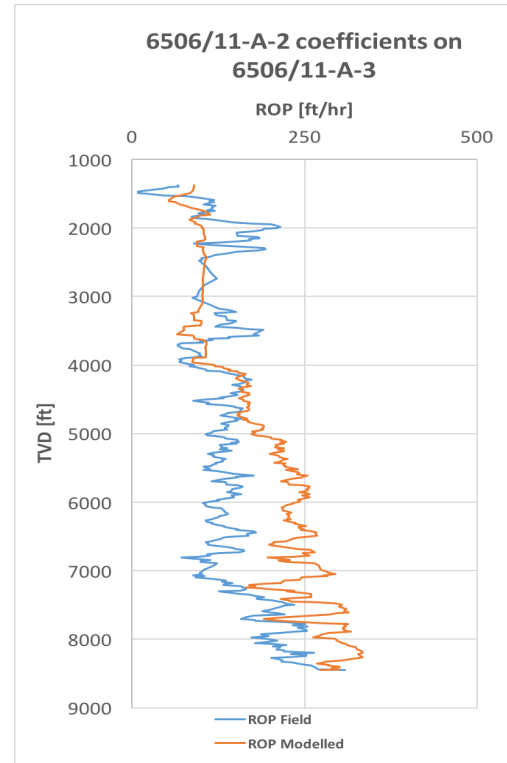
(b) using 6506/11-A-2 regression coefficient values
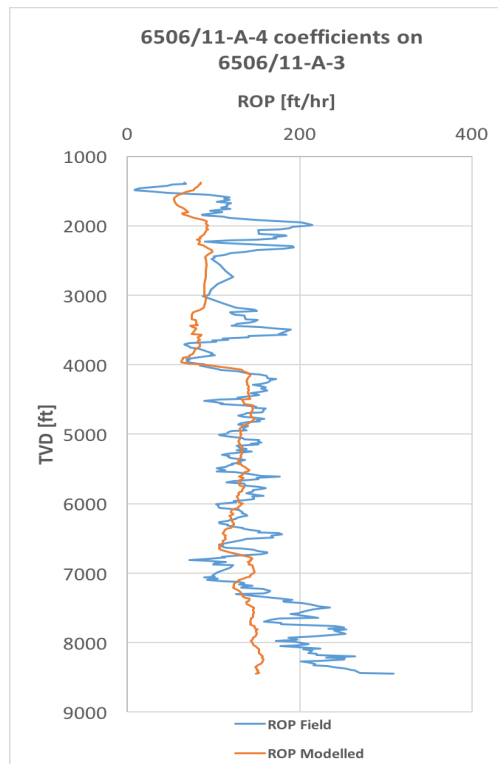
(c) using 6506/11-A-4 regression coefficient values

Figure 5.8: Multiple regression model - Nearby and far-away regression coeff. on 6506/11-A-3.
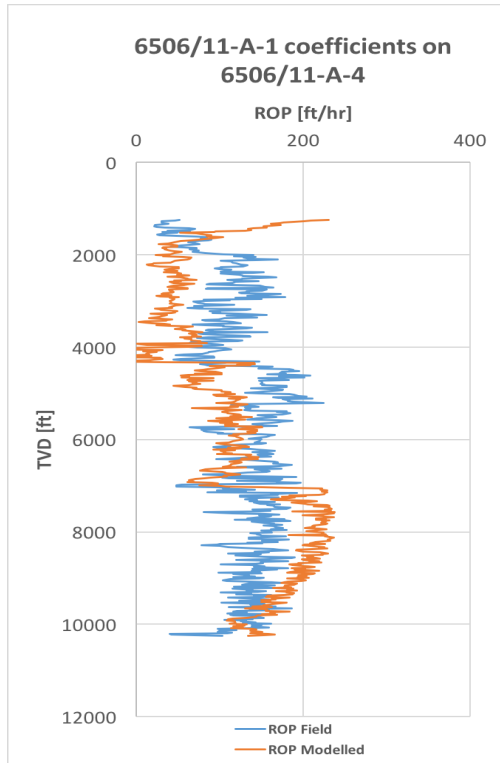
50

(a) using 6506/11-A-1 regression coefficient values
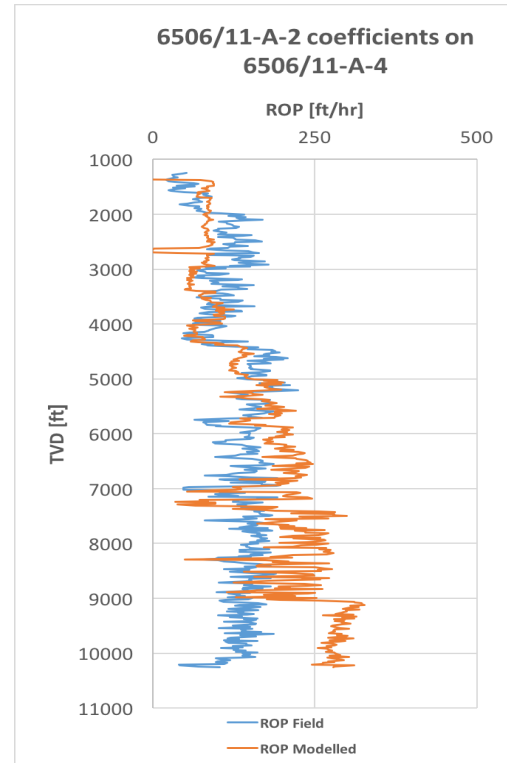
(b) using 6506/11-A-2 regression coefficient values
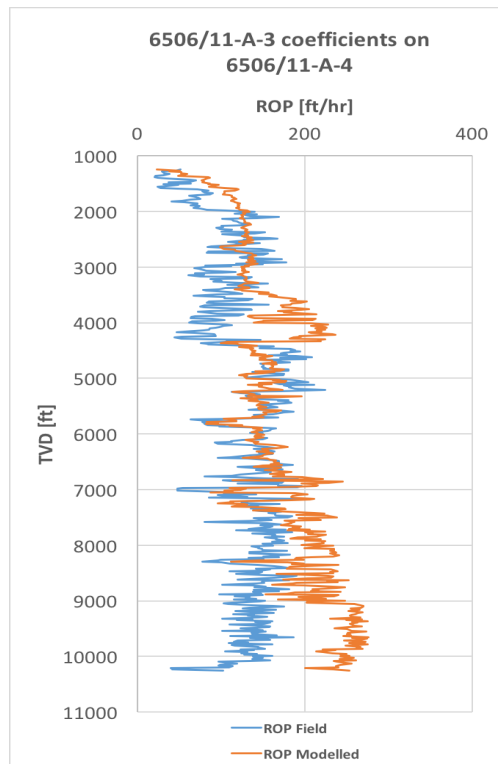
(c) using 6506/11-A-3 regression coefficient values

Figure 5.9: Multiple regression model - Nearby and far-away regression coeff. on 6506/11-A-4.

The results are showed in Figure 5.6. The model coefficients obtained from well 6506/11-A-2 and 6506/11-A-3 predict well 6506/11-A-1 quite good. However, at the deeper section associated with the Cromer Knoll group, the model predictions deviate. The three wells have the same formations (Lysning, Lange and Lyr Formations), which consist of claystone, stringers of either minor limestone or dolomite. However, the homogeneity is not the same in the three wells. The application on well 6506/11-A-4 shows poor correlation.

Similarly, the application on the nearby and far-away wells (6506/11-A-1, A-3 and A-4) on well 6506/11-A-2 show a quite poor prediction. Furthermore, the application of well 6506/11-A-1, 6506/11-A-2 and 6506/11-A-4 on well 6506/11-A-3 show a good prediction. The reason for this could be due to the fact that when applying the models, all wells have the same depth since well 6506/11-A-3 is shorter than the rest. These results suggest developing a new scenario called "Same well depth from mudline", as shown in chapter 5.1.3.

The results displayed in Figure 5.9 is the application of the three well models on well 6506/11-A-4. Since the well 6506/11-A-4 data contains a lot of spikes, it is difficult to model the details. The ROP of the well might experience a lot of axial vibrations. Due to the disturbances on the ROP data, the model could not capture the ROP of the measured data. From the model testing results, one can observe that the application of the models on the nearby and far-away wells is sometimes good enough and sometimes bad. The main reasons associated with this are the quality of the data inputs used, and the lateral geology dissimilarities between the wells.

5.1.3 Same Well Depth From Mudline Scenario

In this modelling scenario, all the wells are set to have the same depth of 8450 ft in order to correlate for the same depths. Figure 5.10 shows a sketch of the well depths.
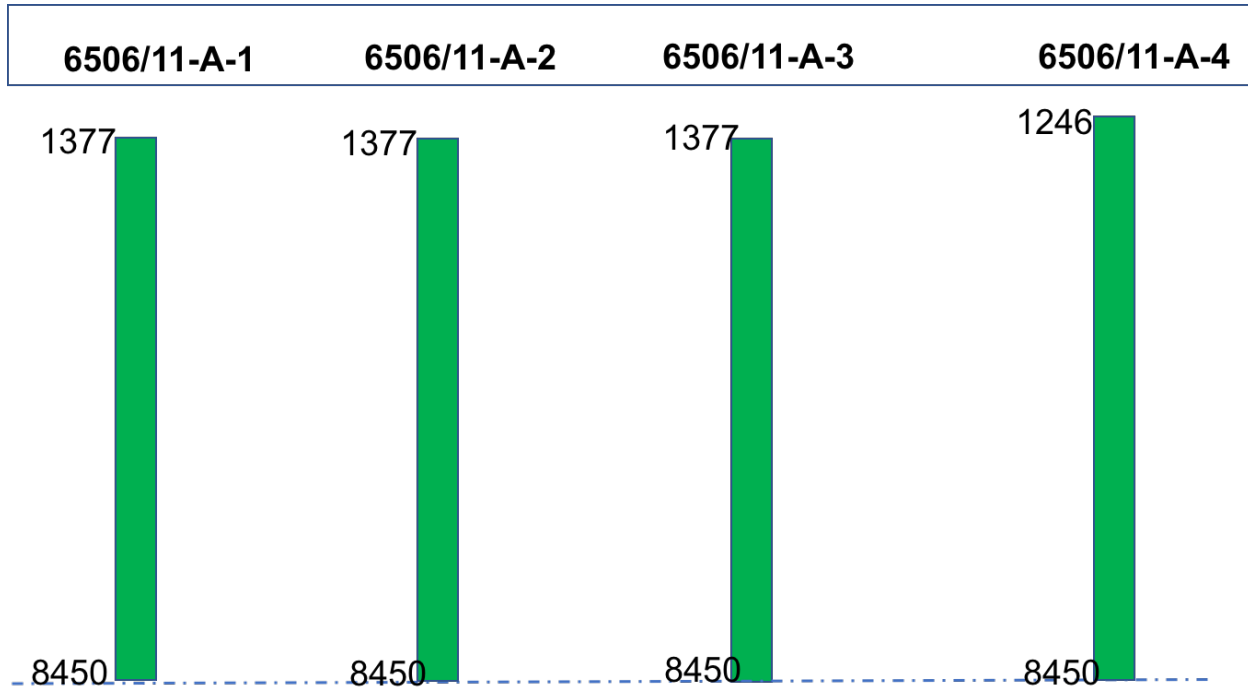
Figure 5.10: Illustration of "Same well depth from the mudline".

Table 5.3 provides the value of the regression coefficients and the results are plotted in Figure 5.12 to 5.15

Table 5.3: Same well depth from mudline - Regression coefficient values.

Well	C_0	C_1	C_2	C_3	C_4	C_5	C_6	R^2
6506/11-A-1	234.328	0.001	0.005	-0.142	-0.342	-0.170	28.615	0.605
6506/11-A-2	-41.376	-0.001	0.005	0.270	33.460	-0.128	-60.739	0.728
6506/11-A-3	-211.664	-0.002	-0.002	0.478	32.210	0.105	-141.171	0.553
6506/11-A-4	-235.965	-0.001	0.006	-0.252	9.010	0.135	84.250	0.520

The UCS profiles of the "Same Well Depth From Mudline" are displayed in Figure 5.11. At shallow depths until 2500 ft, all the wells exhibited the same UCS values. One can also observe that until 7000 ft, except for well 6506/11-A-2, the UCS profiles seem nearly equivalent and deviates afterward. On the other hand, well 6506/11-A-2 shows a stronger UCS between 2500 ft - 7000 ft. The strength reduces afterward. Remember that the calculation results depend on the measured drilling parameters in each well.
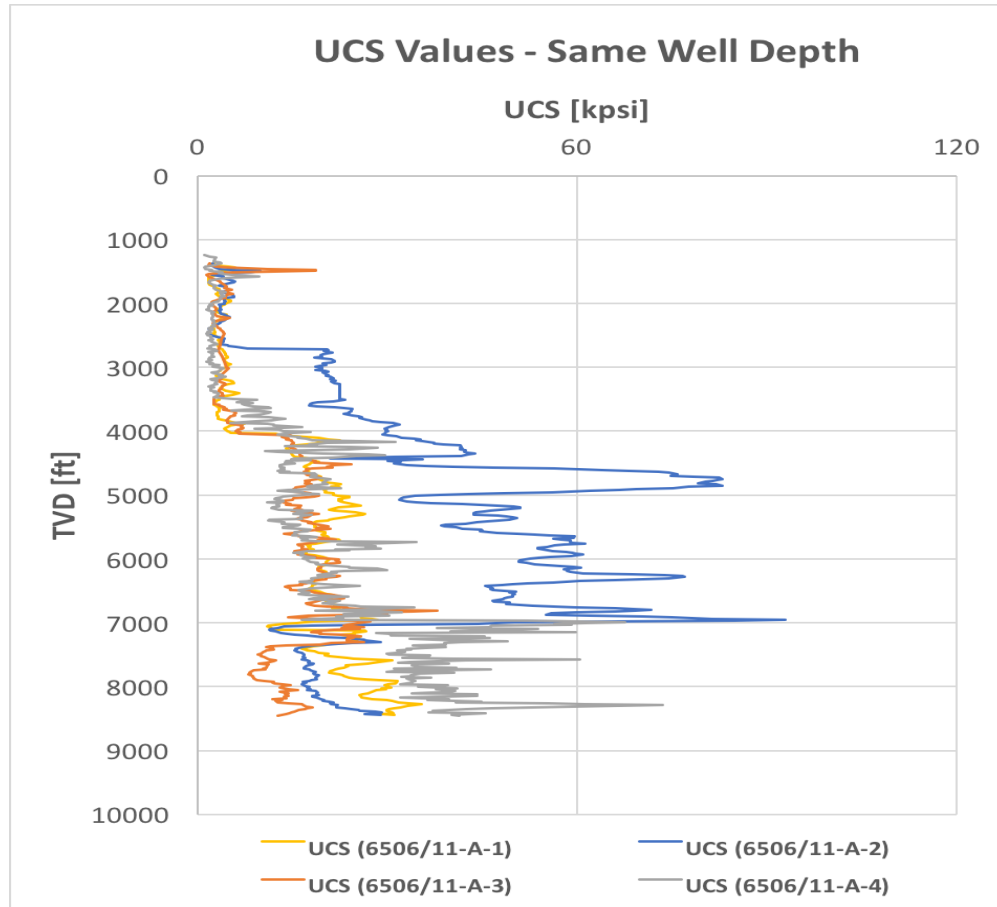
Figure 5.11: Same well depth from mudline - UCS values.

Testing coefficients from nearby and far-away wells

The ROP results obtained by implementing the nearby and far-away coefficient values on each well are plotted in Figure 5.12 - 5.15.
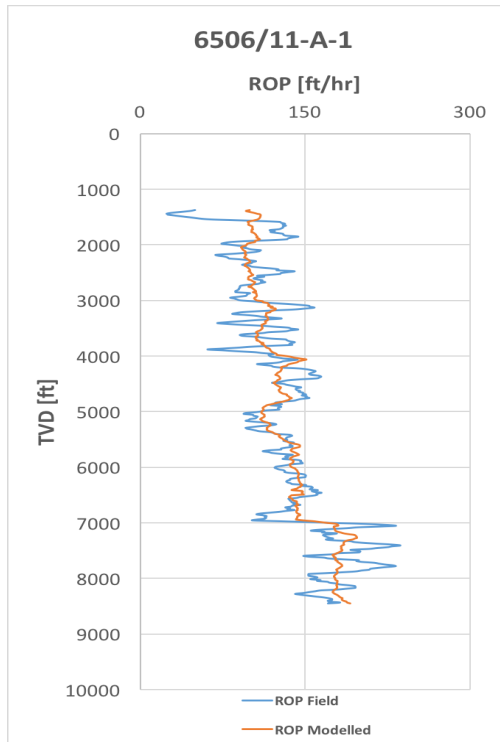
(a) 6506/11-A-1 regression coeff. on itself.
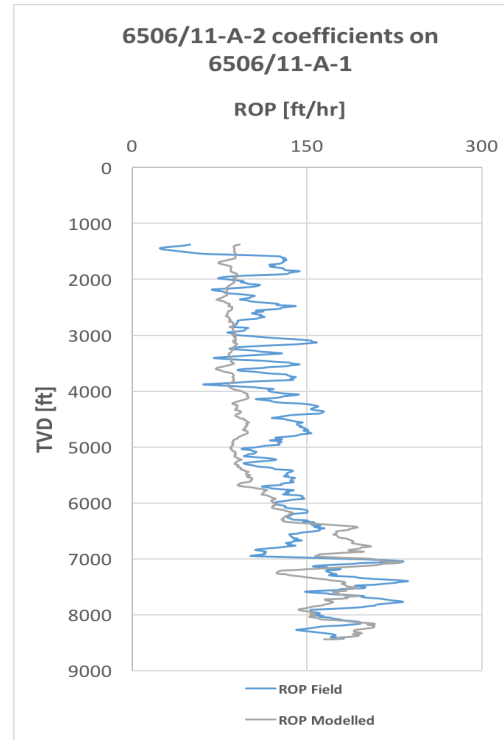
(b) 6506/11-A-2 regression coeff. applied on 6506/11-A-1
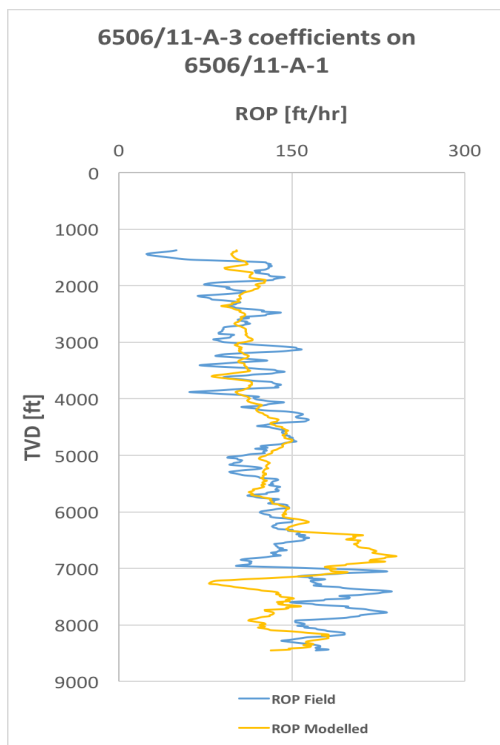
(c) 6506/11-A-3 regression coeff. applied on 6506/11-A-1
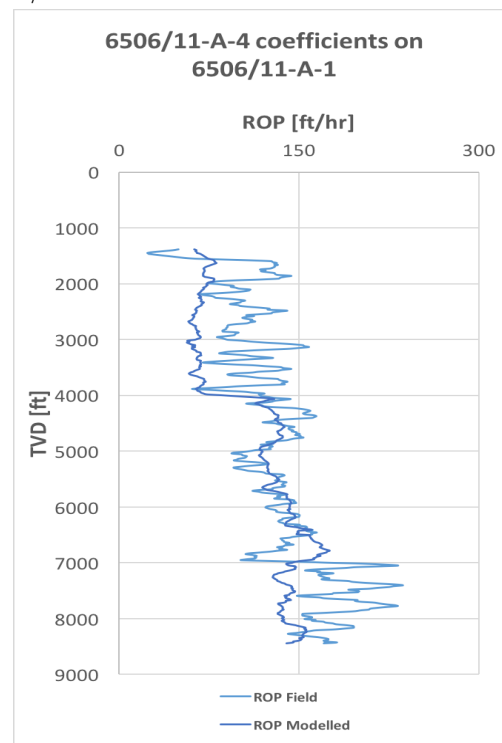
(d) 6506/11-A-3 regression coeff. applied on 6506/11-A-1

Figure 5.12: Same well depth from mudline - 6506/11-A-1.
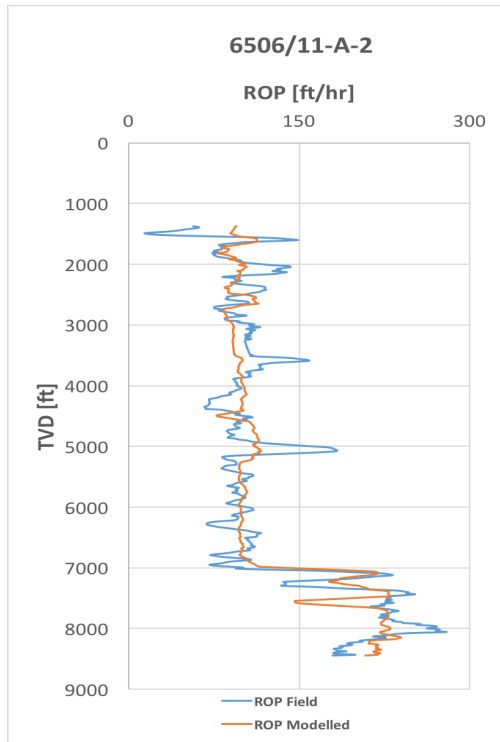
(a) 6506/11-A-2 regression coeff. on itself
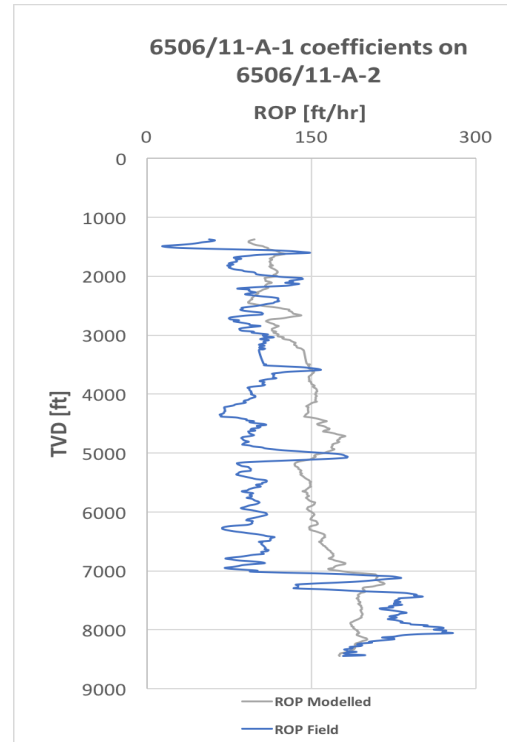
(b) 6506/11-A-1 regression coeff. applied on 6506/11-A-2
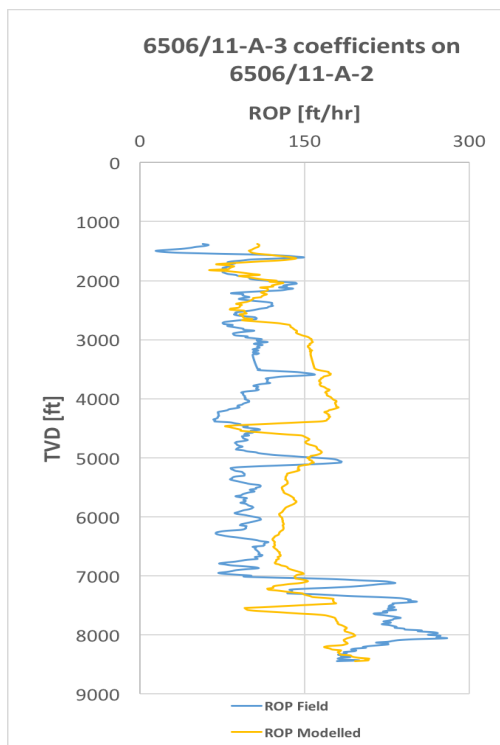
(c) 6506/11-A-2 regression coeff. applied on 6506/11-A-2
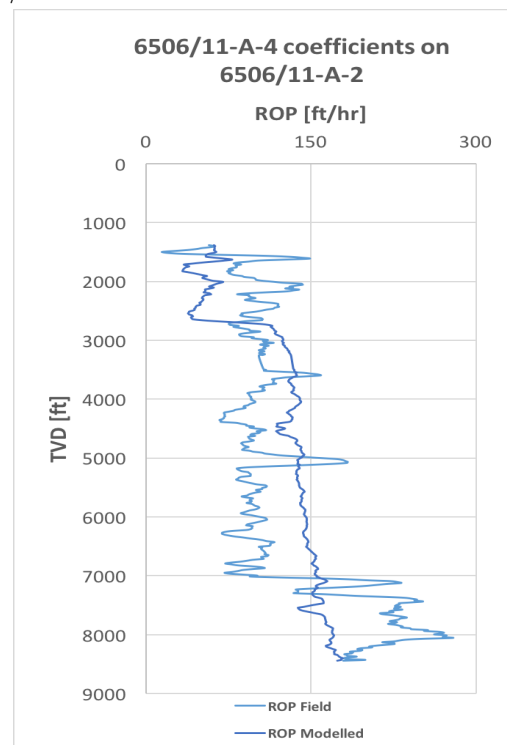
(d) 6506/11-A-4 regression coeff. applied on 6506/11-A-2

Figure 5.13: Same well depth from mudline - 6506/11-A-2.
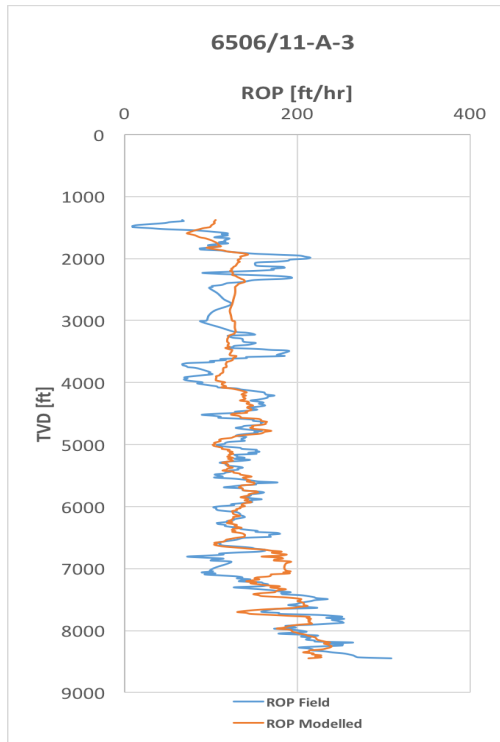
(a) 6506/11-A-3 regression coeff. on itself
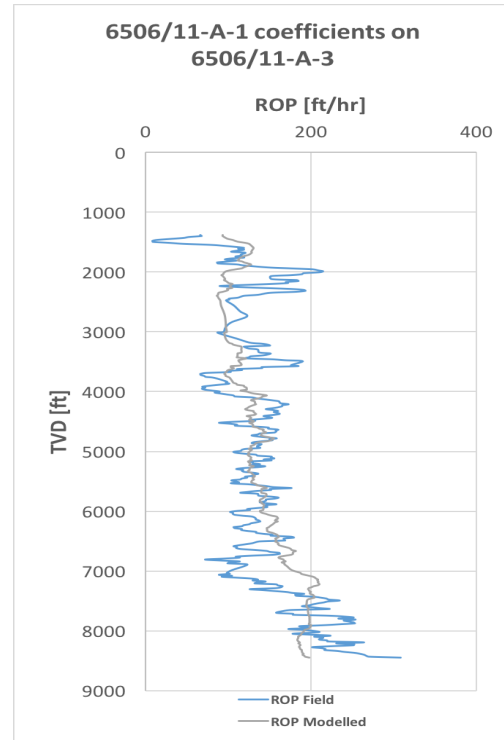
(b) 6506/11-A-1 regression coeff. applied on 6506/11-A-3
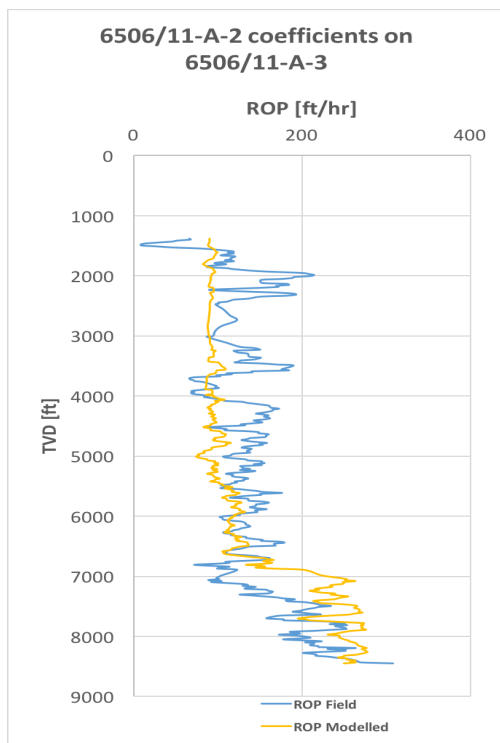
(c) 6506/11-A-2 regression coeff. applied on 6506/11-A-3
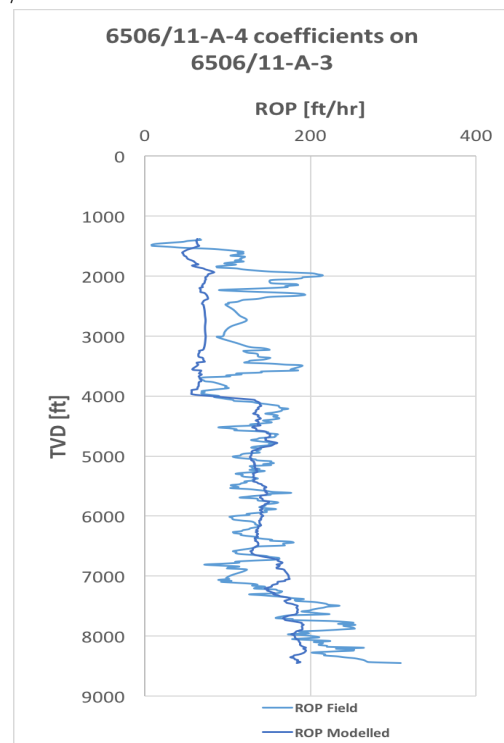
(d) 6506/11-A-4 regression coeff. applied on 6506/11-A-3

Figure 5.14: Same well depth from mudline - 6506/11-A-3.
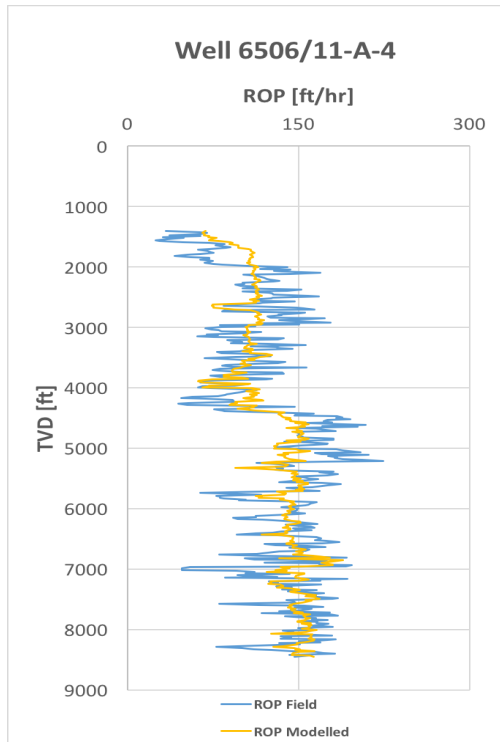
(a) 6506/11-A-4 regression coeff. on itself
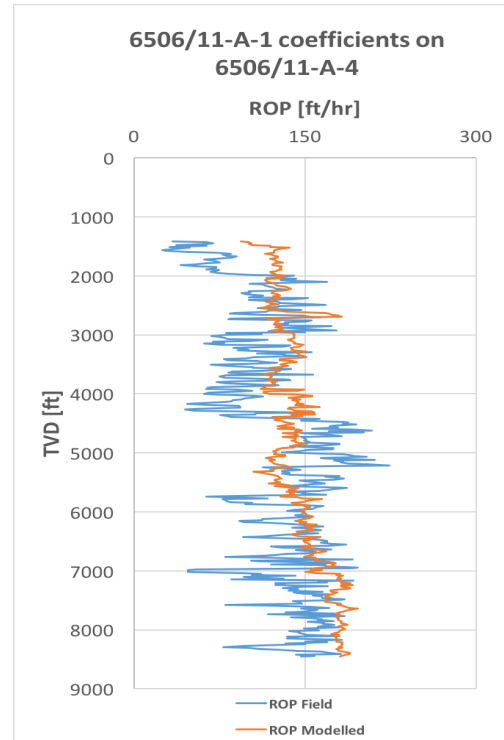
(b) 6506/11-A-1 regression coeff. applied on 6506/11-A-4
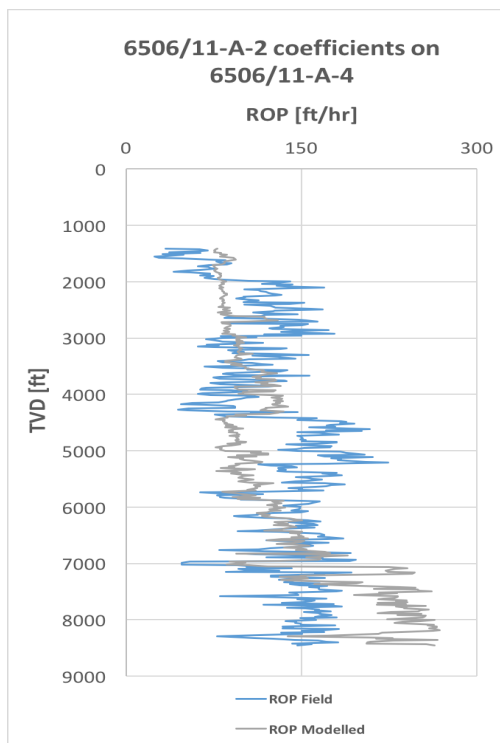
(c) 6506/11-A-2 regression coeff. applied on 6506/11-A-4
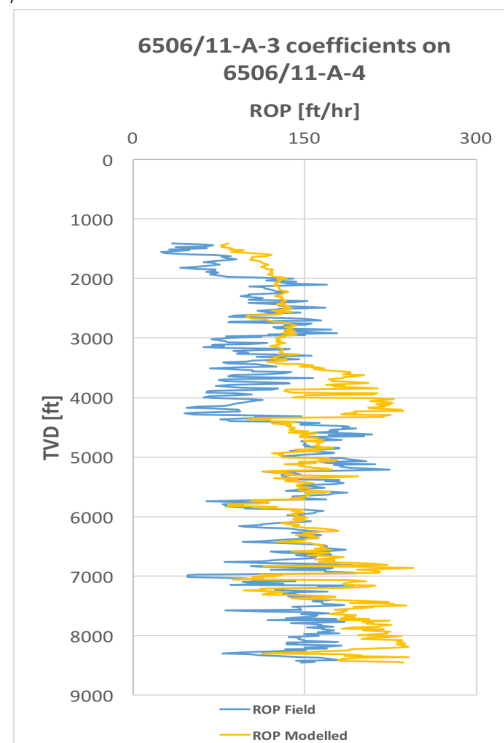
(d) 6506/11-A-3 regression coeff. applied on 6506/11-A-4

Figure 5.15: Same well depth from mudline - 6506/11-A-4.

Figure 5.12 shows the application of the model derived from well 6506/11-A-1 on its own and on distance wells (6506/11-A-2, A-3 and A-4). The prediction seems quite well, but not perfect. However, it is interesting to observe that the same depth based modelling application on the nearby wells show better prediction compared with the entire well data based modelling presented in chapter 5.1.2

Similarly, the testing of well 6506/11-A-2 on its own and far distance wells (6506/11-A-1, A-3, A-4) demonstrated nearly the same performance. In general, one can observe the poor quality of the data sets that show several spikes, which could be associated with torsional or axial vibrations. Therefore, the model predictions based on the considered dataset (entire well or same depth) estimate without capturing the details. This suggest in developing a new modelling scenario called drilling ahead based modelling. The main reason was that as shown in the model application, the models predict best when applying on its own well.

5.1.4   Drilling Ahead ROP Prediction Scenario

The most important question here is how can we apply the modelling approach for practical design and analysis purposes. The idea of this scenario is to continuously model and predict the ROP. From the model, one can obtain the highly ROP dominating drilling parameters in order to optimize them and hence increase ROP. For this, only two wells have been considered for modelling as sketched in Figure 5.16. During modelling, the limitation and the reliability of the concept for predicting ROP ahead of the drilling will be investigated. In this scenario, four different data points will be considered to model well 6506/11-A-1 and 6506/11-A-4. In Figure 5.16 the red area of the well is already modelled. Based on the coefficients generated from Multiple regression model, the coefficients are implemented in the green area, and ROP is modelled for the rest of the well.

Figure 5.16: Illustration of "Drilling Ahead ROP Prediction Scenario".

1. Well 6506/11-A-1

First, the model approach is tested for well 6506/11-A-1 using different numbers of observation points (OP). Figure 5.17 represents the results when ROP is predicted. Table 5.4 provides the value of the regression coefficients.

Table 5.4: Drilling Ahead ROP Prediction Scenario - 6506/11-A-1 coefficient values.

Model	C_0	C_1	C_2	C_3	C_4	C_5	C_6	R^2	OP
100 % Data	151.272	-0.002	-0.013	0.632	9.318	-0.114	68.29	0.625	792
90.7 % Data	170.727	-0.002	-0.010	0.685	9.676	-0.115	31.282	0.549	719
87.3 % Data	169.824	-0.002	-0.010	0.692	9.970	-0.117	30.589	0.516	692
75 % Data	184.866	-0.002	-0.003	0.887	19.273	-0.155	-78.664	0.464	592
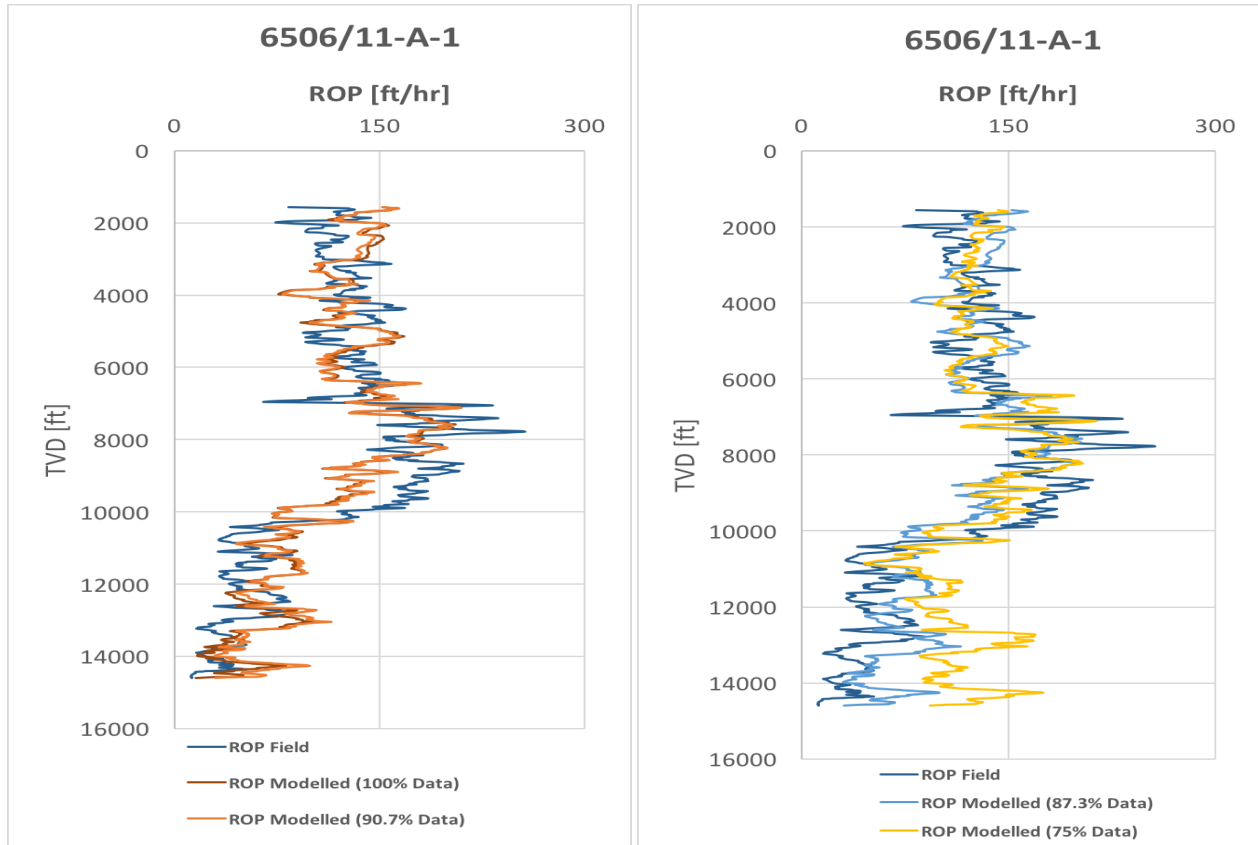
Figure 5.17: Drilling Ahead ROP Prediction Scenario - 6506/11-A-1.

Based on the results in the figure above, the correlation between field ROP and the modelled ROP is greater, the more observation points. For example in the model where $90.7\,\%$ of the data points are used, the correlation is greater than for the case with $75.0\,\%$ of the data points.

2. Well 6506/11-A-4

Secondly, the model approach is tested on well 6506/11-A-4 using different numbers of observation points (OP). Figure 5.5 represents the result when ROP is predicted. Table 5.5 provides the value of the coefficients and the number of observation points.

Table 5.5: Drilling Ahead ROP Prediction Scenario - 6506/11-A-4 coefficient values.

Model	C_0	C_1	C_2	C_3	C_4	C_5	C_6	R^2	OP
100 % Data	151.272	-0.002	-0.013	0.632	9.318	-0.114	68.29	0.625	792
90.7 % Data	170.727	-0.002	-0.010	0.685	9.676	-0.115	31.282	0.549	719
87.3 % Data	169.824	-0.002	-0.010	0.692	9.970	-0.117	30.589	0.516	692
75 % Data	184.866	-0.002	-0.003	0.887	19.273	-0.155	-78.664	0.464	592
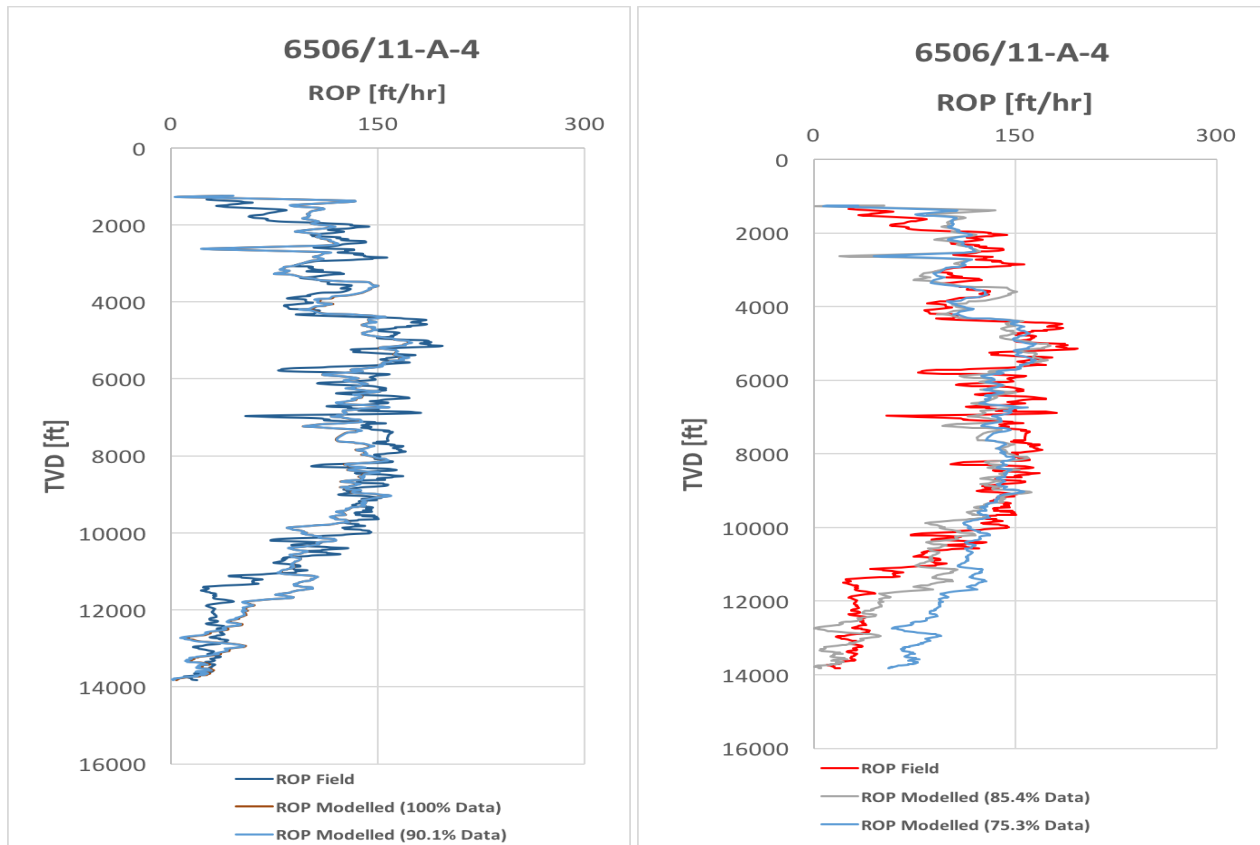
Figure 5.18: Drilling Ahead ROP Prediction Scenario - 6506/11-A-4.

The second model yields the same results as well 6506/11-A-1. The more observation points, the higher correlation between the modelled and field ROP. From the studies, one can observe the prediction works best when 90 % of the dataset is used for modelling and the application is limited to 10 % of drilling ahead.

5.1.5   Section by Section Scenario

In general, the modelling results based on entire well modelling and its application showed a quite good prediction as presented in the previous section. In order to minimize the percentile error deviations, this scenario presents section by section based modelling. The drilled sections are 36", 26", 17.5" and 12.25". For comparison purpose, the section by section modelling result is presented with the entire hole section.

Figure 5.19 illustrates a sketch of the wells modelled using "Section by Section". The results show that the Multiple regression model by using section by section match excellent when it is applied on its own well. Figure 5.20 presents the results for the four wells.
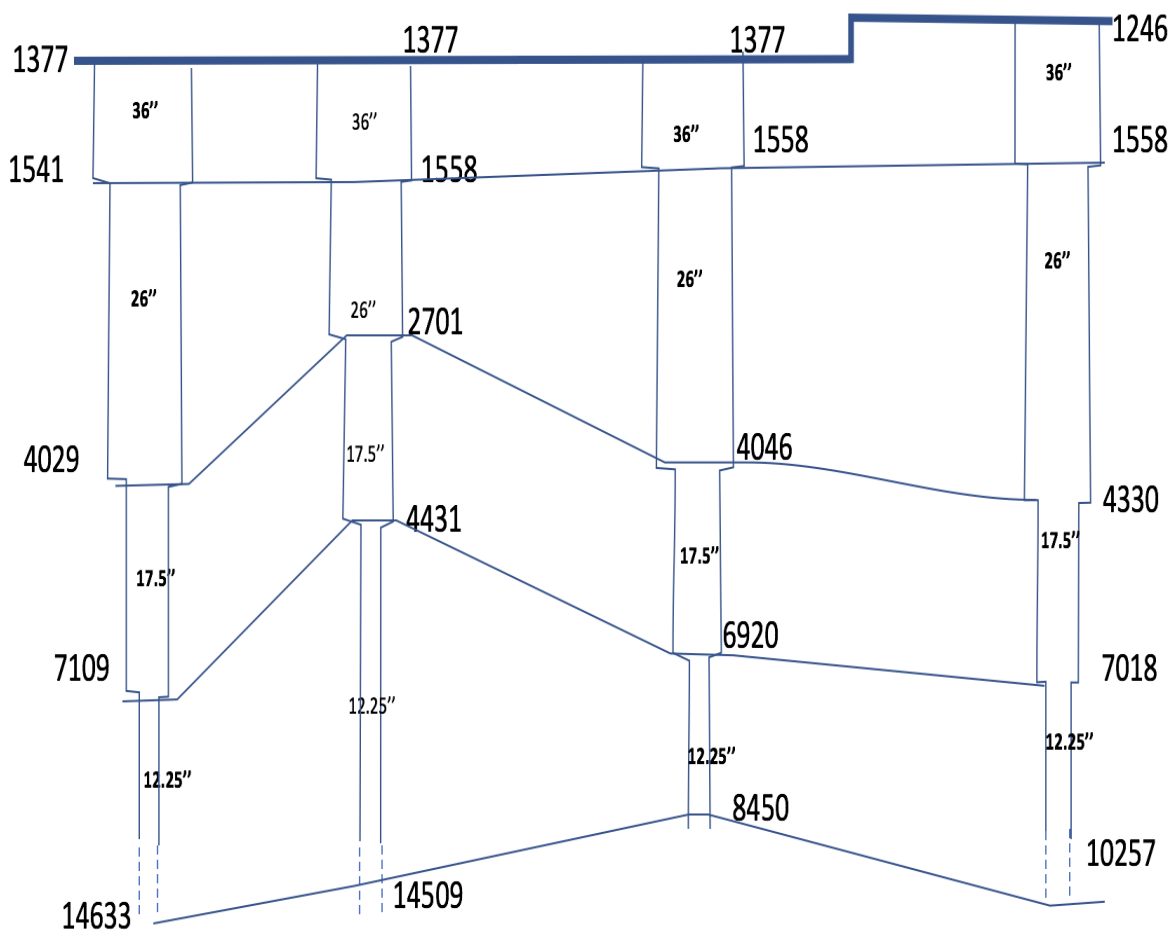
Figure 5.19: Illustration of "Section by section scenario".

Table 5.6: Section by section - 6506/11-A-1 coefficient values.

Section	C_0	C_1	C_2	C_3	C_4	C_5	C_6	R^2
36"	1706.493	-0.008	0.011	0.525	0	1.742	0	0.970
26"	-687.472	0.002	-0.007	1.095	89.881	-0.018	-39.144	0.646
17.5"	1097.755	0.004	0.007	0.204	17.002	-0.538	-363.847	0.701
12.25"	3180.788	-0.001	-0.001	0.168	17.763	-0.420	-1683.480	0.880

Table 5.7: Section by section - 6506/11-A-2 coefficient values.

Section	C_0	C_1	C_2	C_3	C_4	C_5	C_6	R^2
36"	-550.903	-0.007	0.042	2.691	0	0.222	0	0.984
26"	617.540	-0.005	0.026	-0.152	0	0.238	-730.472	0.873
17.5"	-1682.185	0.001	0.008	-1.481	234.235	0.083	-209.419	0.378
12.25"	-720.283	0.002	-0.001	-0.095	65.723	0.309	2.295	0.763

Table 5.8: Section by section - 6506/11-A-3 coefficient values.

Section	C_0	C_1	C_2	C_3	C_4	C_5	C_6	R^2
36"	978.620	-0.007	-0.026	-6.452	0	-0.178	0	0.986
26"	864.150	-0.005	0.034	0.599	-52.552	-0.151	-305.878	0.428
17.5"	621.417	0.002	-0.004	0.714	49.836	0.055	-741.234	0.525
12.25"	-2620.787	0.001	0.062	-0.947	25.322	0.166	1011.350	0.858

Table 5.9: Section by section - 6506/11-A-4 coefficient values.

Section	C_0	C_1	C_2	C_3	C_4	C_5	C_6	R^2
36"	-30.892	0.007	-0.018	0.722	10.409	-0.038	0	0.968
26"	-477.802	-0.003	0.004	-0.062	75.446	0.014	-51.679	0.446
17.5"	-452.742	0.001	0.002	-0.386	22.542	0.433	64.956	0.593
12.25"	160.161	0.001	-0.008	0.267	6.501	-0.098	22.822	0.531
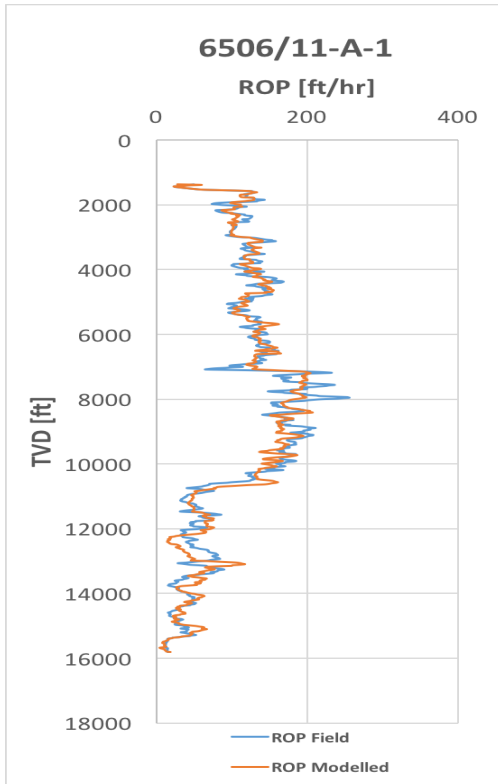
(a) 6506/11-A-1
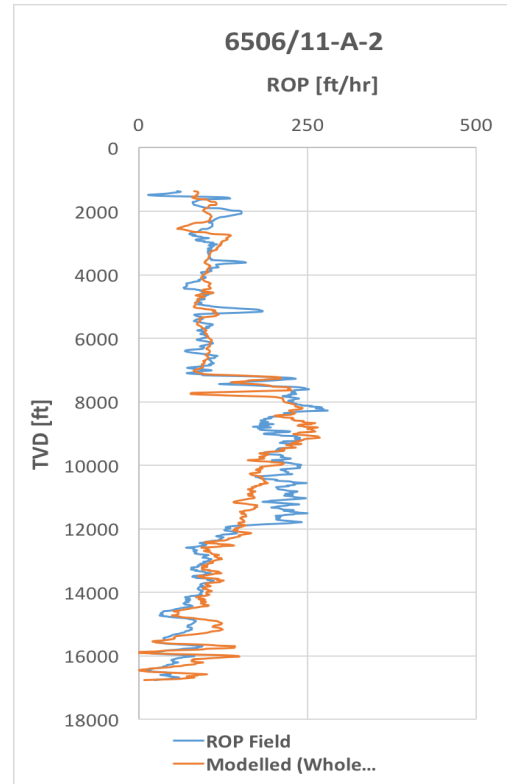
(b) 6506/11-A-2
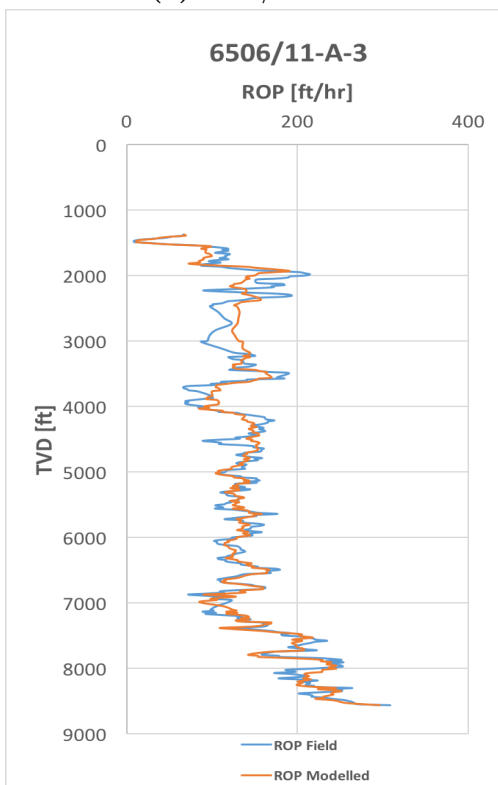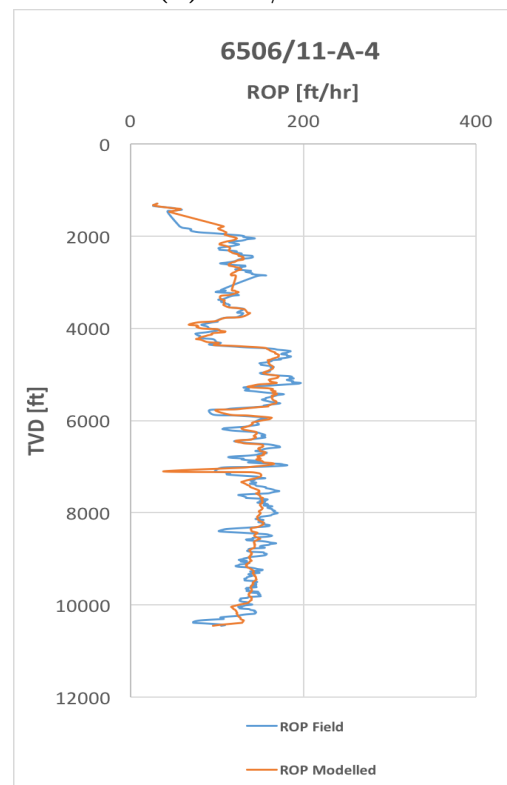
(c) 6506/11-A-3

(d) 6506/11-A-4

Figure 5.20: Section by section modelling results.

5.1.6 Geological Groups Scenario

In this modelling approach, all the wells will be modelled by regression coefficients extracted from each lateral geological group. However, due to the provided well report doesn't cover all the geological groups of the wells, this modelling approach is only implemented on geological groups that cover the given drilling dataset. Table 5.10 - 5.13 provides the regression coefficient values for geological groups of the different wells. In Figure 5.21 the results are illustrated.

As shown in the tables, the modelling R^2 values indicate good correlations. The results displayed in Figure 5.21 show a very good match between the model predictions and the measured ROPs. The results show that the geological groups based modelling scenario is better than the entire well data based modelling.

Table 5.10: Geological Groups - Regression coefficient values from 6506/11-A-1.

Well 6506/11-A-1								
Geo. Groups	C_0	C_1	C_2	C_3	C_4	C_5	C_6	R^2
Nordaland Gr.	33.424	0.002	0.008	-0.547	-0.660	0.239	-135.447	0.939
Hordaland Gr.	-2416.160	0.002	-0.001	1.614	17.020	-0.089	1376.243	0.939
Rogaland Gr.	-1599.056	0.006	-0.025	-3.387	42.863	1.382	481.222	0.913
Shetland Gr.	3458.036	-0.003	0.012	-0.109	0.155	0.476	-1761.236	0.885
Cromer Knoll Gr.	1015.939	0.001	-0.004	-0.100	15.576	-0.190	-506.013	0.981

Table 5.11: Geological Groups - Regression coefficient values from 6506/11-A-2.

Well 6506/11-A-2								
Geo. Groups	C_0	C_1	C_2	C_3	C_4	C_5	C_6	R^2
Hordaland Gr.	-6963.215	0.001	-0.009	-12.520	-44.591	3.336	3558.822	1
Rogaland Gr.	36464.453	-0.001	0.039	1.243	29.603	-40.778	-2865.695	0.943
Shetland Gr.	3970.562	0.007	-0.015	-0.037	39.022	-0.493	-2121.362	0.429
Cromer Knoll Gr.	-16.239	0.001	0.001	-0.210	27.140	0.338	-273.279	0.935

Table 5.12: Geological Groups - Regression coefficient values from 6506/11-A-3.

Well 6506/11-A-3								
Geo. Groups	C_0	C_1	C_2	C_3	C_4	C_5	C_6	R^2
Hordaland Gr.	-2528.383	0.005	0.008	-4.714	20.140	0.147	1040.791	0.999
Rogaland Gr.	-10435.953	0.001	0.032	-0.492	34.608	0.347	5640.873	0.979
Shetland Gr.	1008.025	-0.002	0.053	-0.268	11.424	-0.030	-893.068	0.712

Table 5.13: Geological Groups - Regression coefficient values from 6506/11-A-4.

Well 6506/11-A-4								
Geo. Groups	C_0	C_1	C_2	C_3	C_4	C_5	C_6	R^2
Rogaland Gr.	379.545	0.002	0.014	0.836	17.410	0.056	0	0.406
Shetland Gr.	253.568	-0.002	0.009	0.450	14.110	-0.469	-39.640	0.571
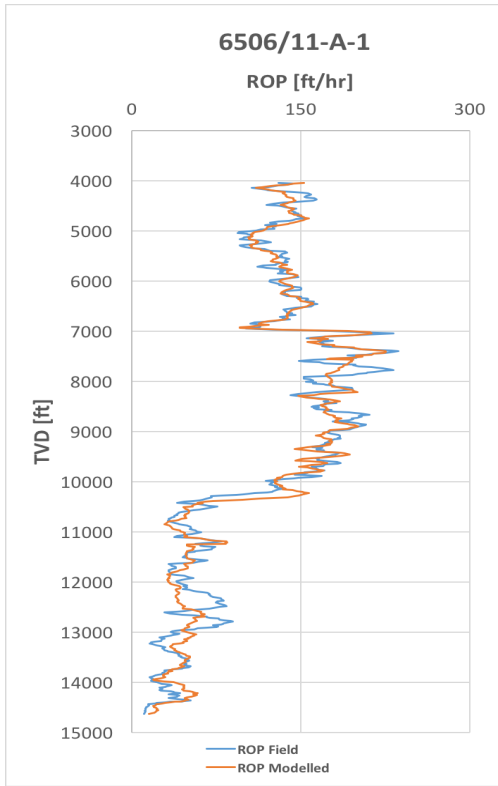
(a) 6506/11-A-1
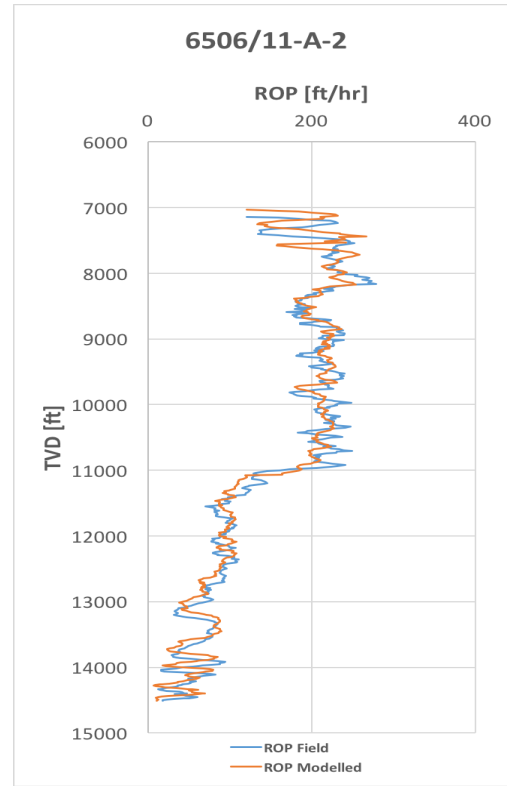
(b) 6506/11-A-2
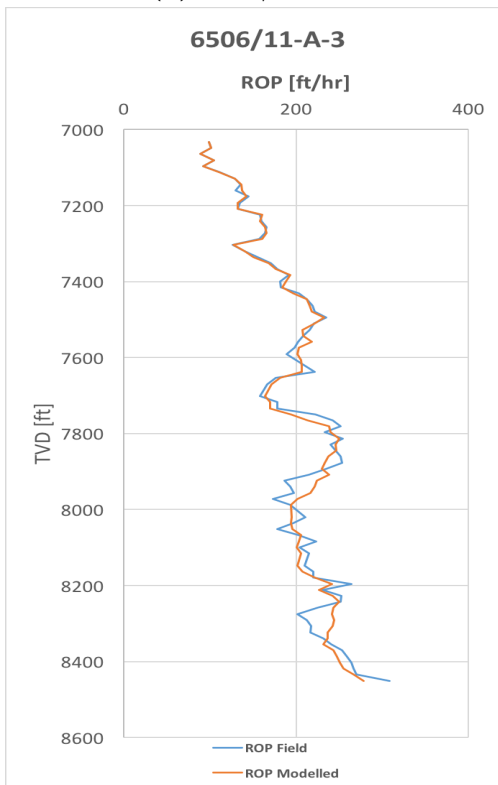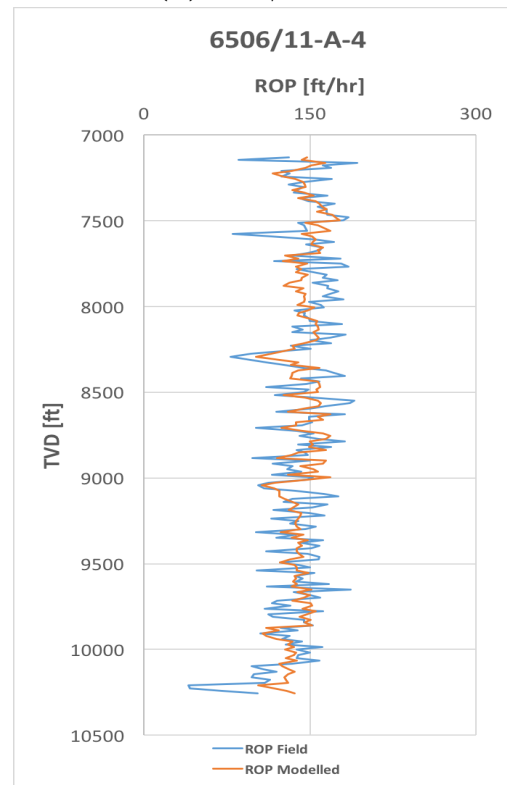
(c) 6506/11-A-3

(d) 6506/11-A-4

Figure 5.21: Geological Groups modelling results.

5.1.7   Drilling Ahead ROP Prediction for Geological Groups

The "Drilling Ahead ROP Prediction Scenario" was examined in chapter 5.1.4. The idea of
the scenario is to continuously model and predict the ROP with the objective of obtaining the
highly dominant drilling parameters and optimize parameters to increase ROP. However, in
this chapter, all the four wells 6506/11-A-1, 6506/11-A-2, 6506/11-A-3 and 6506/11-A-4 have
been considered for modelling with Multiple regression modelling approach. Furthermore,
Drilling Ahead ROP Prediction for geological groups previously showed the model was most
reliable when around 90 % of the data points (red region), were used for modelling. As
illustrated in Figure 5.22, for each of the wells 90 % of the data points for each geological
group is used to predict ROP in 10 % of the modelled depth section (green area), based on
coefficient values generated from the red areas.
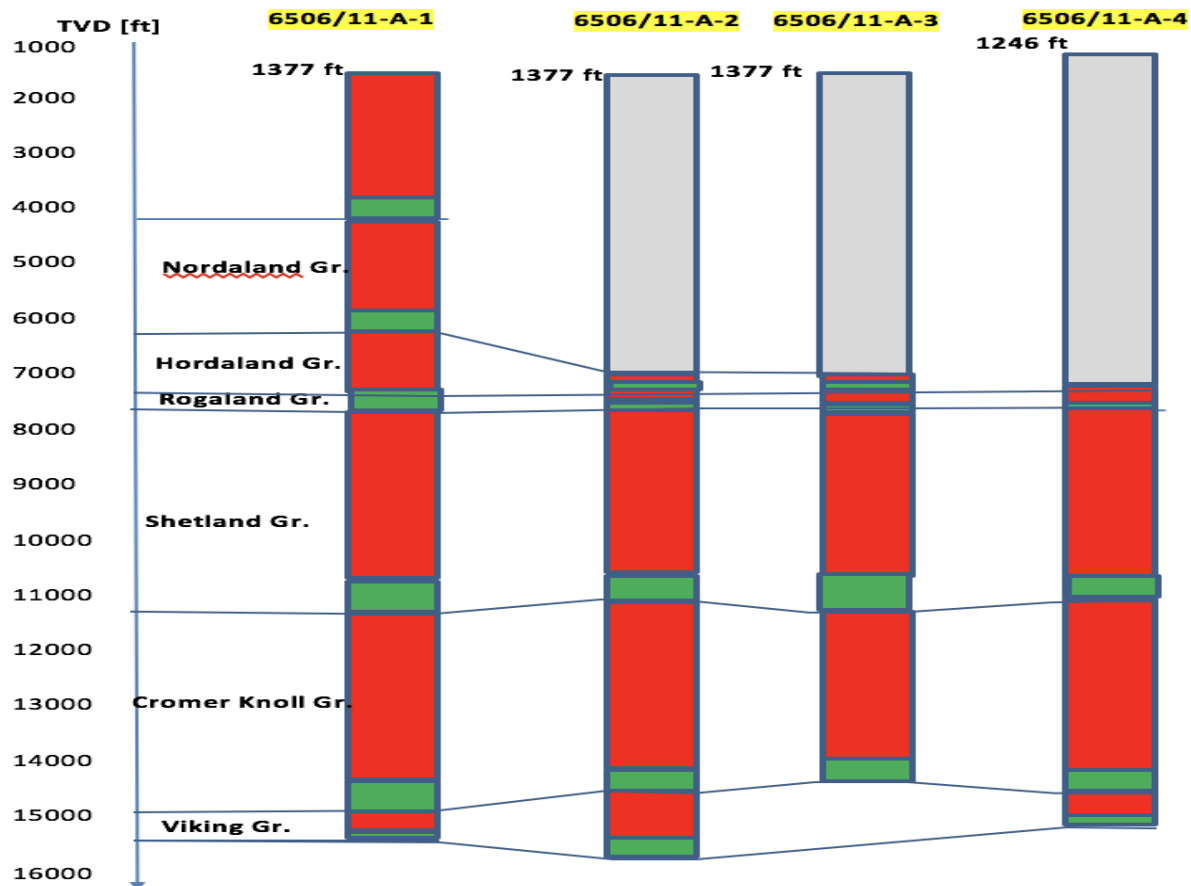
Figure 5.22: Illustration of "Drilling Ahead ROP Prediction" for geological groups.

This modelling approach is very similar to the work done in chapter 5.1.6, except for ROP only being based on the coefficients extracted from 90 % of the data points. In Table 5.14 - 5.17 the regression coefficients values for all four wells are presented and Figure 5.23 displays the comparisons between the models and the measurements.

The results show that 90 % data of geological groups based modelling and application on the 10 % of the data, forecast the measured data perfectly. This indicates the reliability of the modelling approach and can be used in real-time while drilling operations goes on.

Table 5.14: Drilling Ahead ROP Prediction for Geological Groups 6506/11-A-1 regression coeff. values.

Well 6506/11-A-1							
Geo. Groups	C_0	C_1	C_2	C_3	C_4	C_5	C_6
Nordaland Group	20.999	0.002	0.007	-0.763	-10.623	0.289	-78.687
Hordaland Group	-2237.047	0.002	-0.006	1.181	17.167	-0.070	1334.217
Rogaland Group	-506.712	0.008	-0.027	-4.705	51.529	0.749	183.849
Shetland Group	3604.634	-0.003	0.015	-0.205	-3.407	-0.535	-1801.527
Cromer Knoll Group	674.636	0	-0.001	0.022	8.492	-0.118	-333.427

Table 5.15: Drilling Ahead ROP Prediction for Geological Groups 6506/11-A-2 regression coeff. values.

Well 6506/11-A-2							
Geo. Groups	C_0	C_1	C_2	C_3	C_4	C_5	C_6
Hordaland Group	-2429.315	-0.010	-0.045	-25.433	42.492	5.788	0
Rogaland Group	33594.045	-0.002	0.053	1.279	48.793	-35.456	-3874.747
Shetland Group	1958.537	0.004	-0.009	0.308	27.984	-0.461	-945.204
Cromer Knoll Group	338.072	0.002	-0.004	0.062	38.966	0.145	-440.657

Table 5.16: Drilling Ahead ROP Prediction for Geological Groups 6506/11-A-3 regression coeff. values.

Well 6506/11-A-3							
Geo. Groups	C_0	C_1	C_2	C_3	C_4	C_5	C_6
Hordaland Group	-2797.239	0.005	0.078	-4.201	20.366	0.156	1169.209
Rogaland Group	-9891.379	0.001	0.036	-0.453	39.310	0.311	5275.435
Shetland Group	91.208	0.005	0.012	-0.683	20.634	-0.238	-20.776

Table 5.17: Drilling Ahead ROP Prediction for Geological Groups 6506/11-A-4 regression coeff. values.

Well 6506/11-A-4							
Geo. Groups	C_0	C_1	C_2	C_3	C_4	C_5	C_6
Rogaland Group	-419.254	0.003	0.017	0.282	19.369	0.144	0
Shetland Group	293.259	0.001	0.005	0.172	14.352	-0.411	-37.726
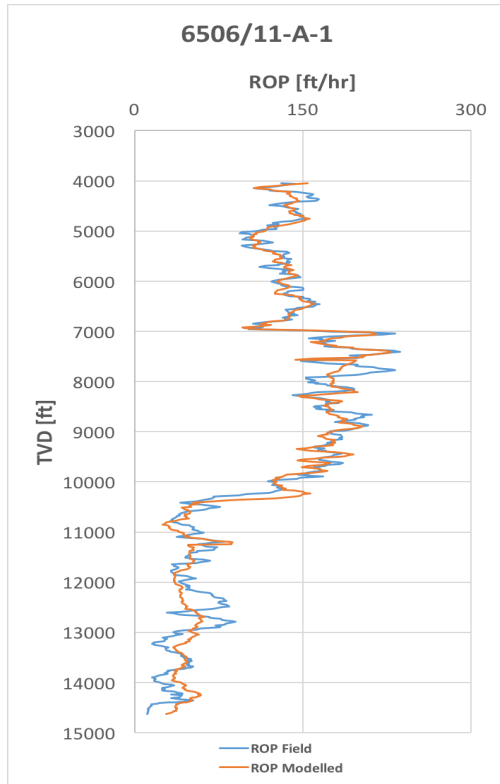
(a) 6506/11-A-1
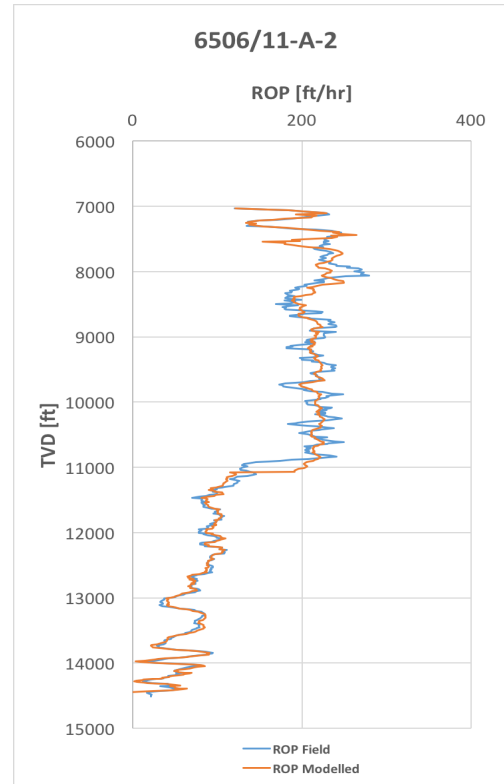
(b) 6506/11-A-2
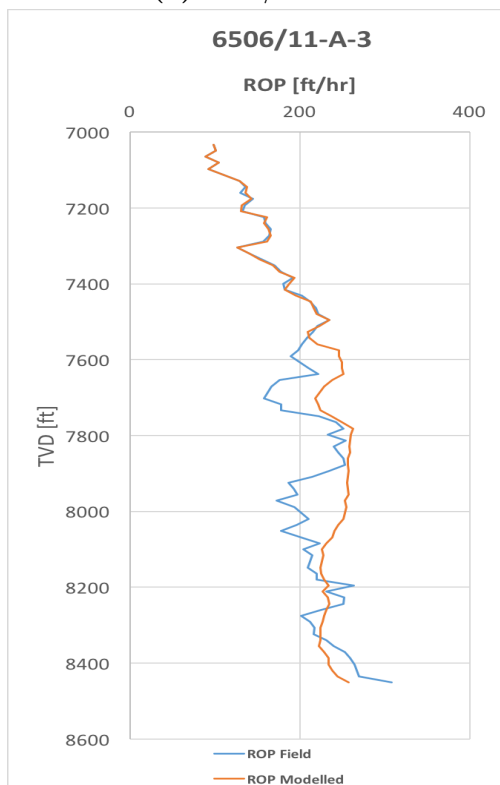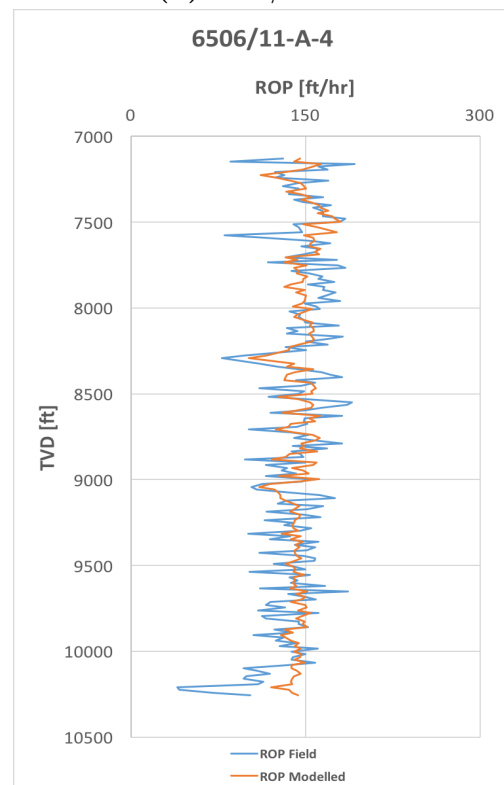
(c) 6506/11-A-3

(d) 6506/11-A-4

Figure 5.23: Drilling Ahead ROP Prediction for geological groups - Using their own regression coeff. values.

5.2   MSE Modelling

The concept of MSE modelling was proposed by Teale in 1965. The model is a function of several drilling parameters such as WOB, Torque and RPM. The MSE model is based on the assumption that the amount of energy required to drill a certain volume of rock is correlative for the nearby and far-away wells. However, in reality this correlation between the wells creates inaccuracy when applying this model and is invalid when applied on remote wells. This is a result of MSE being a function of compressive strength and geostatic pressure, these values vary within the wells.

The modelling technique in this section is based on the MSE workflow presented in Chapter 4.1 and the final results are presented in subfigures in Figure 5.25. Note that the TVD is correlated for TVD of each depth of each well, therefore the resulting plots doesn't yield the same TVD for all cases.

In Figure 5.24 all the UCS values are plotted against each other as a function of TVD (ft). All the wells show promising correlations in the shallowest section. However, as the depth increases well 6506/11-A-2 deviates from the other wells. This is an indication that the wells have very similar lateral geology, and well 6506/11-A-2 exhibited relatively stronger mechanical strength within 2500 ft - 7000 ft compared to the other wells. Moreover, well 6506/11-A-4 differs from the other wells as we exceed 7000 ft because UCS increases rapidly.

Figure 5.24: Computed UCS values for the four wells.

(a) 6506/11-A-1

(b) 6506/11-A-2

(c) 6506/11-A-3

(d) 6506/11-A-4

Figure 5.25: MSE modelling results.

When UCS values from well 6506/11-A-2, 6506/11-A-3 and 6506/11-A-4 are applied on 6506/11-A-1, the results are showed in subfigure 5.25a. The modelled ROPs correlates fairly with the filtered ROP. The model wit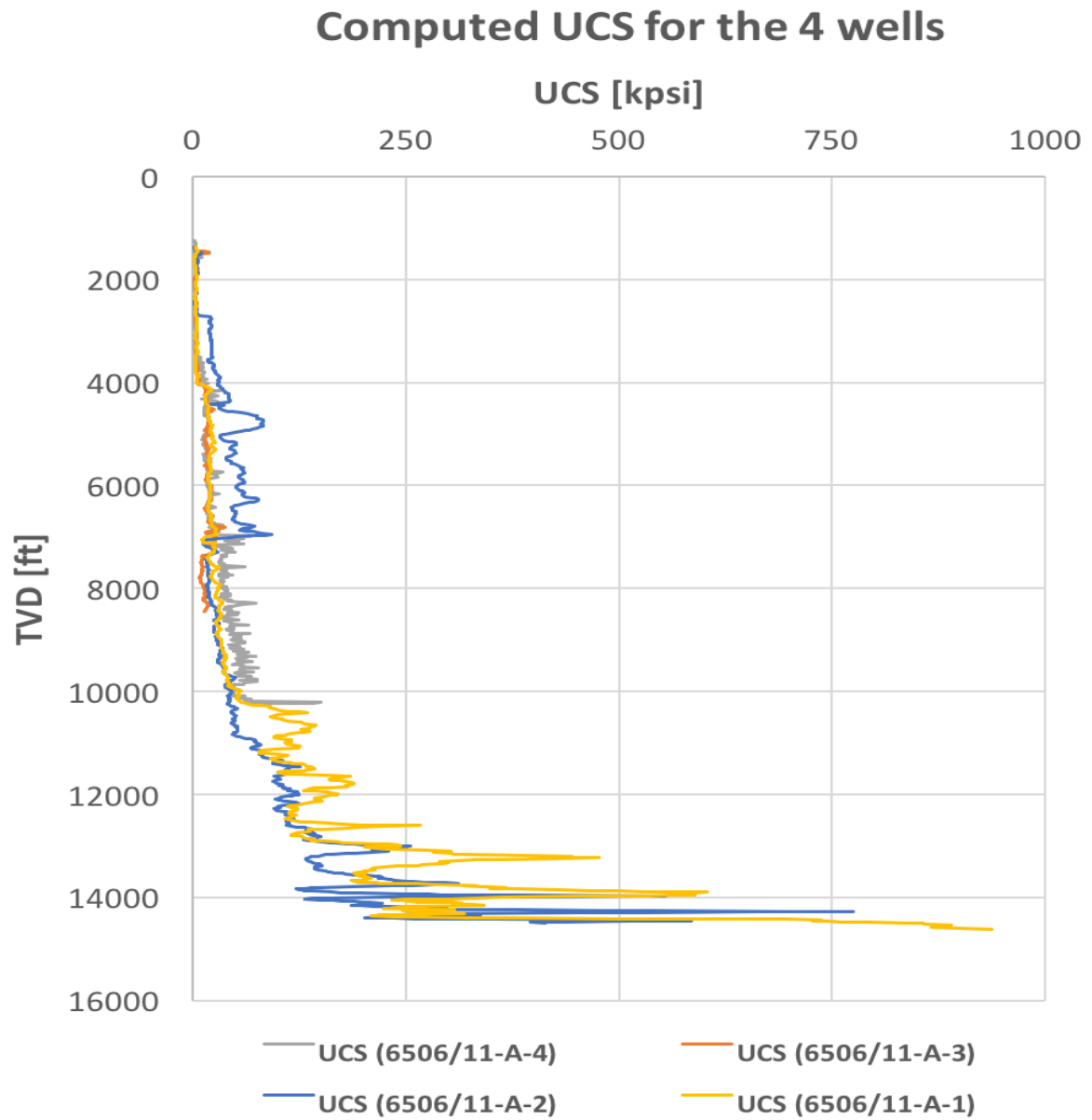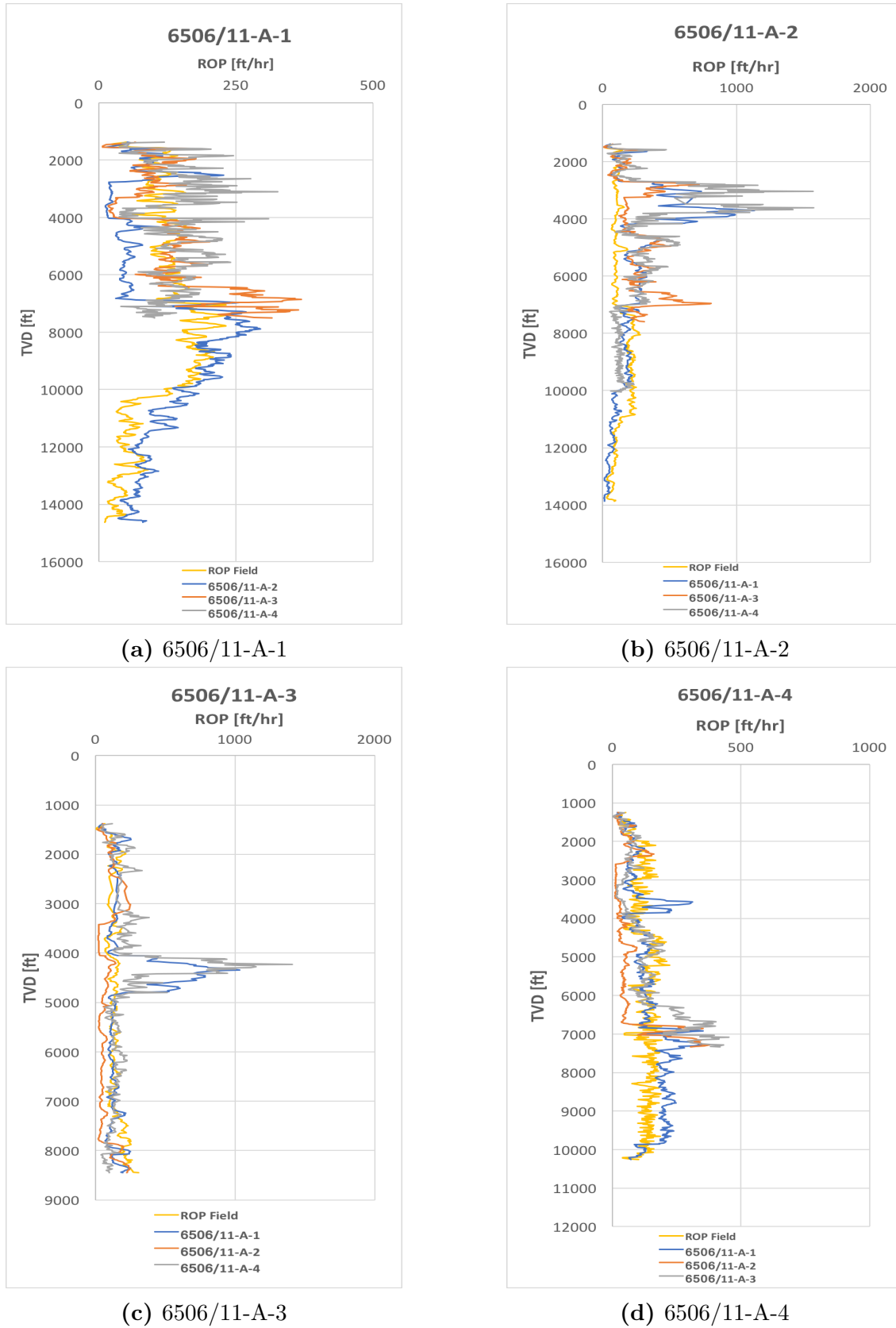h UCS values from 6506/11-A-2 underestimates the ROP in the depth of 1377 ft - 7000 ft, before catching the filtered ROP.

The MSE model with UCS values from well 6506/11-A-1, 6506/11-A-3 and 6506/11-A-4 applied on 6506/11-A-2 is shown in subfigure 5.25b. When applying UCS values from the other wells, well 6506/11-A-3 has the most similar lateral geological features and is most correlative. UCS values from well 6506/11-A-1 and 6506/11-A-4 overestimates penetration rates in the depth of 2400 ft - 2900 ft, meaning there is different geology in this depth sections.

In subfigure 5.25b the MSE model with UCS values from well 6506/11-A-1, 6506/11-A-2 and 6506/11-A-4 applied on 6506/11-A-3 is shown. In this modelling technique, UCS values from well 6506/11-A-2 correlates best with 6506/11-A-3 which confirms geological similarities between the wells. Also in this modelling case well 6506/11-A-1 and 6506/11-A-4 have very high amplitudes at 4000 ft - 5000 ft. However, they correlate decently with the filtered ROP after this depth, indicating the same geological features.

Finally, in the last subfigure 5.25d is well 6506/11-A-4, where nearby and far-away wells values are implemented is illustrated. UCS values from 6506/11-A-2 deviates from the filtered ROP as there are geological differences. Except for a few high amplitudes, the ROP model with UCS values from well 6506/11-A-1 and 6506/11-A-3 correlates fairly with the measured ROP.

5.3   D-exponent Modelling

This chapter will present the results of Drillability exponent, and the results are presented in Figure 5.27. The modelling procedure for D-exp is previously described in Chapter 4.3 (D-Exponent Workflow). In general, the D-exponent is a drilling parameter that gives information about the drillability of the formation.

The drilling exponent increases with the depth of the formation for normally pressurized formations and is proportional to the formation strength. The harder it is to penetrate through the formation, the greater will the D-exp value be. The D-exponent model is built on the assumption that the drillability of the different wells are more correlative, the more lateral geology of the wells are similar.
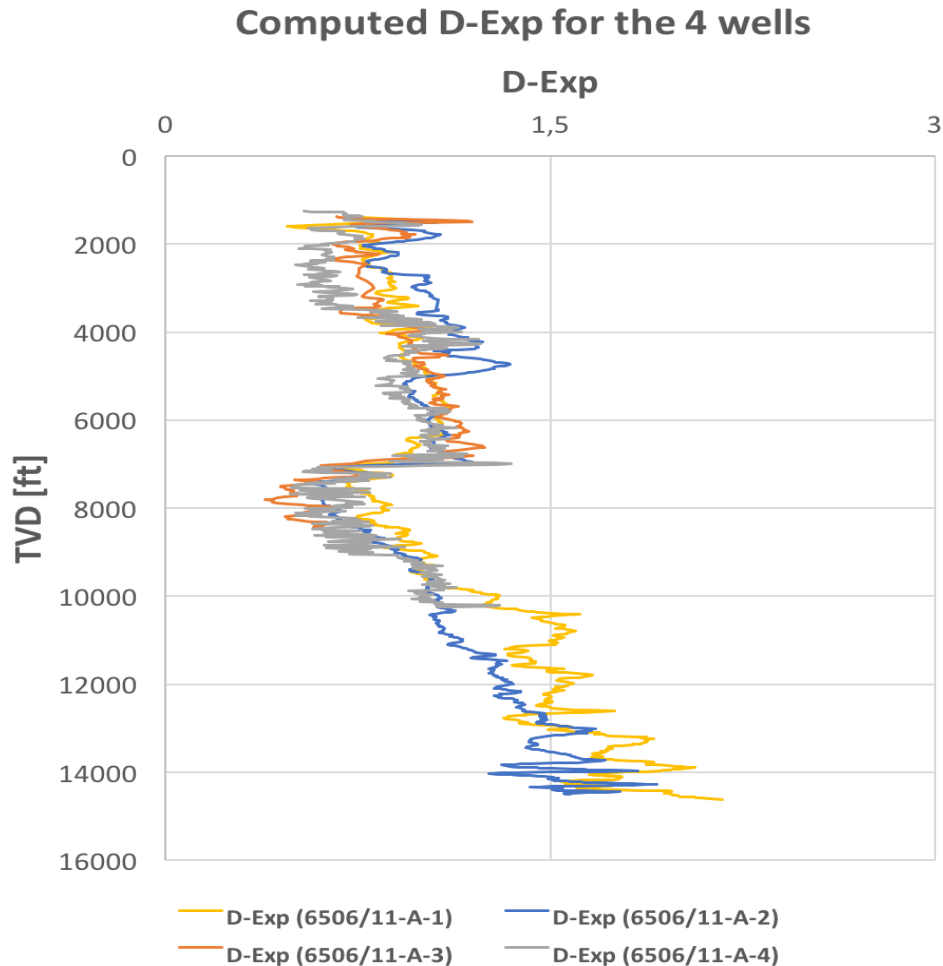
Figure 5.26: Computed D-exponent for the four wells.

By studying Figure 5.26 we observe up to 9000 ft the D-exponent for all the wells are almost similar, meaning the drillabillity of the formations are very similar. Furthermore, by exceeding the vertical depth of 9000 ft, we observe that the D-exponent for well 6506/11-A-1 and 6506/11-A-2 starts to deviate from one and another, as the formation in well 6506/11-A-1 is harder to penetrate through.

(a) 6506/11-A-1

(b) 6506/11-A-2

(c) 6506/11-A-3
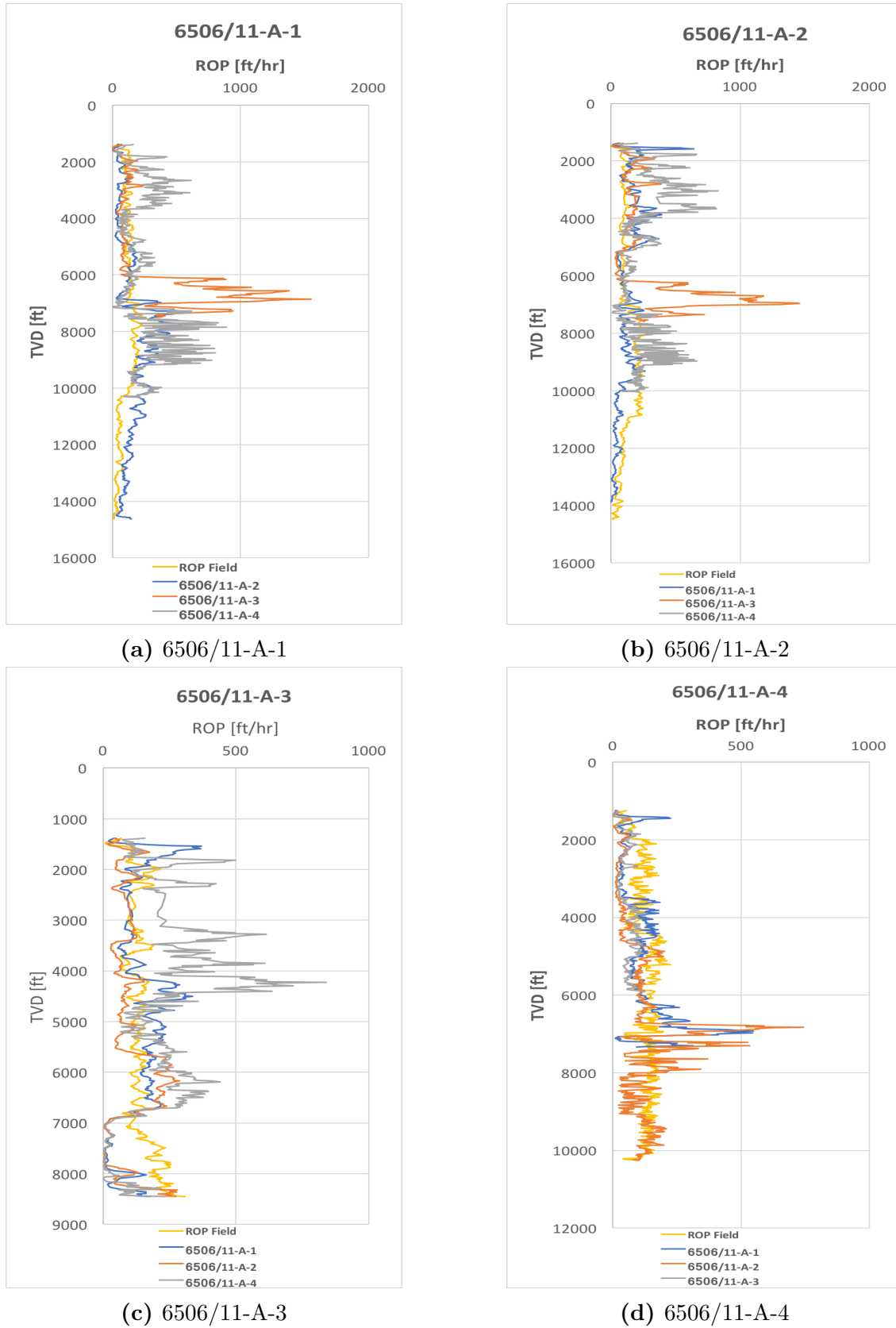
(d) 6506/11-A-4

Figure 5.27: D-exponent modelling results.

In subfigure 5.27a, the D-exponent obtained from well 6506/11-A-2, 6506/11-A-3 and 6506/11-A-4 are substituted into well 6506/11-A-1. The penetration rate is very similar until the drilling reaches the Kai formation in Nordaland group (6000 ft). Initially, well 6506/11-A-3 result is greatly larger than the filtered ROP for well 6506/11-A-1. Well 6506/11-A-4 also deviates from the filtered ROP as we approach Hordaland group at 7800 ft - 8500 ft.

Subfigure 5.27b shows the D-exponent values generated from well 6506/11-A-1, 6506/11-A-3 and 6506/11-A-4 implemented in well 6506/11-A-2. This case is very similar to the first case with well 6506/11-A-1, as well 6506/11-A-3 and 6506/11-A-4 starts to deviate, when we approach Nordaland and Hordaland Groups. Besides that Figure 5.27b shows promising results.

The results of applying the D-exponent values from the other three wells on well 6506/11-A-3 is shown in subfigure 5.27c. Here, the ROP with D-exp from well 6506/11-A-4 is deviating from the filtered ROP for well 6506/11-A-3, showing very high peaks.

In the last subfigure 5.27d, well 6506/11-A-4 is tested with well 6506/11-A-1, 6506/11-A-2 and 6506/11-A-3 drillability exponents. The figure shows good correlation, except for high peaks at approximately 6800 ft for ROPs with D-exponent from well 6506/11-A-1 and 6506/11-A-2. This indicates that for most of the depth sections, the drillability to penetrate through the formations is quite similar.

5.4   Warren Modelling

Warren model is a function of several drilling parameters as stated in equation 3.13 in chapter 3.3. The modelling technique is based on Warrens imperfect-cleaning model. Furthermore, the Warren model constants "a", "b" and "c" are generated using MATLAB. The workflow used modelling the field data is presented in Figure 4.9 in Chapter 4.3.4.
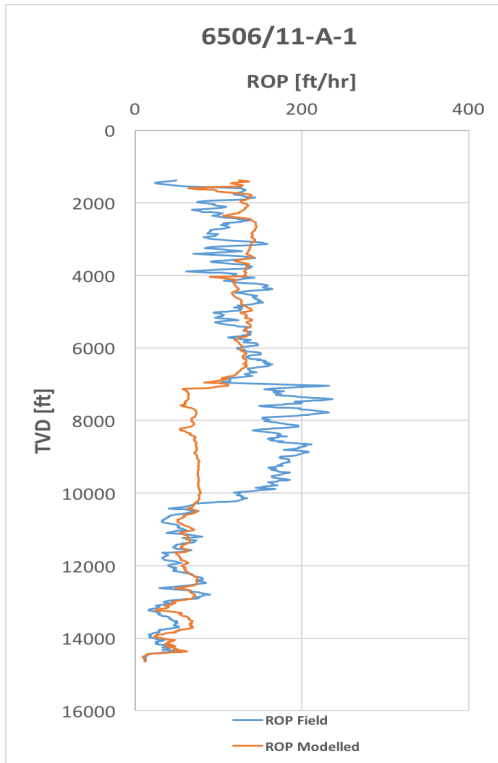
5.4.1   Modelling by Entire Well Data

In this section the wells 6506/11-A-1, 6506/11-A-2, 6506/11-A-3 and 6506/11-A-4 are modelled with Warren constants extracted from each of their well. The ROP results modelled for the wells are presented in Figure 5.28. Warren constants "a", "b" and "c" are shown in Table 5.18.

Figure 5.28 shows the application of Warren model on its own well by using the coefficients presented in Table 5.18. The results show that the model prediction on well 6506/11-A-1 is quite good at the top and bottom part of the well. However, in the middle section, the model deviates from the measurement. On well 6506/11-A-3, the model deviates from the well throughout the drilling depth. Well 6506/11-A-2 and 6506/11-A-4 also show quite big discrepancy between the model and the measurement. The overall results suggest that the entire well data based modelling approach is not good enough when using Warren model. In the next section, the performance of the Warren model on section by section approach will be evaluated.

Table 5.18: Warren Model - Warren constant values for entire well data.

Well	a	b	c
6506/11-A-1	1.364E-05	16.525	4.279E-07
6506/11-A-2	1.169E-05	8.0492	4.996E-07
6506/11-A-3	1.273E-06	16.388	-1.185E-06
6506/11-A-4	0	0	1.521E-06

(a) 6506/11-A-1
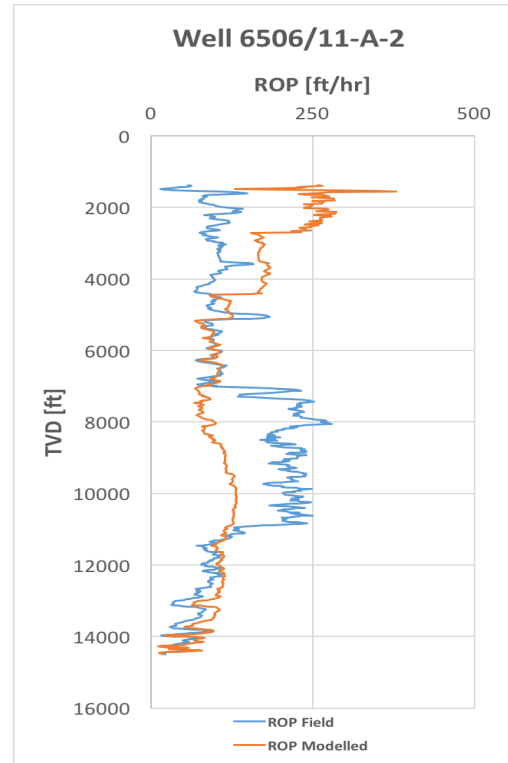
(b) 6506/11-A-2
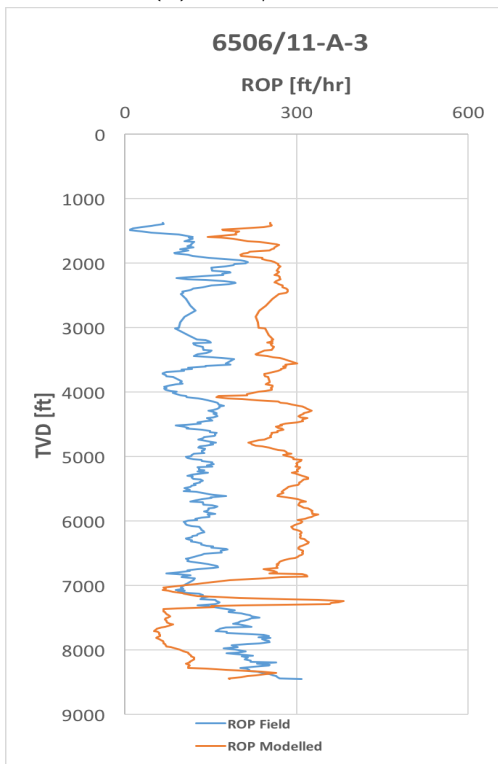
(c) 6506/11-A-3

(d) 6506/11-A-4

Figure 5.28: Warren model - Using their own Warren constant values for entire well data.

5.4.2 Modelling by Hole Sections

In this section the well 6506/11-A-1, 6506/11-A-2, 6506/11-A-3 and 6506/11-A-4 are modelled by correlating the hole sections to the overburden section of the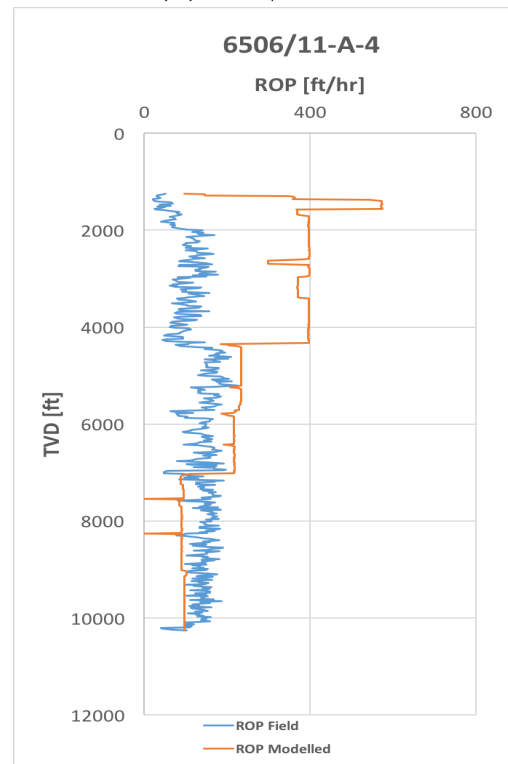 wells, i.e 36", 26", 17,5" and 12,25", respectively. In the first case, the wells are modelled with Warren constants extracted from their own wells. Table 5.19 - 5.22 provides the values for Warren constants and the results are shown in Figure 5.29

When modelling Warren model using section by section approach, the results are better compared to the entire well data approach. However, the model fails to capture some parts of the drilling data. It can be noted that the prediction is not consistent, which may be due to the input parameters.

Table 5.19: Warren Model - Warren constant values for 6506/11-A-1 for hole sections.

Well 6506/11-A-1			
Hole Section	**a**	**b**	**c**
36"	2.313E-04	180.938	-5.159E-05
26"	-4.339E-07	-3.843	6.231E-06
17.5"	6.827E-06	7.568	1.439E-06
12.25"	1.252E-05	-25.939	3.940E-06

Table 5.20: Warren Model - Warren constant values for 6506/11-A-2 for hole sections.

Well 6506/11-A-2			
Hole Section	**a**	**b**	**c**
36"	1.650E-04	3.585	6.279E-06
26"	-1.950E-05	7.639	3.990E-06
17.5"	9.745E-05	-1.427	2.370E-06
12.25"	1.134E-05	-9.878	2.051E-06

Table 5.21: Warren Model - Warren constant values for 6506/11-A-3 for hole sections.

Well 6506/11-A-3			
Hole Section	**a**	**b**	**c**
36"	1.019E-04	164.175	-3.358E-05
26"	1.193E-04	28.691	-1.752E-06
17.5"	4.790E-05	-7.375	3,397E-06
12.25"	1.336E-06	-1.477	8.494E-07

Table 5.22: Warren Model - Warren constant values for 6506/11-A-4 for hole sections.

Well 6506/11-A-4			
Hole Section	**a**	**b**	**c**
36"	1.742E-05	61.518	-3.529E-06
26"	1.413E-04	5.189	1.810E-06
17.5"	8.306E-05	-7.616	2.440E-06
12.25"	0	0	1.048E-06
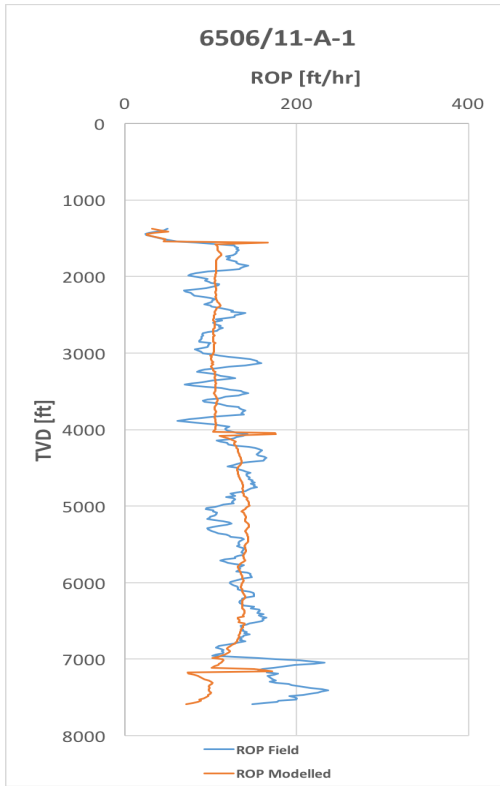
(a) 6506/11-A-1
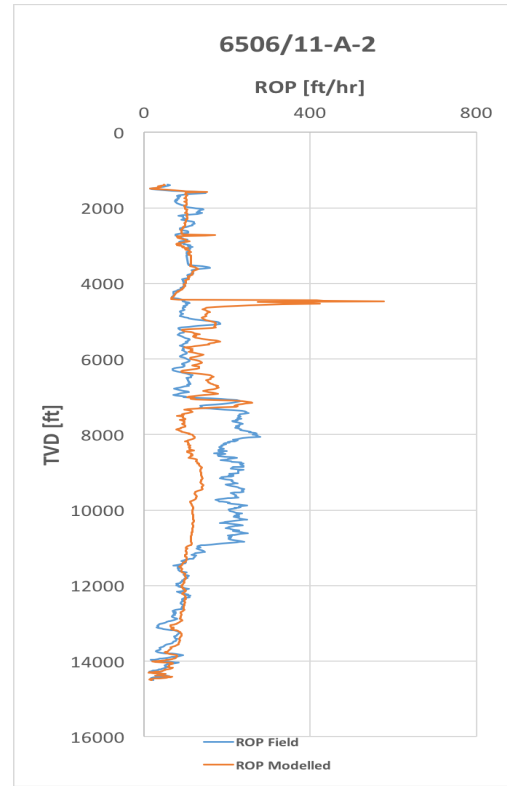
(b) 6506/11-A-2
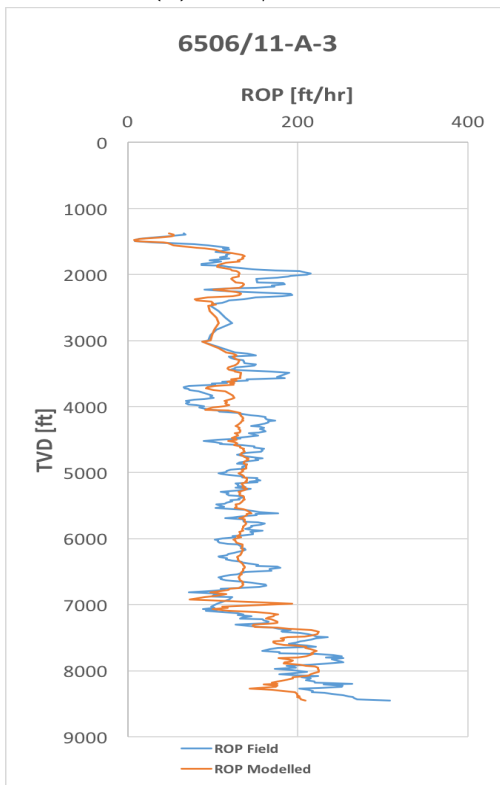
(c) 6506/11-A-3

(d) 6506/11-A-4

Figure 5.29: Warren model - Using their own Warren constant values for hole sections.

5.4.3   Modelling by Geological Groups

The test method for "Modelling by geological groups" is executed by dividing the well depths into different geological groups as illustrated in Figure 4.3 in Chapter 4.1.2. The depths of the wells had to be in terms of the same lateral geological groups. Table 5.23 - 5.26 provides the Warren constant values for the geological groups of the different wells.

Table 5.23: Warren Model - Warren constant values for 6506/11-A-1 for geological groups.

Well 6506/11-A-1			
Group	**a**	**b**	**c**
Nordaland Group	4.425E-05	-13.043	3.775E-06
Hordaland Group	9.056E-06	57.870	-4.718E-06
Rogaland Group	-1.236E-06	-10.725	1.812E-06
Shetland Group	2.049E-05	60.641	-4.116E-06
Cromer Knoll Group	1.145E-05	14.403	1.555E-06

Table 5.24: Warren Model - Warren constant values for 6506/11-A-2 for geological groups.

Well 6506/11-A-2			
Group	**a**	**b**	**c**
Hordaland Group	1.880E-05	-0.248	5.708E-07
Rogaland Group	-3.7616E-06	0.705	6.831E-07
Shetland Group	1.506E-06	-4.834	1.1396E-06
Cromer Knoll Group	1.014E-05	-0.410	1.738E-06

Table 5.25: Warren Model - Warren constant values for 6506/11-A-3 for geological groups.

Well 6506/11-A-3			
Group	**a**	**b**	**c**
Hordaland Group	1.245E-06	-4.912	1.569E-06.
Rogaland Group	1.741E-07	-2.557	1.108E-06
Shetland Group	-1.900E-07	0.645	5.425E-07

Table 5.26: Warren Model - Warren constant values for 6506/11-A-4 for geological groups.

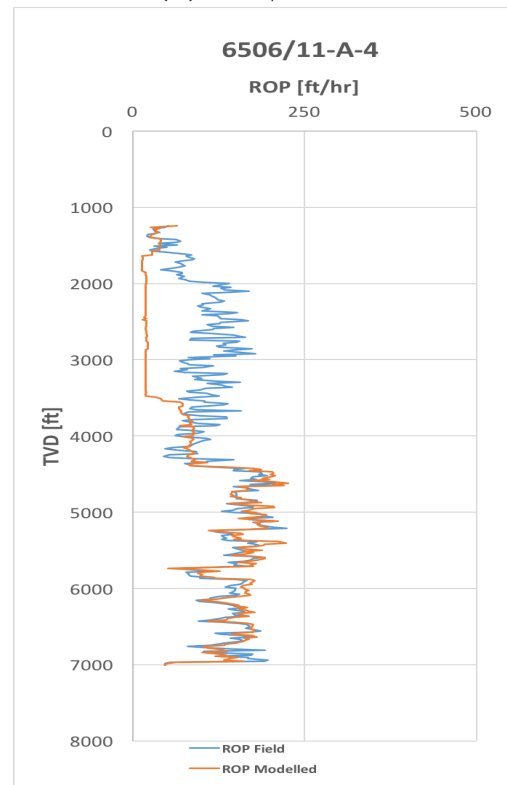| Well 6506/11-A-4			
Group	**a**	**b**	**c**
Rogaland Group	0	0	1.023E-06
Shetland Group	3.816E-09	9.883	2.997E-07

(a) 6506/11-A-1

(b) 6506/11-A-2

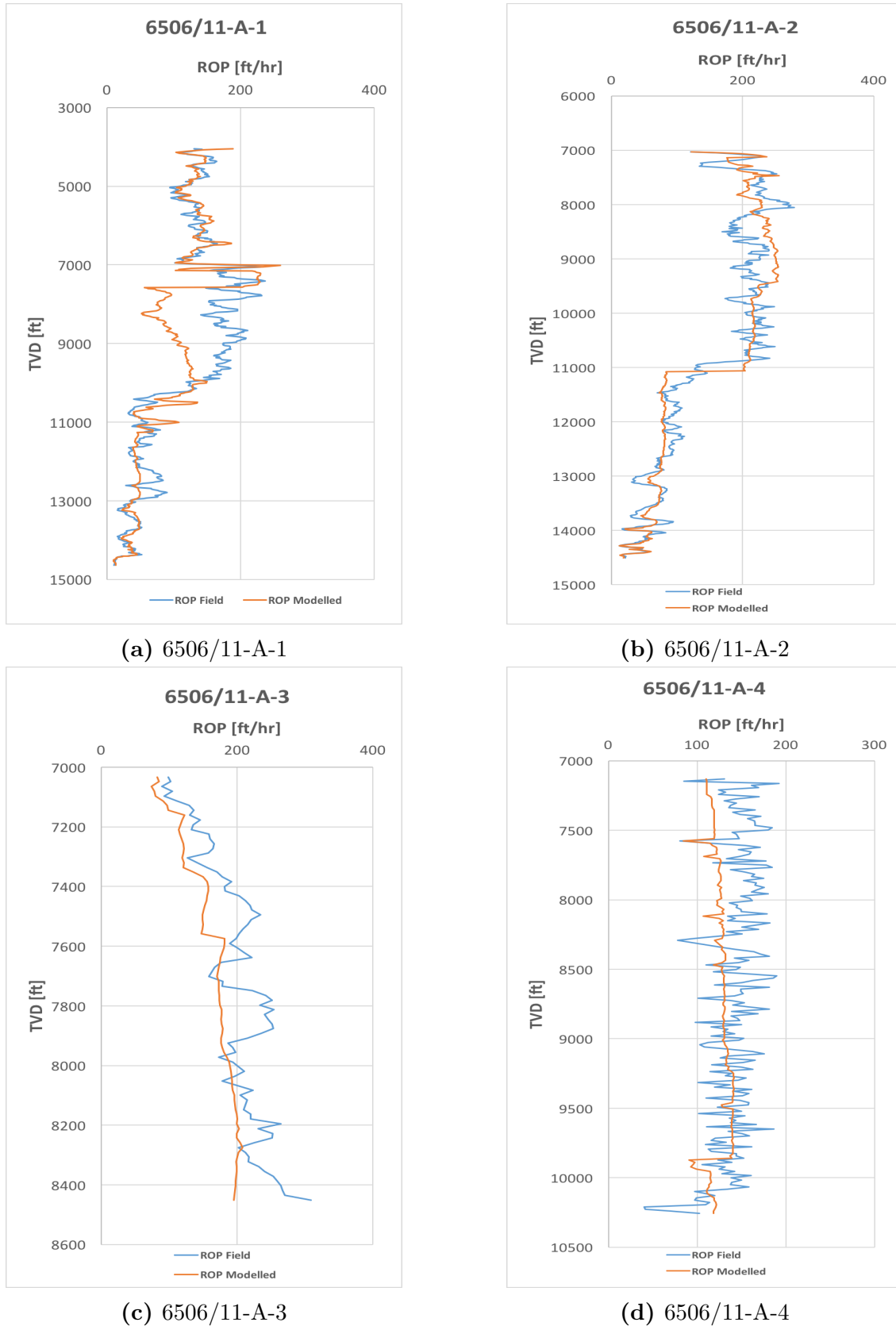**(c)** 6506/11-A-3

(d) 6506/11-A-4

Figure 5.30: Warren model - Using their own Warren constant values for geological groups.

In subfigure 5.30a, ROP Warren constants are extracted from Nordaland, Hordaland, Rogaland, Shetland and Cromer Knoll Groups. From the modelled ROP the correlation between actual and modelled ROPs are very good in all group sections. The modelled ROP in Shetland Group (7500 ft - 10,000 ft) overestimates the field ROP.

When modelling by geological groups using Warren constants in well 6506/11-A-2, the correlation is very promising. However, the model is slightly limited as it doesn't generate a good representation of the high and low peaks of ROP. Overall modelled ROP yields satisfying results.

Modelling well 6506/11-A-3 by geological groups, the modelled ROP gives poor correlation with field ROP. The modelled ROP follows the trendline of actual ROP, but underestimates the prediction of ROP in most depths of the well.

Well 6506/11-A-4 is hard to model as signal is very sensitive to disturbances. The geological groups Rogaland and Shetland Groups where the constants are extracted from, generates the poor result.

5.4.4   Drilling Ahead ROP Prediction for Geological Groups

The Warren model application method in this testing results follows the same procedure in chapter 5.1.7, where the Warren constants are extracted from the red area in Figure 5.22.

Warren modelling approach for all the four wells are presented in Figure 5.31 and the Warren constant values are shown in Table 5.27 - 5.30 below:

Table 5.27: Drilling Ahead ROP Prediction for Geological Groups 6506/11-A-1 Warren constants values.

Well 6506/11-A-1			
Geo. Groups	**a**	**b**	**c**
Nordaland Group	4.3245E-05	-13.347	3.926E-06
Hordaland Group	1.109E-05	46.215	-3.420E-06
Rogaland Group	-1.543E-06	-12.697	2.139E-06
Shetland Group	1.746E-05	59.646	-4.324E-06
Cromer Knoll Group	2.363E-05	27.686	-2.266E-06

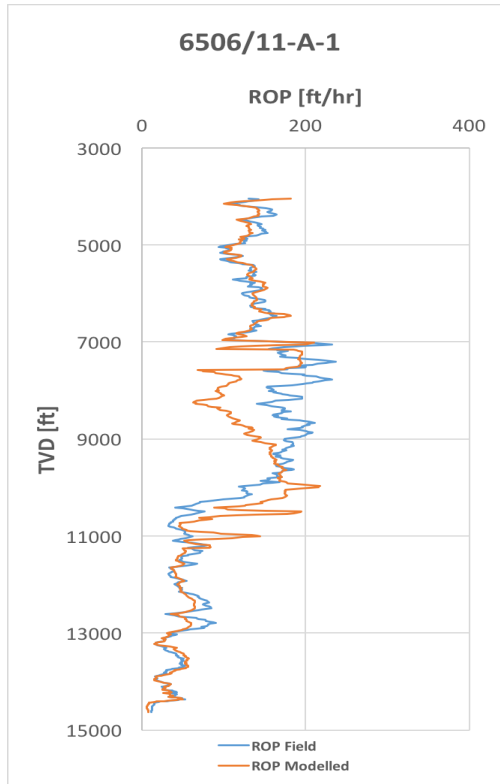**Table 5.28:** Drilling Ahead ROP Prediction for Geological Groups 6506/11-A-2 Warren constants values.

Well 6506/11-A-2			
Geo. Groups	**a**	**b**	**c**
Hordaland Group	1.554E-05	-3.600	1.174E-06
Rogaland Group	-1.208E-06	-1.464	5.725E-07
Shetland Group	9.237E-07	-0.992	8.360E-07
Cromer Knoll Group	1.467E-05	39.729	-1.552E-06

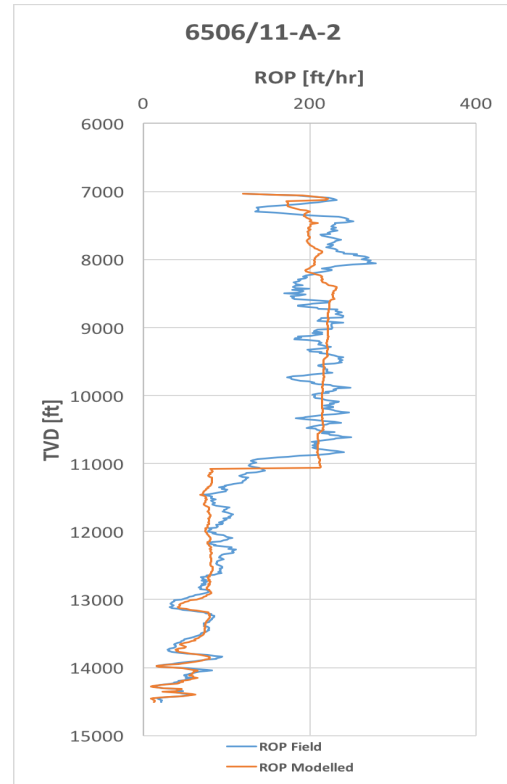**Table 5.29:** Drilling Ahead ROP Prediction for Geological Groups 6506/11-A-3 Warren constant values.

Well 6506/11-A-3			
Geo. Groups	**a**	**b**	**c**
Hordaland Group	1.170E-06	-4.749	1.327E-06
Rogaland Group	4.249E-07	-2.354	9.053E-07
Shetland Group	-5.117E-07	-0.133	5.962E-07

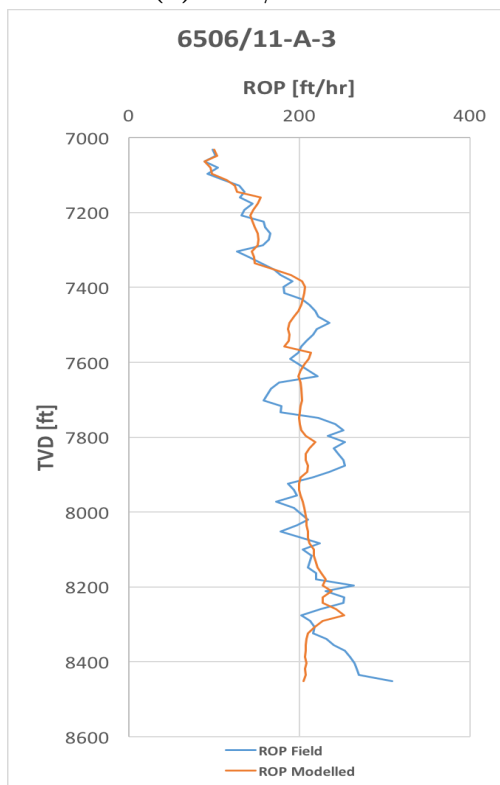**Table 5.30:** Drilling Ahead ROP Prediction for Geological Groups 6506/11-A-4 Warren constant values.

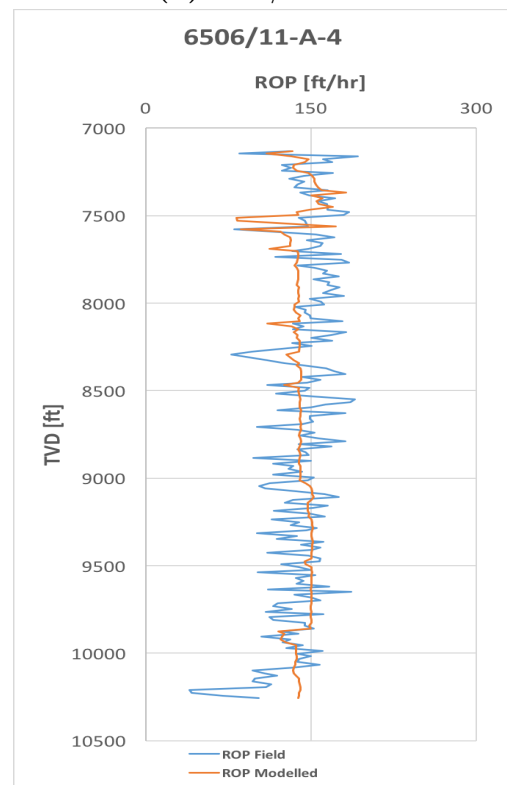| Well 6506/11-A-4			
Geo. Groups	**a**	**b**	**c**
Rogaland Group	1.806E-08	-24.209	2.345E-06
Shetland Group	4.312E-09	4.123	5.770E-07

(a) 6506/11-A-1

(b) 6506/11-A-2

(c) 6506/11-A-3

(d) 6506/11-A-4

Figure 5.31: Drilling Ahead ROP Prediction for geological groups - Using their own Warren constant values.

In subfigure 5.31a, drilling ahead ROP prediction for well 6506/11-A-1 is illustrated. The well is very well predicted in all the geological groups, although it underestimates in Rogaland and Shetland Groups at 7100 ft - 9000 ft. We can summarize by concluding with well 6506/11-A-1 being good predicted.

Well 6506/11-A-2 prediction is showed in subfigure 5.31b. The ROP prediction for this well is very alternating as the bottom and top sections of the well are excellently modelled. However, the modelled ROP is unpleasant in Shetland Group as it is poor to model the ROP peaks. The result in well 6506/11-A-2 when modelling by drilling ahead ROP prediction the modelled ROP is viewed to be acceptable.

The result generated in subfigure 5.31c with well 6506/11-A-3 is good, although it doesn't match fully with the field ROP.

In subfigure 5.31d well 6506/11-A-4 is modelled using drilling ahead ROP prediction. Earlier results show that Warren model is moderate when generating ROP peaks. Therefore modelling well 6506/11-A-4 suffers from this condition. The ROP prediction for well 6506/11-A-4 in this section yields the poorest results.
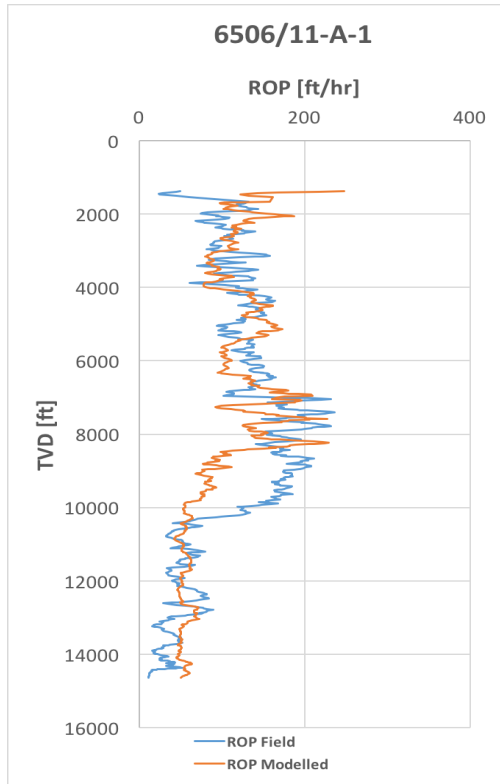
5.5   Bourgoyne & Young Modelling

The analysis of Bourgoyne & Young model is presented in chapter 4.3.5. As described earlier in the thesis, Bourgoyne & Young Model is based on multiple drilling parameters.

Table 5.31 presents Bourgoyne & Young Model coefficient values extracted from each well and in Figure 5.32 the coefficient values are plotted in the well against field ROP.

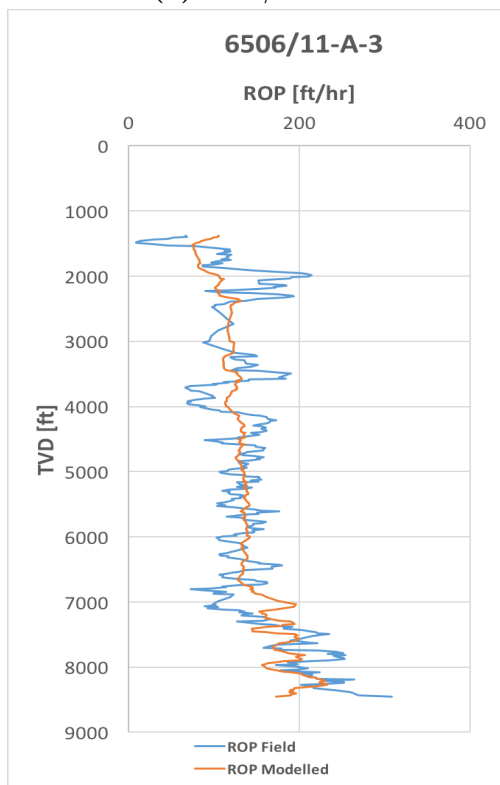**Table 5.31:** Bourgoyne & Young model - B&Y coeff. values for entire well data.

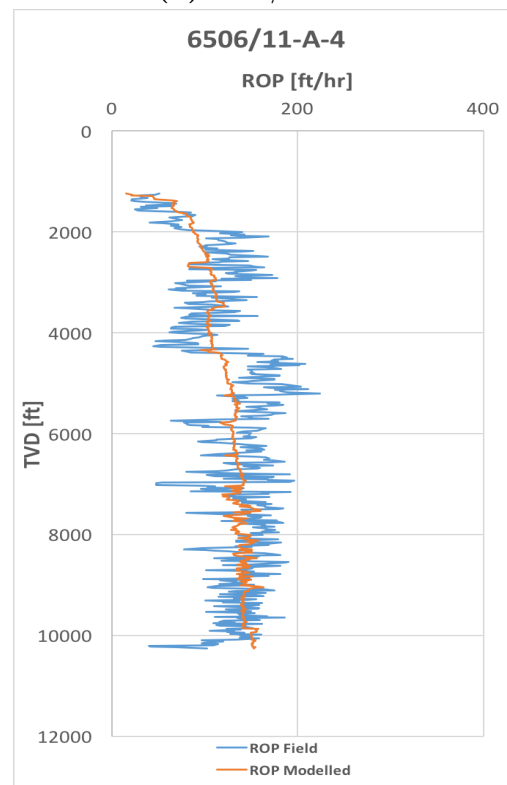| Well	a_1	a_2	a_4	a_6	a_8	R^2
6506/11-A-1	1.881	0.031	-0.732	0.490	1.249	0.440
6506/11-A-2	0.008	0.312	-0.593	0.430	1.540	0.231
6506/11-A-3	1.465	0.393	-0.209	0.268	0.279	0.321
6506/11-A-4	0.009	0.592	-0.058	-0.169	0.832	0.397

(a) 6506/11-A-1
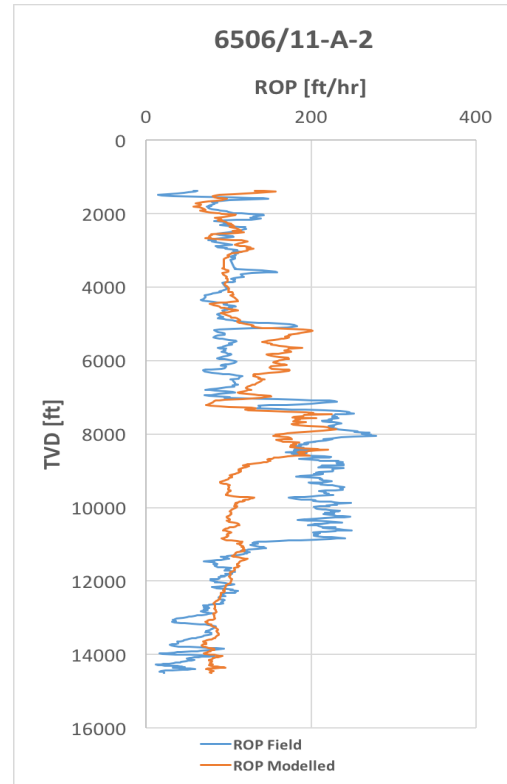
(b) 6506/11-A-2

(c) 6506/11-A-3

(d) 6506/11-A-4

Figure 5.32: Bourgoyne & Young Model - Using their own B&Y coeff. values for entire well data.

The results show that the "Entire well data" based coefficients provide very well predictions of the field ROP. Although the model clearly deviates from the actual ROP in Shetland Group at 8300 ft - 10300 ft. One of the main reasons for the deviation was that the measured WOB was very low compared with the upper-lying formation dataset. However, the overall results show satisfactory.

In the figure above (Figure 5.32b) the wells give poor estimations of the field ROP. The deviation is significant at 5000 ft - 7000 ft (12.25" hole section) and Shetland at 8500 ft - 11100 ft. However, the modelled ROP follows the trendline, presenting a fair correlation.

The Bourgoyne & Young model fails to predict the high and low peaks of ROP in well 6506/11-A-3. Therefore the correlation factor, R^2 is low. The modelled ROP in this well gives good result in terms of the trendline, but doesn't fit the details of the ROP values.

As described in the previous cases with the other wells, the Bourgoyne & Young model is poor to capture the ROP peaks. Therefore ROP in well 6506/11-A-4 which is very sensitive to disturbances it isn't favorable when it comes to modelling. Even though R^2 is greater than for well 6506/11-A-2 and 6506/11-A-3, the model is not sufficient to model ROP.

The model is a five parameter model, which is missing some important ROP governing parameters. This could be the reason for the weakness of the model. This suggests the need to modify the model. The next section deals with the modification and testing process.

5.6   Modified Bourgoyne & Young Modelling

The Bourgoyne & Young model results presented in Chapter 5.5 show that equation (3.19) is limited when it comes to predicting field ROP. Therefore, in this thesis a new improved model developed with the idea of improving the predictive power of Bourgoyne & Young model is modified. The background for the model improvement is the results obtained from chapter 5.1.1. Here, the work done was in an attempt to investigate the ROP dependent parameters.

The new model proposed is built on the assumption of equation (3.19) being correlated for the depth of the wellbore and being simplified with respect to the core real-time drilling optimization variables. As demonstrated in chapter 5.1.1, the ROP depends on torque (T), formation pressure (FM) and mud weight (MW). The Modified Bourgoyne & Young model is expressed as:

$$ROP = \gamma_1 D^{\gamma_2} WOB^{\gamma_3} RPM^{\gamma_4} q^{\gamma_5} T^{\gamma_6} FP^{\gamma_7} MW^{\gamma_8} \qquad (5.6)$$

The workflow for solving ROP is the same as the one presented for Bourgoyne & Young in Figure 4.10 in chapter 4.3.5, p. 37.

5.6.1 Modelling by Entire Well Data

In this chapter well 6506/11-A-1, 6506/11-A-2, 6506/11-A-3 and 6506/11-A-4 are modelled by Bourgoyne & Young coefficients extracted from the entire well. The resultant coefficient values, γ_1 - γ_8, are presented in Table 5.32. The coefficient values are implemented in equation (5.6) on well 6506/11-A-1, 6506/11-A-2, 6506/11-A-3 and 6506/11-A-4. The outcomes are presented in Figure 5.33.

Table 5.32: Modified Bourgoyne & Young model - Modified B&Y coeff. values for entire well data.
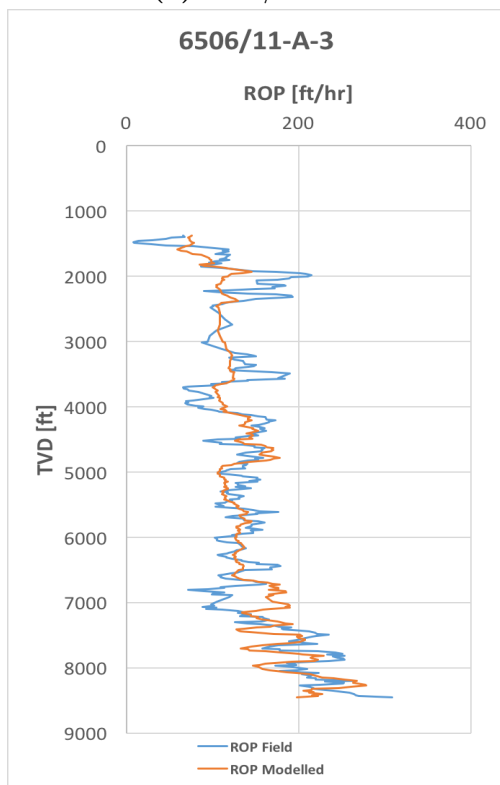
Well	γ_1	γ_2	γ_3	γ_4	γ_5	γ_6	γ_7	γ_8	$\mathbf{R^2}$
6506/11-A-1	62037.7223	-0.0335	-0.532	0.082	1.022	-0.775	0.252	2.501	0.492
6506/11-A-2	4.547E-11	-0.579	0.025	0.267	3.251	-0.372	5.420	2.382	0.757
6506/11-A-3	2.849E-05	0.151	-0.262	0.447	0.349	1.125	1.039	-1.731	0.427
6506/11-A-4	0.018	-0.052	-0.080	-0.146	0.595	0.723	-0.233	1.016	0.467
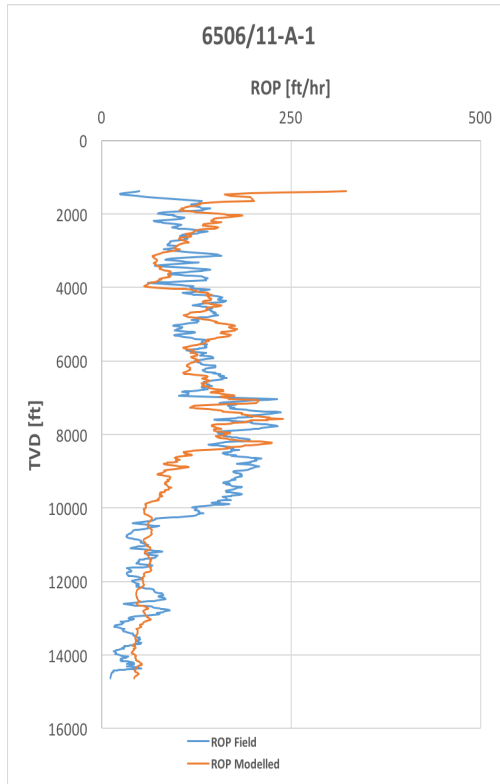
(a) 6506/11-A-1
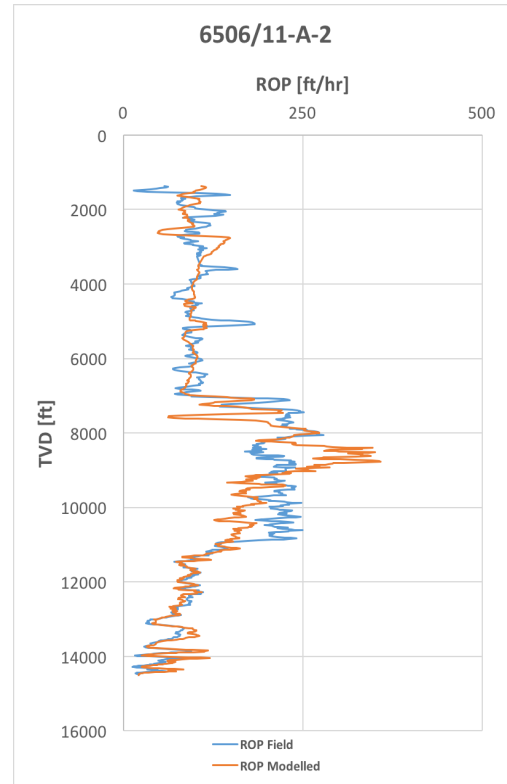
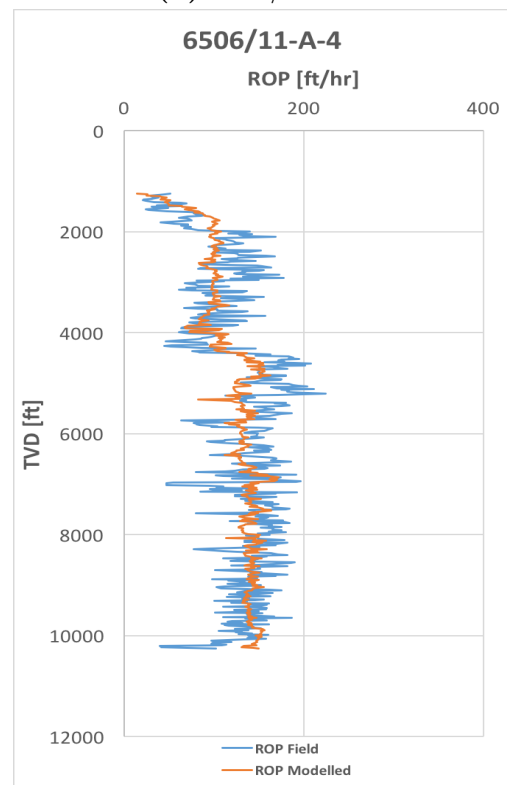**(b)** 6506/11-A-2

(c) 6506/11-A-3

(d) 6506/11-A-4

Figure 5.33: Modified Bourgoyne & Young Model - Using their own B&Y coeff. values for entire well data.

The modelled ROPs in subfigures 5.33a and 5.33b have great correlation factors for all the four wells. However, the generated penetration rates aren't extremely predictive for field ROP, the model is clearly improved. The model tends to minimize the geological areas where the deviation was large, especially in well 6506/11-A-1.

As the modelling results in subfigures 5.33d and 5.33c showed good correlation with field ROP, the coefficients from the reference well are tested on the nearby and far-away wells in order to model ROP model with respect to the measured one. However, note that well 6506/11-A-4 is not included as this well were hard to predict with this modified model, and produced poor results when implemented with its own coefficients.

Testing Mod. B&Y coeff. from nearby and far-away wells

The coefficient values achieved from well 6506/11-A-1 seen in Table 5.32 are implemented from nearby and far-away wells for well 6506/11-A-1, 6506/11-A-2 and 6506/11-A-3. The resultant ROPs are presented in Figure 5.34 - 5.36.
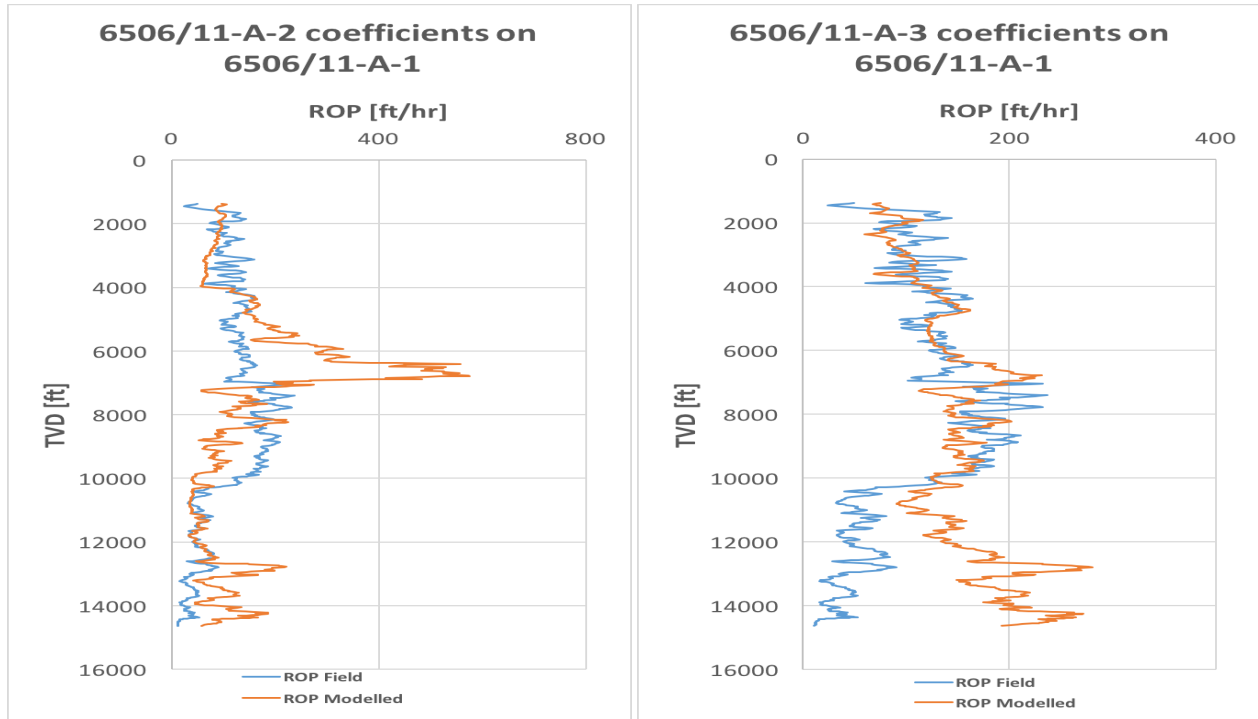
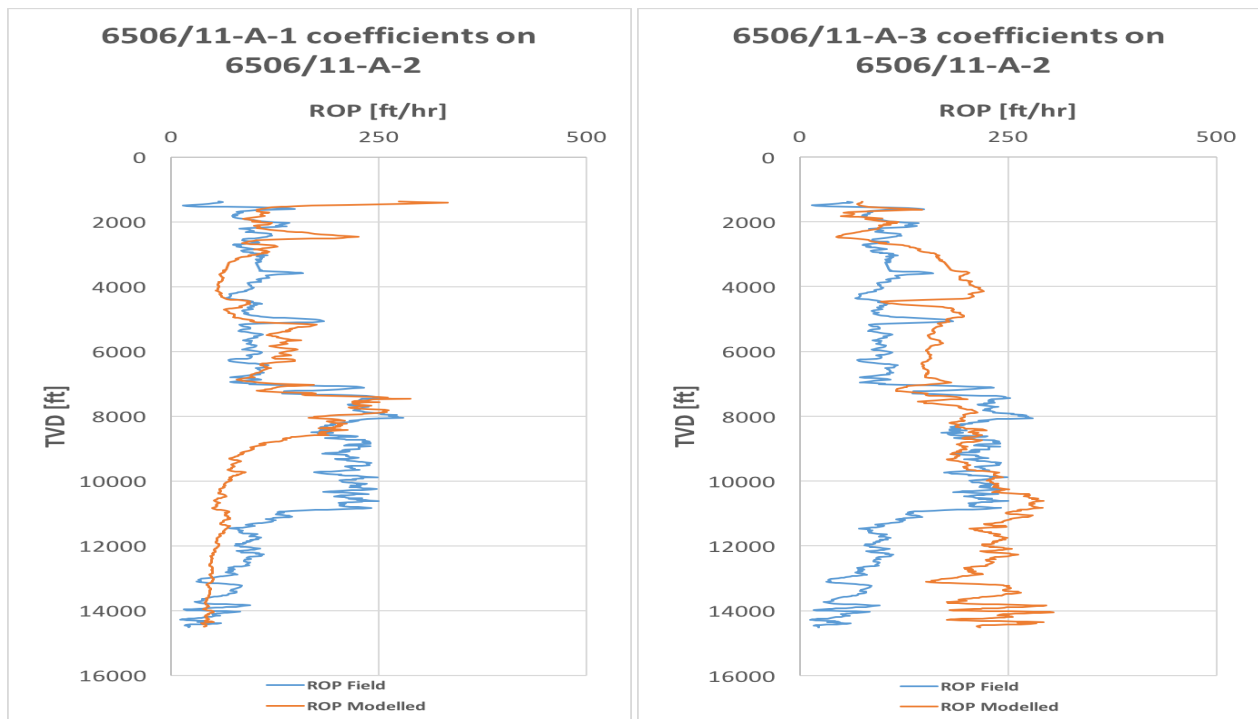**Figure 5.34:** Modified Bourgoyne & Young Model - 6506/11-A-1 using 6506/11-A-2 and 6506/11-A-3 B&Y coeff. values.

Figure 5.35: Modified Bourgoyne & Young Model - 6506/11-A-2 using 6506/11-A-1 and 6506/11-A-3 B&Y coeff. values.
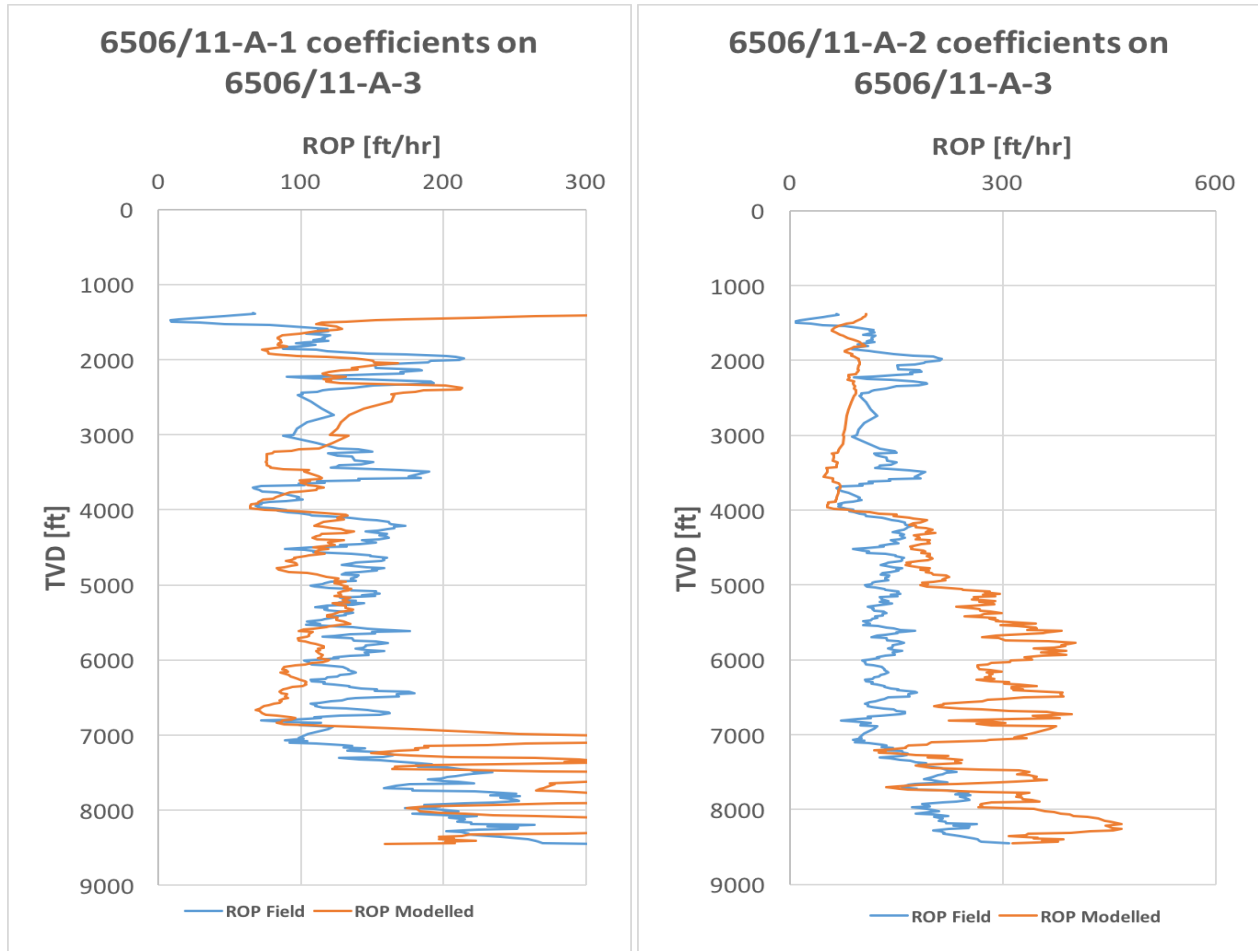
Figure 5.36: Modified Bourgoyne & Young Model - 6506/11-A-3 using 6506/11-A-1 and 6506/11-A-2 B&Y coeff. values.

Figure 5.34 show a decent correlation throughout most sections of the wells. When ROP is modelled with well 6056/11-A-2 coefficients a large deviation occurs in Nordaland and Hordaland Group at 4800 ft - 7000 ft. For ROP with coefficients from well 6506/11-A-3 the modelled ROP highly overestimates field ROP as we drill through Shetland Group at 10000 ft.

When coefficients from well 6506/11-A-1 are implemented in well 6506/11-A-2, the modelled ROP prediction is weaker than when well 6506/11-A-1 is implemented with its own coefficients. Some minor high-value peaks occur in the shallowest sections and the model tends to deviate from the measured ROP at 8500 ft in Shetland Group.

Applying coefficients from well 6506/11-A-3, the result is fluctuating. However, in this case also with coefficients from well 6506/11-A-1 deviates clearly as we approach Shetland Group.

We observe that the results obtained in well 6506/11-A-3 are very alternating for both cases. In the first case with coefficients from well 6506/11-A-1 the model shows a very promising correlation until the last 2000 ft of the well. In the second case with coefficients from well 6506/11-A-2 it is poor to predict ROP with a large offset at around 4000 ft.

5.6.2 Modelling by Hole Sections

Furthermore, well 6506/11-A-1, 6506/11-A-2, 6506/11-A-3 and 6506/11-A-4 are divided into intervals depending on the hole sections. The wells are modelled by correlating the hole sections to the overburden section. The wells are first modelled with their own coefficients extracted from each hole section of the wells.

Table 5.33 - 5.36 provides the Bourgoyne & Young coefficient values extracted from the hole sections. The result is shown in Figure 5.33 - 5.36.

Results show that the application of the model on its own well where they are derived from predicts the measured ROP perfectly. This suggests the applicability of the model as well as the hole section based modelling. The modelling approach could describe the same geological sections. However, it may also contain other geological groups as well. To be more specific the next chapter (5.6.3), will look at geological groups based modelling.

Table 5.33: Modified Bourgoyne & Young model - Modified B&Y coeff. for 6506/11-A-1 hole sections.

Well 6506/11-A-1									
Hole section	γ_1	γ_2	γ_3	γ_4	γ_5	γ_6	γ_7	γ_8	R^2
36"	0.847	2.979	-0.833	-5.061	5.394	-3.30	0	0	0.962
26"	-33.130	-0.246	0.113	-0.238	-3.866	0.372	49.707	-7.900	0.176
17.5"	6.614	-1.137	0.233	0.340	-1.854	0.595	1.147	0.812	0.584
12.25"	17.912	-7.426	1.294	0.635	-0.177	0.817	4.448	-2.374	0.934

Table 5.34: Modified Bourgoyne & Young model - Modified B&Y coeff. values for 6506/11-A-2 hole sections.

Well 6506/11-A-2									
Hole section	γ_1	γ_2	γ_3	γ_4	γ_5	γ_6	γ_7	γ_8	$\mathbf{R^2}$
36"	167.612	10.616	-2.439	2.321	-65.797	0	0	0	0.737
26"	-1.812	0.133	-0.464	0.257	1.476	0	0	-2.638	0.561
17.5"	18.059	-2.921	-0.524	0	-2.255	2.683	-8.766	6.989	0.804
12.25"	17.912	-7.426	1.294	0.635	-0.177	0.817	4.448	-2.374	0.934

Table 5.35: Modified Bourgoyne & Young model - Modified B&Y coeff. values for 6506/11-A-3 hole sections.

Well 6506/11-A-3									
Hole section	γ_1	γ_2	γ_3	γ_4	γ_5	γ_6	γ_7	γ_8	$\mathbf{R^2}$
36"	177.796	-29.797	2.458	-18.251	-2.350	-13.510	0	0	0.912
26"	2.569	-0.390	-0.599	0.728	-1.664	1.782	0.233	-2.521	0.540
17.5"	-7.140	-2.900	0.599	1.089	-1.526	0.334	3.955	1.320	0.728
12.25"	-21.881	0.446	-0.078	-0.406	0.530	3.979	0.903	20.373	0.872

Table 5.36: Modified Bourgoyne & Young model - Modified B&Y coeff. values for 6506/11-A-4 hole sections.

Well 6506/11-A-4									
Hole section	γ_1	γ_2	γ_3	γ_4	γ_5	γ_6	γ_7	γ_8	$\mathbf{R^2}$
36"	22.837	-10.705	1.081	-1.346	0.769	-1.076	13.179	0	0.552
26"	-3.210	0.485	-0.524	-0.292	0.725	0.589	1.806	0	0.266
17.5"	-5.939	-1.505	0.223	-0.553	2.964	0.267	3.991	-0.352	0.684
12.25"	7.011	-3.232	-0.019	0.556	-1.626	2.486	1.210	-0.332	0.450

(a) 6506/11-A-1

(b) 6506/11-A-2

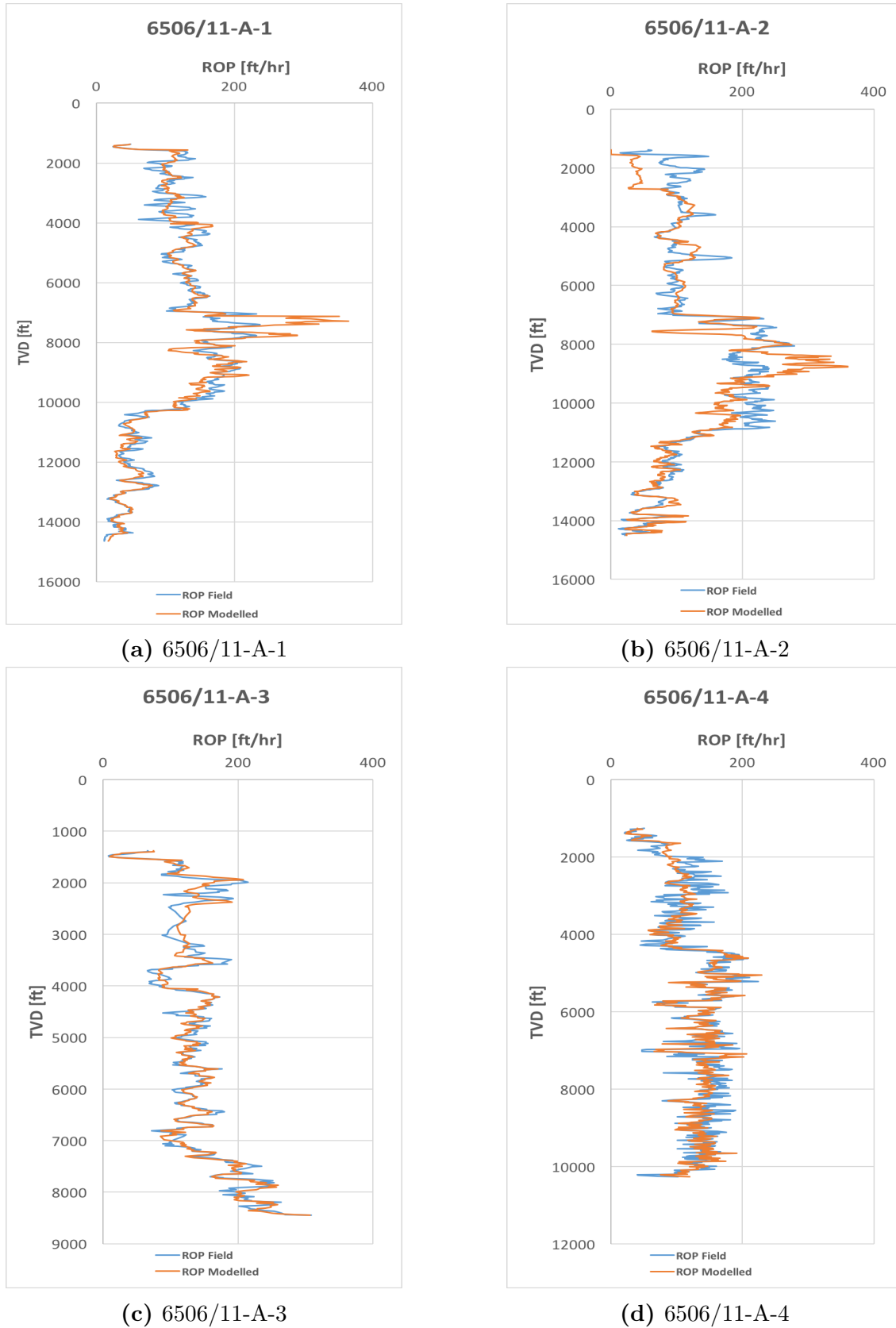**(c)** 6506/11-A-3

(d) 6506/11-A-4

Figure 5.37: Modified Bourgoyne & Young Mode - Using their own B&Y coeff. values for hole section.

5.6.3   Modelling by Geological Groups

In this chapter well 6506/11-A-1, 6506/11-A-2, 6506/11-A-3 and 6506/11-A-4 are modelled by coefficients extracted from the geological groups. This modelling technique approach is similar to the explanation in chapter 5.1.6 and 5.4.3

Table 5.37 - 5.40 presents the Modified Bourgoyne & Young coefficients obtained from the four wells. Figure 5.38 shows that the the Modified Bourgoyne & Young model perfectly capture the field ROPs. Results also show that geological group based model prediction improved the one obtained from the section by section modelling method.

The results presented in Figure 5.40 are application of the geological groups based model on its own well, showing there is an excellent match with the field ROP.

Table 5.37: Modified Bourgoyne & Young model - Modified B&Y coeff. values for 6506/11-A-1 geological groups.

Well 6506/11-A-1									
Geo. Groups	γ_1	γ_2	γ_3	γ_4	γ_5	γ_6	γ_7	γ_8	R^2
Nordaland Group	-7.153	-2.031	0.765	0.346	2.915	0.392	2.463	-0.737	0.884
Hordaland Group	6.995	-3.306	0.044	1.034	-0.449	0.542	1.072	16.887	0.950
Rogaland Group	17.109	-6.761	0.143	-1.011	3.377	-0.974	3.013	17.243	0.935
Shetland	2.955	-6.624	0.369	0.352	1.635	4.197	2.281	-5.381	0.976
Cromer Knoll Group	35.266	-10.484	1.712	0.847	-1.859	-0.202	6.317	-1.428	0.976

Table 5.38: Modified Bourgoyne & Young model - Modified B&Y coeff. values for 6506/11-A-2 geological groups.

Well 6506/11-A-2									
Geo. Groups	γ_1	γ_2	γ_3	γ_4	γ_5	γ_6	γ_7	γ_8	R^2
Hordaland Group	-6.674	0	0.628	-0.541	-0.529	2.515	-1.212	0	1
Rogaland Group	370.397	12.216	0.337	-0.350	-142.707	-0.647	2.658	-10.665	0.952
Shetland	15.474	-5.372	-0.220	0.764	-1.178	1.894	1.267	-0.833	0.790
Cromer Knoll Group	3.484	-4.762	0.841	0.137	1.524	1.093	4.727	-0.346	0.968

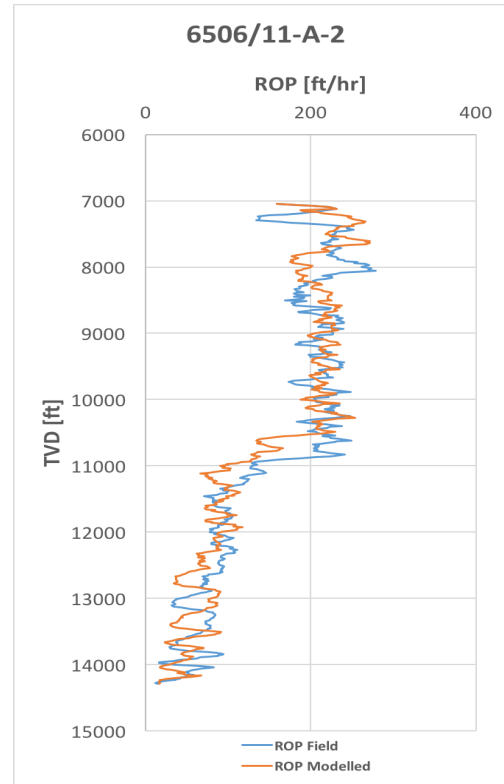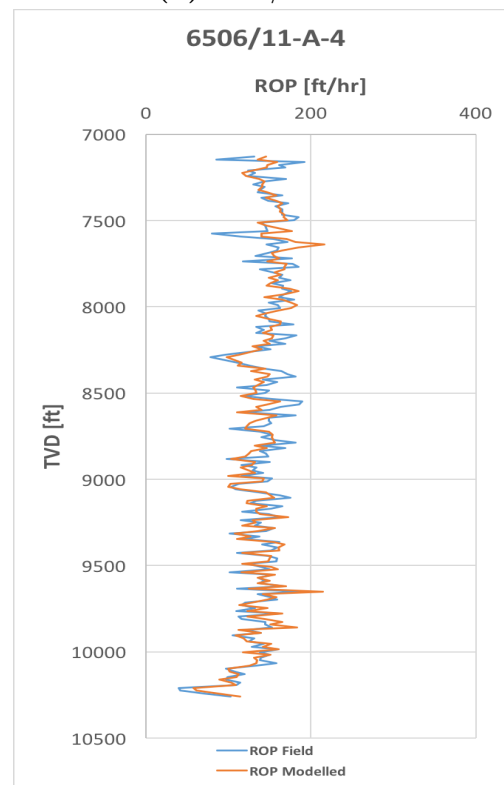**Table 5.39:** Modified Bourgoyne & Young model - Modified B&Y coeff. values for 6506/11-A-3 geological groups.

Well 6506/11-A-3									
Geo. Groups	γ_1	γ_2	γ_3	γ_4	γ_5	γ_6	γ_7	γ_8	$\mathbf{R}^2$
Hordaland Group	-23.229	-4.484	0.164	-2.239	1.024	9.071	2.513	16.911	1
Rogaland Group	-22.065	-0.735	0.008	-0.203	1.292	2.991	2.817	37.209	0.980
Shetland Group	-7.294	0.452	-0.042	-0.047	-0.537	2.517	0.812	-6.451	0.718

Table 5.40: Modified Bourgoyne & Young model - Modified B&Y coeff. values for 6506/11-A-4 geological groups.

Well 6506/11-A-4									
Geo. Groups	γ_1	γ_2	γ_3	γ_4	γ_5	γ_6	γ_7	γ_8	$\mathbf{R}^2$
Rogaland Group	-7.270	-0.096	0.058	0.467	0.863	1.157	1.346	0	0.398
Shetland Group	8.383	-5.596	-0.039	0.349	-0.589	3.899	0.786	0.053	0.692
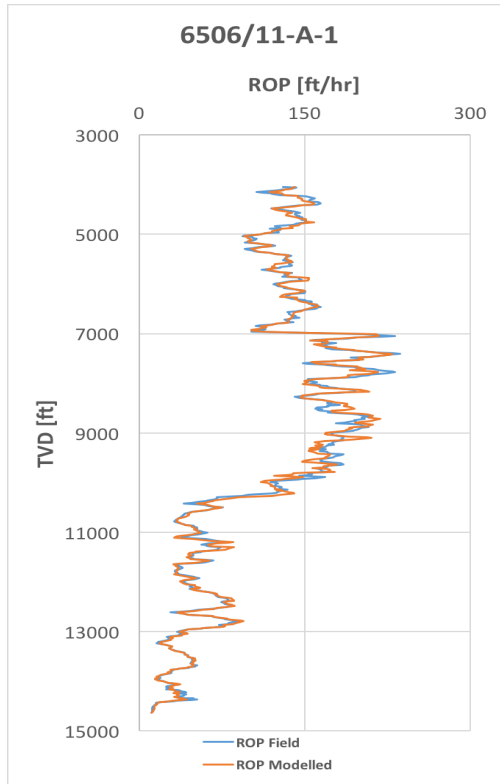
(a) 6506/11-A-1

(b) 6506/11-A-2
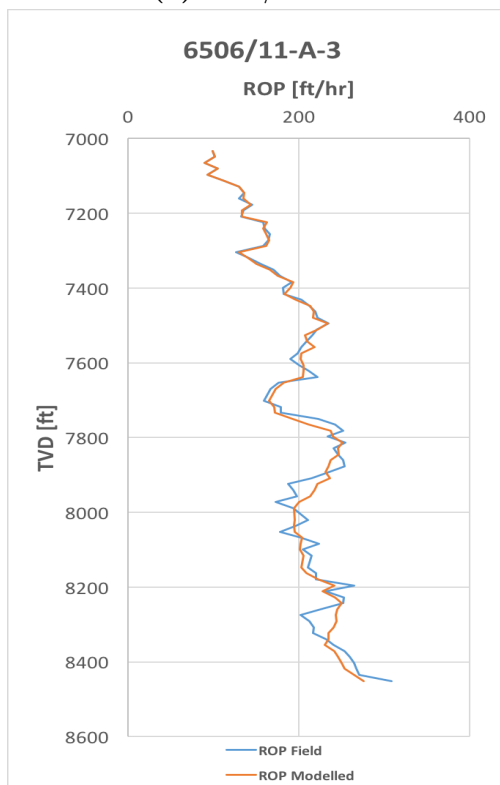
(c) 6506/11-A-3

(d) 6506/11-A-4

Figure 5.38: Modified Bourgoyne & Young Model - Using their own B&Y coeff. values for geological groups.

5.6.4 Drilling Ahead ROP Prediction for Geological Groups

In this chapter, the wells are modelled by Modified Bourgoyne & Young coefficients extracted from the red area in Figure 5.22 in page 69. The modelling technique is similar to the application method in Chapter 5.1.7 in page 69. Table 5.41 - 5.44 provides the coefficient values and in Figure 5.31 the resulting plots are plotted.

In subfigure 5.39a ROP is perfectly modelled for all geological groups of the well. A high-value ROP prediction occurs at bottom of Hordaland Group. Well 6506/11-A-1 can be concluded with that it generates excellent results using the Modified Bourgoyne & Young model when drilling ahead ROP prediction is applied.

Subfigure 5.39b illustrates drilling ahead ROP prediction for well 6506/11-A-2. This well also experiences the deviation as well 6506/11-A-1 when high-value ROP is generated in Hordaland Group, but note that this section isn't for where drilling ahead ROP prediction is applied.

In subfigures 5.39c and 5.39d, well 6506/11-A-3 and 6506/11-A-4 are respectively modelled. The outcome results are viewed to be the finest results, generating perfect ROP prediction in all geological groups. This is an indication that these two wells behave perfectly under this modelling application.

Table 5.41: Drilling Ahead ROP Prediction for Geological Groups 6506/11-A-1 Modified B&Y coeff. values.

Well 6506/11-A-1								
Geological Group	γ_1	γ_2	γ_3	γ_4	γ_5	γ_6	γ_7	γ_8
Nordaland	-7.335	-2.022	0.782	0.187	3.225	0.357	1.981	-0.287
Hordaland	6.452	-3.247	0.053	1.111	-0.475	0.597	1.053	16.857
Rogaland	39.481	-9.717	-0.189	-1.191	-0.822	-0.971	-3.775	20.543
Shetland	5.209	-6.976	0.356	0.485	1.079	4.368	2.152	-5.532
Cromer Knoll	31.419	-10.160	1.448	0.932	-1.264	0.270	5.561	0.865

Table 5.42: Drilling Ahead ROP Prediction for Geological Groups 6506/11-A-2 Modified B&Y coeff. values.

Well 6506/11-A-2								
Geological Group	γ_1	γ_2	γ_3	γ_4	γ_5	γ_6	γ_7	γ_8
Hordaland	-7.325	0	0.600	-0.731	0	2.383	-1.099	0
Rogaland	283.224	11.979	0.269	-0.310	-113.125	0.330	3.874	-22.414
Shetland	-0.878	-1.221	-0.165	-0.016	-0.350	1.622	0.791	9.358
Cromer Knoll	8.081	-3.113	1.473	1.179	-0.850	-1.105	6.341	-7.229

Table 5.43: Drilling Ahead ROP Prediction for Geological Groups 6506/11-A-3 Modified B&Y coeff. values.

Well 6506/11-A-3								
Geological Group	γ_1	γ_2	γ_3	γ_4	γ_5	γ_6	γ_7	γ_8
Hordaland	-56.294	0	-0.005	0.515	1.778	12.956	0.123	0
Rogaland	-26.524	0.793	0.015	-0.171	0.799	3.149	2.939	33.398
Shetland	-5.856	0.057	-0.066	-0.125	-0.320	1.938	0.955	-6.320

Table 5.44: Drilling Ahead ROP Prediction for Geological Groups 6506/11-A-4 Modified B&Y coeff. values.

Well 6506/11-A-4								
Geological Group	γ_1	γ_2	γ_3	γ_4	γ_5	γ_6	γ_7	γ_8
Rogaland	-33.009	8.468	0.184	-0.059	-3.062	2.073	2.444	0
Shetland	9.294	-3.884	0.005	0.261	-1.310	2.498	1.048	-0.059
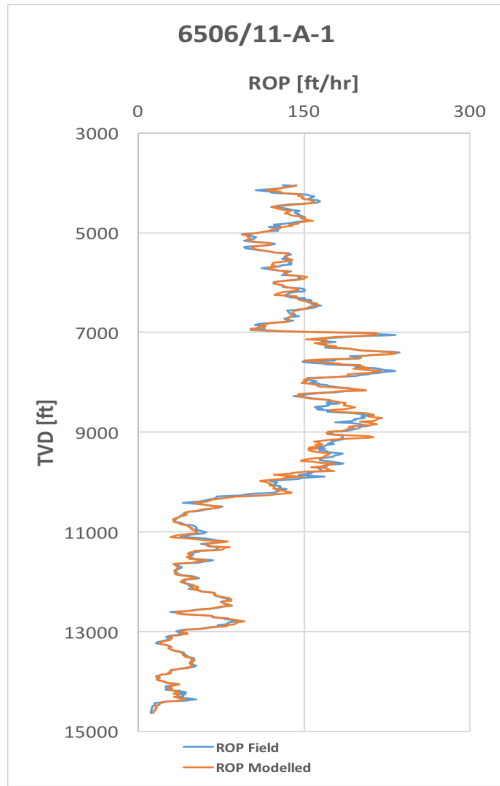
(a) 6506/11-A-1
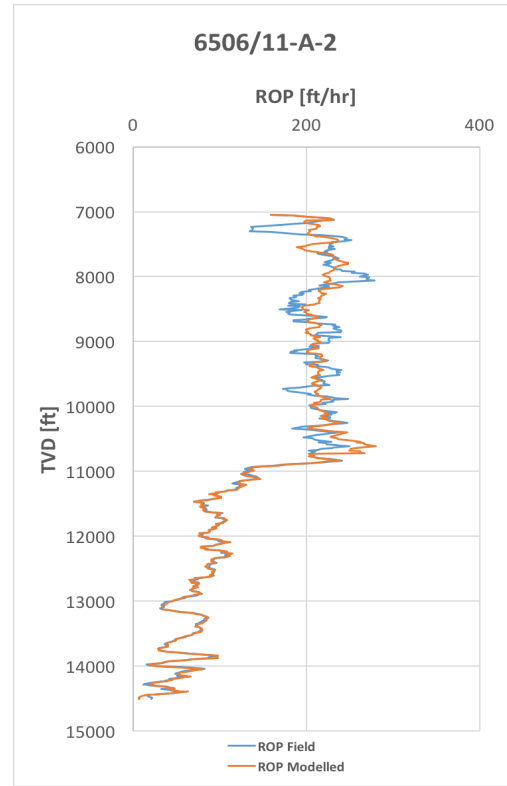
(b) 6506/11-A-2
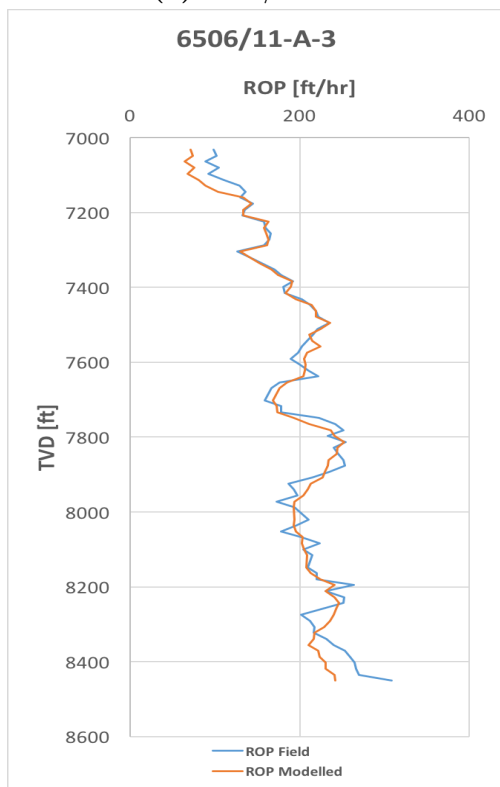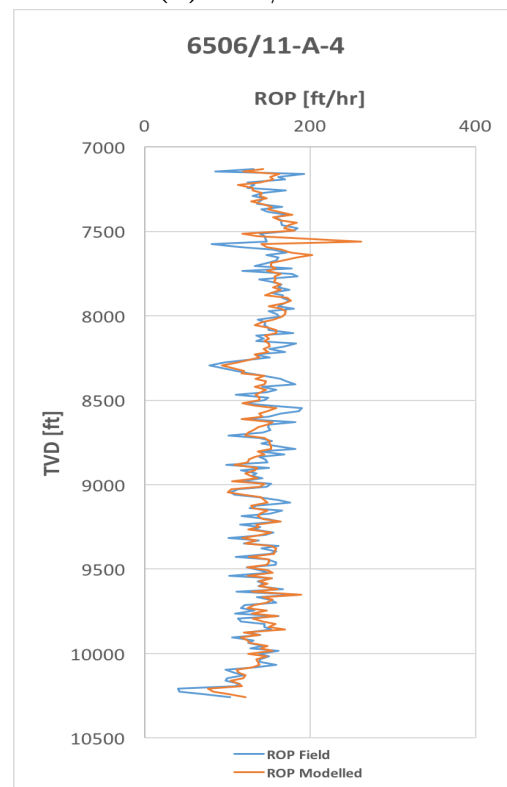
(c) 6506/11-A-3

(d) 6506/11-A-4

Figure 5.39: Drilling Ahead ROP Prediction for geological groups - Using their own B&Y coeff. values.

6. Analysis and Discussion

Chapter 6 summarizes the result and simulation studies work presented in Chapter 5. The previous work presented earlier were presented as qualitative research, however, in this chapter results of the predicted models will be analyzed and be presented as quantitative research. The work in this chapter is based on several outlined analysis methods to test the accuracy of the modelled ROPs.

6.1 Mean Absolute Percentage Error (MAPE)

Mean absolute percentage error (MAPE) measures the size of the errors in percentage terms, where the predicted model deviates from the actual model. MAPE is used to calculate the accuracy of a predicted model. The better the model predicts the actual model, the lower is MAPE value, meaning if modelled dataset is $100\,\%$ accurate, then MAPE value is equal to 0 and there exists no deviation.

In this thesis MAPE evaluation is used to analyse the accuracy for each modelled ROP approach. The objective of this analysis is to observe the deviation between measured and modelled ROP nummerically. MAPE is calculated in Microsoft Excel with the use of equation 6.1 as shown in Table 6.1 - 6.4.

$$MAPE = \frac{100\,\%}{n} \sum_{i=1}^{n} \left| \frac{ROP_{(mod)i} - ROP_{(filt)i}}{ROP_{(filt)i}} \right| \tag{6.1}$$

Where "n" is number of datasets, ROP_{mod} is modelled ROP and ROP_{filt} is actual or filtered ROP.

Table 6.1: MAPE values for Multiple regression model.

MAPE Values	Well			
Multiple Regression Model	6506/11-A-1	6506/11-A-2	6506/11-A-3	6506/11-A-4
Multiple Reg. model - Using its own coeff.	42.121%	26.772%	25.857%	24.480%
Multiple Reg. model - Coeff from 6506/11-A-1		50.690%	40.365%	50.061%
Multiple Reg. model - Coeff from 6506/11-A-2	98.210%		54.673%	54.433%
Multiple Reg. model - Coeff from 6506/11-A-3	120.460%	89.735%		51.715%
Multiple Reg. model - Coeff from 6506/11-A-4	93.461%	72.897%	28.937%	
Same Well Depth - Using its own coeff.	15.611%	18.495%	25.857%	24.432%
Same Well Depth - Coeff from 6506/11-A-1		46.342%	31.861%	47.195%
Same Well Depth - Coeff from 6506/11-A-2	24.136%		34.778%	44.247%
Same Well Depth - Coeff from 6506/11-A-3	23.082%	42.136%		42.888%
Same Well Depth - Coeff from 6506/11-A-4	23.420%	41.470%	27.485%	
Multiple Reg. - Section by section using its own coeff.	20.297%	20.495%	11.576%	9.331%
Multiple Reg. - geological groups using its own coeff.	18.106%	8.550%	4.259%	13.707%
Multiple Reg. - Drilling ahead ROP prediction	22.251%	12.010%	9.624%	14.291%

MAPE Values

Investigating ROP Dependent Parameters	Case 1 26.772%	Case 2 +27.272%	Case 3 55.728%	Case 4 54.893%	
Drilling Ahead ROP Prediction - 6506/11-A-1	100% 41.026%	91.3% 46.328%	90.7% 46.960%	87.3% 47.278%	75% 87.116%
Drilling Ahead ROP Prediction - 6506/11-A-4	100% 33.561%	90.1% 33.606%	85.4% 33.740%	75.3% 63.657%	

Table 6.2: MAPE values for MSE and D-exponent models.

MAPE Values	Well			
MSE & D-Exponent Models	6506/11-A-1	6506/11-A-2	6506/11-A-3	6506/11-A-4
MSE - values from 6506/11-A-1		69.130%	41.884%	37.410%
MSE - values from 6506/11-A-2	108.966%		162.428%	185.035%
MSE - values from 6506/11-A-3	70.800%	53.113%		80.819%
MSE - values from 6506/11-A-4	41.504%	67.937%	55.100%	
D-exp. - values from 6506/11-A-1		110.481%	131.966%	103.263%
D-exp. - values from 6506/11-A-2	67.929%		170.155%	119.238%
D-exp. - values from 6506/11-A-3	62.009%	54.324%		120.114%
D-exp. - values from 6506/11-A-4	66.542%	57.287%	51.086%	

Table 6.3: MAPE values for Warren model.

MAPE Values	Well			
Warren Model	6506/11-A-1	6506/11-A-2	6506/11-A-3	6506/11-A-4
Warren model - Entire well using its own const.	35.121%	53.612%	125.164%	163.276%
Warren model - Section by section using its own const.	31.634%	35.616%	15.431%	23.312%
Warren model - Geological groups using its own const.	23.351%	15.703%	17.416%	19.061%
Warren model - Geological groups const. from 6506/11-A-1		47.935%	111.911%	235.566%
Warren model - Geological groups const. from 6506/11-A-2	78.399%		30.969%	55.166%
Warren model - Geological groups const. from 6506/11-A-3	124.598%	25.761%		170.085%
Warren model - Geological groups const. from 6506/11-A-4	50.231%	38.085%	57.488	
Warren Model - Drilling Ahead ROP prediction	22.664%	14.085%	10.073%	17.175%

Table 6.4: MAPE values for Bourgoyne & Young model.

MAPE Values	Well			
Bourgoyne & Young Model	6506/11-A-1	6506/11-A-2	6506/11-A-3	6506/11-A-4
Bourgoyne & Young model - Entire well using its own coeff.	44.595%	44.293%	27.079%	25.471%
Modified B&Y model - Entire well using its own coeff.	42.863%	21.814%	23.862%	23.239%
Modified B&Y - Entire well coeff. from 6506/11-A-1		44.803	50.569%	
Modified B&Y - Entire well coeff. from 6506/11-A-2	84.532%		79.144%	
Modified B&Y - Entire well coeff. from 6506/11-A-3	233.873%	122.412%		
Modified B&Y model - Section by section using its own coeff.	14.317%	21.339%	9.890%	15.664%
Modified B&Y model - Geological groups using its own coeff.	5.435%	24.045%	4.260%	9.748%
Modified B&Y - Drilling Ahead ROP prediction	-5.843%	6.230%	7.166%	10.069%

Table 6.1 - 6.4 confirms the qualitative modelling reporting in chapter 5. The results obtained in the tables above are quite alternating. However, when the wells are plotted with the coefficients or constants extracted from their own well, gave the best estimation of field ROPs, indicating that they had least errors.

By observing the results achieved in this subchapter its clearly that "Drilling Ahead ROP Prediction for Geological Groups" application gives by far the best correlation between the field and modelled ROP. When this application is applied using Modified Bourgoyne & Young model it gives least errors.

Furthermore, MSE and D-exponent models in Table 6.2, gave the worst correlation to field ROP. Additionally when wells where plotted with coefficients from the nearby and far-away wells often tend to perform the poorest results which are the case in Multiple regression, Warren and Bourgoyne & Young models.

Note – **Well 6506/11-A-4 was not modelled with Modified Bourgoyne & Young model using nearby and far-away coefficient values.**

6.2   Time Analysis

Time analysis is used to evaluate how fast drilling is completed for the wells used for modelling in real-life application. An advantage with time analysis is that it allows models which initially had variations or fluctuations in their data points to still predict ROP and drilling time with decent results. The assumption in this analysis is there is no non-productive time.

When calculating the drilling time for the proposed models generated in Chapter 5 the drilling time for each depth interval is calculated, where the well is divided into multiple depth consisting of two and two data points. The time interval for each intervals are then added together to get the whole drilling time for the well. This steps are performed for both field and modelled ROPs, and the total time deviation is calculated. The equation used for time analysis to present the time deviation are presented in equation 6.2.

$$t_i = 2 \frac{(MD)_{i+1} - (MD)_i}{(ROP)_{i+1} + (ROP)_i}$$

$$T = \sum_{i=1}^{n} t_i$$

$$\% \, Time \; Deviation = \frac{T_{Mod} - T_{Field}}{T_{Field}} \tag{6.2}$$

Where, t_i is time for each section and T is total time.

Table 6.5: Time deviation values for Multiple regression model.

Time Deviation (%)	Well			
Multiple Regression Model	6506/11-A-1	6506/11-A-2	6506/11-A-3	6506/11-A-4
Multiple Reg. model - Using its own coeff.	-21.072%	-58.613%	-11.865%	+17.465%
Multiple Reg. model - Coeff from 6506/11-A-1		-36.910%	+8.690%	-41.204%
Multiple Reg. model - Coeff from6506/11-A-2	-40.754%		-19.321%	-36.980%
Multiple Reg. model - Coeff from 6506/11-A-3	-43.057%	-43.326%		-28.642%
Multiple Reg. model - Coeff from 6506/11-A-4	-41.139%	-28.830%	+10.676%	
Same Well Depth - Using its own coeff.	-5.798%	-5.299%	-11.825%	-8.175%
Same Well Depth - Coeff from 6506/11-A-1		-28.609%	-9.454%	-25.355%
Same Well Depth - Coeff from 6506/11-A-2	+13.029%		+4.619%	-6.472%
Same Well Depth - Coeff from 6506/11-A-3	-4.505%	-22.383%		-25.237%
Same Well Depth - Coeff from 6506/11-A-4	+20.732%	-2.193%	+15.463%	
Multiple Reg. - Section by section using its own coeff.	+3.252%	-15.535%	-4.148%	-3.628%
Multiple Reg. - geological groups using its own coeff.	-11.543%	+5.198%	-50.098	-2.514%
Multiple Reg. - Drilling ahead ROP prediction	-16.779%	+5.698%	-5.644%	-4.805%

Time Deviation (%)					
Investigating ROP Dependent Parameters	Case 1 -58.613%	Case 2 +51.047%	Case 3 -23.581%	Case 4 -23.747%	
Drilling Ahead ROP Prediction - 6506/11-A-1	100% -19.638%	91.3% -27.379%	90.7% -28.035%	87.3% -28.401%	75% -43.482%
Drilling Ahead ROP Prediction - 6506/11-A-4	100% +1.365%	90.1% 11.476%	85.4% +52.535%	75.3% -37.463%	

Table 6.6: Time deviation values for MSE and D-exponent models.

Time Deviation (%)	Well			
MSE & D-Exponent Models	6506/11-A-1	6506/11-A-2	6506/11-A-3	6506/11-A-4
MSE - values from 6506/11-A-1		+6.875%	+50.837%	+6.265%
MSE - values from 6506/11-A-2	+24.045%		-40.419%	-30.780%
MSE - values from 6506/11-A-3	-9.577%	+116.287%		-16.630%
MSE - values from 6506/11-A-4	+1.818%	+200.076%	+53.532%	
D-exp. - values from 6506/11-A-1		-25.607%	+37.782%	-12.716%
D-exp. - values from 6506/11-A-2	+84.745%		-13.761%	-28.660
D-exp. - values from 6506/11-A-3	+116.990%	+247.259%		+176.339%
D-exp. - values from 6506/11-A-4	+70.311%	+155.716%	+166.964	

Table 6.7: Time deviation values for Warren model.

Time Deviation (%)	Well			
Warren Model	6506/11-A-1	6506/11-A-2	6506/11-A-3	6506/11-A-4
Warren model - Entire well using its own const.	-1.746%	-7.568%	-37.543%	-31.996%
Warren model - Section by section using its own const.	-1.048%	-2.162%	+0.307%	-32.425%
Warren model - Geological groups using its own const.	+1.700%	-3.526%	+20.556%	+9.201%
Warren model - Geological groups const. from 6506/11-A-1		+62.590%	+507.315%	+332.851%
Warren model - Geological groups const. from 6506/11-A-2	-34.353%		+52.501%	-20.314%
Warren model - Geological groups const. from 6506/11-A-3	-54.015%	-16.287%		-39.104%
Warren model - Geological groups const. from 6506/11-A-4	-13.220%	+63.470%	+153.940	
Warren Model - Drilling Ahead ROP prediction	+12.415%	+4.669%	+1.571%	-2.374%

Table 6.8: Time deviation values for Bourgoyne & Young model.

Time Deviation (%)	Well			
Bourgoyne & Young Model	6506/11-A-1	6506/11-A-2	6506/11-A-3	6506/11-A-4
Bourgoyne & Young model - Entire well using its own coeff.	-18.581%	-13.843%	-8.167%	-4.445%
Modified B&Y model - Entire well using its own coeff.	-17.693%	-5.714%	-6.915%	-4.020%
Modified B&Y - Entire well coeff. from 6506/11-A-1		+23.031%	-3.218%	
Modified B&Y - Entire well coeff. from 6506/11-A-2	-23.863%		-11.956%	
Modified B&Y - Entire well coeff. from 6506/11-A-3	-52.390%	47.790%		
Modified B&Y model - Section by section using its own coeff.	-5.260%	7.208%	+1.646%	-1.807%
Modified B&Y model - Geological groups using its own coeff.	+0.809%	+13.007%	-0.087%	-0.323%
Modified B&Y - Drilling Ahead ROP prediction	-2.901%	-6.715%	+5.949%	-1.968%

The results obtained in the tables below provide positive and negative percent-values for time deviation. The positive terms mean the estimated drilling time is greater than actual drilling time, while negative values are the other way around.

When using time analysis the results above are very alter when the different ROP models are implemented under different applications, where most of them required less drilling time. Time analysis also confirms the observations calculations made in previous work in both chapter 5 and MAPE analysis, where the best results are obtained when a well is plotted with its own constants or coefficients.

Modified Bourgoyne & Young model gave the least errors, where especially "Drilling ahead ROP Prediction" had the most accurate time estimation. Additionally, in this analysis "Drilling ahead ROP Prediction" for Multiple regression, Warren and Bourgoyne & Young models estimated time very good.

Note – **Well 6506/11-A-4 was not modelled with Modified Bourgoyne & Young model using nearby and far-away coefficient values.**

The wells that are modelled with MSE and D-exp models show the largest time deviation. Also as we observed in chapter 5 and MAPE analysis, the largest time differences occur when wells are modelled with constants or coefficients from nearby and far-way wells.

6.3 Parametric Sensitivity Analysis

Parametric sensitivity analysis was performed in order to figure out the most controlling drilling parameters on ROP. The main objective of this study is to optimize these drilling parameters to increase the rate of penetration and reduce drilling time. The overall results are reflected in the reduction of drilling cost. By doing so, the idea behind this is to give the operator which parameters it should increase or decrease when the new section is to be drilled.

The parametric analysis will be applied on Nordaland Group in well 6506/11-A-1. Furthermore, the drilling parameters used for analysis are WOB, torque and RPM where they are increased or decreased with 10% depending on their coefficient values. The single drilling parameter and their combined effects on the average ROP and drilling time are shown in Figures 6.1 and 6.2, respectively.
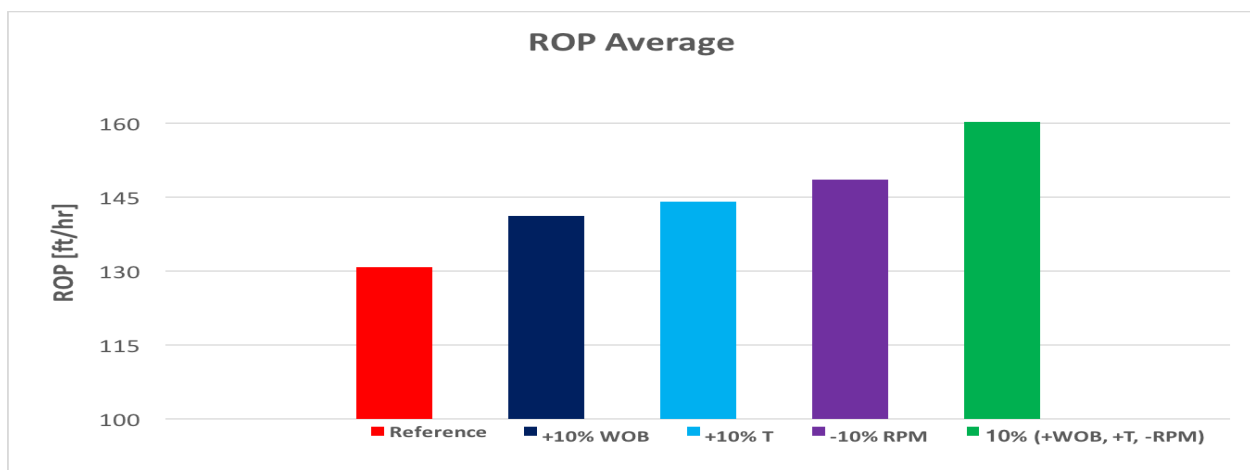
Figure 6.1: Average ROP for Nordaland Group.
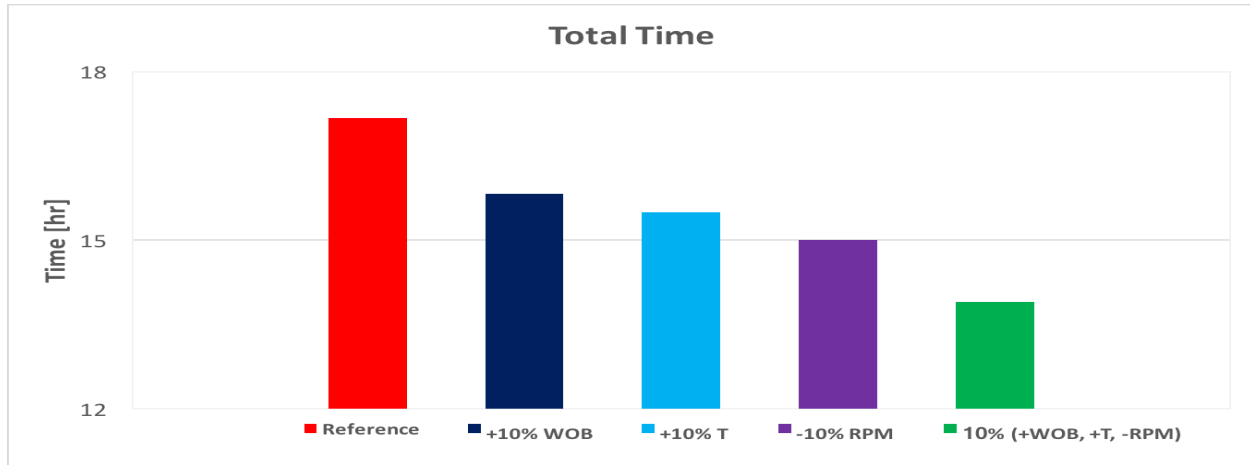
Figure 6.2: Total time for Nordaland Group.

The red column represents the reference well where the values extracted from field measurements. The dark-blue and light-blue columns are 10 % increase in WOB and torque. While purple is a 10 % decrease in RPM. The green bar shown at the left end of the figure is the result of the combined effect of drilling parameters.

Finally, it is clear that the value of the regression coefficient values will directly contribute to the optimization of the ROP. By optimizing WOB, T and RPM with 10 % will increase the average drilling rate by 22 % and reduce the drilling time by 17 %.

6.4 ROP Optimization Process

The main purpose of the ROP optimization is selecting the appropriate drilling parameters, which provides an increase in ROP and reduce drilling time per footage. For this first, verify the applicability of the models. Based on the model coefficients, a sensitivity study will be carried out by changing the drilling parameter to ±10 %. Here, the single and the combined effect of parameters based evaluation will be compared to the reference measured data. Finally, the thesis work presents the systematic optimization procedures.

1. First of all well-to-well and stratigraphic correlations are performed.

2. Remove data outliers and apply Moving average filter to the drilling data.

3. The proposed ROP models are applied in order to generate the coefficients used for modelling.

4. The coefficients values are implemented on either its own, nearby or far-away wells, where it is compared to the field ROP of that well.

5. The model proposed can be verified on modelling pre-drilled nearby and far-away wells and also on its own well.

6. For the pre-drilled well average time and ROP are then computed where it is used as reference well. Furthermore, average time and ROP are then compared to the next well.

7. The drilling parameters with the greatest attribution on the ROP models are defined. These parameters are the ones that have the highest positive coefficient values. Furthermore, a sensitivity analysis is carried out, where the parameters are increased or decreased. Finally, average time and ROP are calculated where they are compared to the reference well specified in step 4.

8. Lastly, if combining larger and smaller coefficient values are combined more sensitivity analysis can be performed. The best-case scenario and the most realistic can be implemented in the future well.

6.5   Uncertainties in Modelling

- Quality of the drilling data parameters.

- Failure or non-optimal LWD and MWD-tools. Also, uncertainties in measurements may cause errors.

- Lateral geological variations between the proposed wells

7. Summary and Conclusion

7.1 Summary

Based on the time and ROP analysis, the application of the models are compared. The model testing was on its own well, nearby and far-away wells. The summary is shown in Table 7.1. The color code in green is to represent an excellent prediction, yellow is very good and red is poor. Results show that the application of coefficients derived from its own well exhibited excellent prediction. However, when applying on the nearby and far-away wells, the prediction is not as on its own well. The main reason is due to the lateral geological variations in terms of type and strength. The analysis shows that Multiple regression, MSE and D-exponent based ROP models works good on the nearby-well. On the other hand, the rest of the models show poor both on the nearby and far-away wells.

Table 7.1: Modelling limitation summary for the ROP models.

ROP Model	On its own	Nearby	Far-away
Multiple Regression Model (Chapter 5.1)	- Excellent in modelling by entire well, section by section and geological groups.	- Very good in modelling by entire well. Poor modelling by section by section and geological groups.	- Acceptable in modelling by entire well. Poor modelling section by section and geological groups.
MSE (Chapter 5.2)	- Excellent correlation between field and calculated UCS values.	- Acceptable correlation between field and calculated ROP	- Acceptable correlation between field and calculated ROP
D-Exponent Model (Chapter 5.3)	- Excellent correlation between field and calculated D-exp values.	- Acceptable correlation between field and calculated ROP	- Poor correlation between field and calculated ROP
Warren Model (Chapter 5.4)	- Very good in modelling by section by section and geological groups. Poor in entire well	- Acceptable in modelling by section by section. Poor modelling by entire well and geological groups.	- Poor in modelling by entire well, section by section and geological groups.
Bourgoyne & Young Model (Chapter 5.5)	- Acceptable in modelling by entire well.	- Poor in modelling by entire well.	- Poor in modelling by entire well.
Modified Bourgoyne & Young Model (Chapter 5.6)	- Excellent in modelling by entire well, section by section and geological groups.	- Poor in modelling by entire well, section by section and geological groups.	- Acceptable in modelling by entire well. Poor in modelling by section by section and geological groups

7.2   Conclusion

In this thesis work, six models were implemented on four different modelling scenarios. The model predictions were evaluated on its own, nearby and far-away wells. The overall analysis results are summarized as:

- The primary step is to filter out the raw drilling data with respect to spikes and removal of outliers. It is important to remove unmeasured and data with noises before modelling is performed.

- The application of the models on the wells derived from its own well gave excellent predictions. However, applying on distance wells reduced the prediction.

- Modelling based on geological group found out to be the best on all the ROP models.

- All the modelling methods are found to be applicable on "Drilling ahead ROP Prediction for Geological Groups" scenario. The drilling ahead method can be applied on entire well data, section by section and geological groups data. From the analysis, it was found out that modelling part with 90 % of data gave excellent results. Decreasing the number of data points will deteriorate the prediction.

- Best drilling ahead prediction is the geological groups based modelling and application. For instance, modelling 90 % of the geological sections (eg. Shetland Group) and applying the model for the 10 % of the Shetland Group, the model works magnificently. The values obtained from one geological group can't be used in predicting other geological groups. Therefore, each group is modelled with their own values extracted from 90 % of the drilling data.

- In this thesis, the Bourgoyne & Young model was modified by including torque, formation pressure and mud weight drilling parameters. The results showed excellent predictions, when using drilling ahead with 90 % of the data. The Modified Bourgoyne & Young provided the best and most reliable results.

References

[1] John Rogers Smith et al. "Energy demand creates new opportunities and challenges for drilling". In: *Journal of Canadian Petroleum Technology* 40.05 (2001).

[2] Australian Drilling Industry Training Committee Limited. *Drilling: the manual of methods, applications, and management*. CRC Press, 1997.

[3] R Teale. "The concept of specific energy in rock drilling". In: *International journal of rock mechanics and mining sciences & geomechanics abstracts*. Vol. 2. 1. Elsevier. 1965, pp. 57–73.

[4] Hussain Rabia. *Oilwell drilling engineering : principles and practice*. London, 1985.

[5] *Rotary drilling mechanism*. `https://petrowiki.org/File:Devol2_1102final_Page_223_Image_0002.png`. (Accessed on 06/30/2020).

[6] Robert F Mitchell. *Fundamentals of Drilling Engineering*. eng. SPE Textbook Series. 2010. ISBN: 9781555633387.

[7] Amardeep Singh and Sujian Huang. *Cutting structure for roller cone drill bits*. US Patent 6,374,930. Apr. 2002.

[8] *Introduction to Roller-Cone and Polycrystalline Diamond Drill Bits*. Vol. 2. Richardson, Tex.: Society of Petroleum Engineers, 2015, p. 221. ISBN: 9781555631260.

[9] *File:Devol2 1102final Page 242 Image 0001.png - PetroWiki*. `https://petrowiki.org/File:Devol2_1102final_Page_242_Image_0001.png`. (Accessed on 06/30/2020).

[10] EK Morton, WR Clements, et al. "The Role of Bit Type and Drilling Fluid Type in Drilling Performance". In: *International Meeting on Petroleum Engineering*. Society of Petroleum Engineers. 1986.

[11] Paolo Macini et al. "Bit performance evaluation revisited by means of bit Index and formation drillability catalogue". In: *SPE/IADC Middle East Drilling and Technology Conference*. Society of Petroleum Engineers. 2007.

[12] TM Warren, WK Armagost, et al. "Laboratory drilling performance of PDC bits". In: *SPE drilling engineering* 3.02 (1988), pp. 125–135.

120

[13]   Adam T Bourgoyne Jr, FS Young Jr, et al. "A multiple regression approach to optimal drilling and abnormal pressure detection". In: *Society of Petroleum Engineers Journal* 14.04 (1974), pp. 371–384.

[14]   A.T. Bourgoyne and F.S. Young. "A Multiple Regression Approach to Optimal Drilling and Abnormal Pressure Detection". eng. In: *Society of Petroleum Engineers Journal* 14.04 (1974), pp. 371–384. ISSN: 0197-7520.

[15]   Mahmood Bataee, Mohammadreza Kamyab, Rahman Ashena, et al. "Investigation of various ROP models and optimization of drilling parameters for PDC and roller-cone bits in shadegan oil field". In: *International oil and gas conference and exhibition in China*. Society of Petroleum Engineers. 2010.

[16]   Xuyue Chen et al. "Real-time optimization of drilling parameters based on mechanical specific energy for rotating drilling with positive displacement motor in the hard formation". In: *Journal of Natural Gas Science and Engineering* 35 (2016), pp. 686–694.

[17]   *Typical response of ROP to WOB.* `https : / / www . researchgate . net / figure / Typical – response – of – ROP – to – WOB _ fig1 _ 328649750 ? fbclid = IwAR3BfiLP – lSekvPkJgqi0nShILBU_WpcNhJK5HfZdrsEg8PQIGox8qmNzpo`. (Accessed on 03/05/2020).

[18]   Kien Ming Lim, GA Chukwu, et al. "Bit hydraulics analysis for efficient hole cleaning". In: *SPE Western Regional Meeting*. Society of Petroleum Engineers. 1996.

[19]   Ong Kai Sheng. "PDC Bit Hydraulic and Mud Rheological Simulation to Model Pressure Drop across Bit". In: IRC. 2016.

[20]   *Assessment of Mechanical Specific Energy Aimed at Improving Drilling Inefficiencies and Minimize Wellbore Instability.* `https : / / www . longdom . org / open – access / assessment-of-mechanical-specific-energy-aimed-at-improving-drillinginefficiencies-and-minimize-wellbore-instability-2157-7463-1000309.pdf?fbclid=IwAR1dzdS_jymOlLyMAHVlB2Huh59xG1fPsOz1nQnPwgR8w88Mi0POAfMd_nc`. (Accessed on 03/03/2020).

[21]   Williams Kingsley Amadi, Ibiye Iyalla, et al. "Application of mechanical specific energy techniques in reducing drilling cost in deepwater development". In: *SPE Deepwater Drilling and Completions Conference*. Society of Petroleum Engineers. 2012.

[22]   Fred E Dupriest, William L Koederitz, et al. "Maximizing drill rates with real-time surveillance of mechanical specific energy". In: *SPE/IADC Drilling Conference*. Society of Petroleum Engineers. 2005.

[23]   RC Pessier, MJ Fear, et al. "Quantifying common drilling problems with mechanical specific energy and a bit-specific coefficient of sliding friction". In: *SPE Annual Technical Conference and Exhibition*. Society of Petroleum Engineers. 1992.

[24]   Yully P Solano et al. "A modified approach to predict pore pressure using the d exponent method:: an example from the carbonera formation, colombia". In: *CTF-Ciencia, Tecnologia y Futuro* 3.3 (2007), pp. 103–112.

[25]   JR Jorden, OJ Shirley, et al. "Application of drilling performance data to overpressure detection". In: *Journal of Petroleum Technology* 18.11 (1966), pp. 1–387.

[26]   P. Ablard et al. "The expanding role of mud logging". In: *Oilfield Review* 24.1 (2012), pp. 24–41. ISSN: 09231730.

[27]   Bill Rehm, Ray McClendon, et al. "Measurement of formation pressure from drilling data". In: *Fall Meeting of the Society of Petroleum Engineers of AIME*. Society of Petroleum Engineers. 1971.

[28]   TM Warren et al. "Penetration rate performance of roller cone bits". In: *SPE Drilling Engineering* 2.01 (1987), pp. 9–18.

[29]   EM Galle, HB Woods, et al. "Best constant weight and rotary speed for rotary rock bits". In: *Drilling and production practice*. American Petroleum Institute. 1963.

[30]   Tommy M Warren et al. "Drilling model for soft-formation bits". In: *Journal of Petroleum Technology* 33.06 (1981), pp. 963–970.

[31]   Mohammad Rastegar et al. "Optimization of multiple bit runs based on ROP models and cost equation: a new methodology applied for one of the Persian Gulf carbonate fields". In: *IADC/SPE Asia Pacific Drilling Technology Conference and Exhibition*. Society of Petroleum Engineers. 2008.

[32]   MG Bingham. "How rock properties are related to drilling". In: *Oil & Gas Journal* 62.94 (1964), pp. 96–98.

[33] Behrad Rashidi, Geir Hareland, Runar Nygaard, et al. "Real-time drill bit wear prediction by combining rock energy and drilling strength concepts". In: *Abu Dhabi International Petroleum Exhibition and Conference*. Society of Petroleum Engineers. 2008.

[34] Andreas Nascimento et al. "Mathematical modeling applied to drilling engineering: an application of Bourgoyne and young ROP model to a presalt case study". In: *Mathematical Problems in Engineering* 2015 (2015).

[35] Ekaterina Wiktorski, Artem Kuznetcov, Dan Sui, et al. "ROP optimization and modeling in directional drilling process". In: *SPE Bergen One Day Seminar*. Society of Petroleum Engineers. 2017.

[36] DT Kutas et al. "A study of the applicability of Bourgoyne & Young ROP model and fitting Reliability through Regression". In: *International petroleum technology conference*. International Petroleum Technology Conference. 2015.

[37] Determining Bourgoyne and Young Model Coefficients Using Genetic. "Algorithm to Predict Drilling Rate". In: *Journal of Applied Sciences* 8.17 (2008), pp. 3050–3054.

[38] *Field - Factpages - NPD*. https://factpages.npd.no/en/field/pageview/all/4966234. (Accessed on 03/29/2020).

[39] *Morvin - equinor.com*. https://www.equinor.com/en/what-we-do/norwegian-continental-shelf-platforms/morvin.html. (Accessed on 03/29/2020).

[40] *Moving Average Filter in Python and Matlab – GaussianWaves*. https://www.gaussianwaves.com/2010/11/moving-average-filter-ma-filter-2/?fbclid=IwAR1Cb7CyQUBAA2bWmibrROveFjeYCNDuSaoOPduDjA-FoVSopgy-PI3-J_k. (Accessed on 03/03/2020).

[41] S Deviant. *The Practically Cheating Statistics Handbook–*. Lulu. com, 2011.

[42] Barbara G Tabachnick, Linda S Fidell, and Jodie B Ullman. *Using multivariate statistics*. Vol. 5. Pearson Boston, MA, 2007.

[43] Douglas C Montgomery, Elizabeth A Peck, and G Geoffrey Vining. *Introduction to linear regression analysis*. Vol. 821. John Wiley & Sons, 2012.

[44] G Hareland, PR Rampersad, et al. "Drag-bit model including wear". In: *SPE Latin America/Caribbean Petroleum Engineering Conference*. Society of Petroleum Engineers. 1994.

8. APPENDICES

8.1 APPENDIX A

The main objective of the modelling and testing process was to figure out which modeling and application methods are practically acceptable. The results presented in the main report are the qualified ones. However, applications on the nearby and far-away wells found out to be poor. Therefore in the following Appendix, the poor results are displayed.

- Chapter 8.1.1: Multiple Regression Model - Modelling by Geological Groups on Nearby and Far-Away Wells.

- Chapter 8.1.2: Warren Model - Modelling by Entire Well Data on Nearby and Far-Away Wells.

- Chapter 8.1.3: Warren Model - Modelling by Section by Sections on Nearby and Far-Away Wells.

- Chapter 8.1.4: Warren Model - Modelling by Geological Groups on Nearby and Far-Away Wells.

- Chapter 8.1.5: Bourgoyne & Young - Modelling by Entire Well Data on Nearby and Far-Away Wells.

- Chapter 8.1.6: Modified Bourgoyne & Young - Modelling by Entire Well Data on Nearby and Far-Away Wells.

- Chapter 8.1.7: Modified Bourgoyne & Young - Modelling by Section by Section on Nearby and Far-away Wells.

- Chapter 8.1.8: Modified Bourgoyne & Young - Modelling by Geological Groups on Nearby and Far-Away Wells.

Multiple Regression Model - Modelling by Geological Groups on Nearby and Far-Away Wells
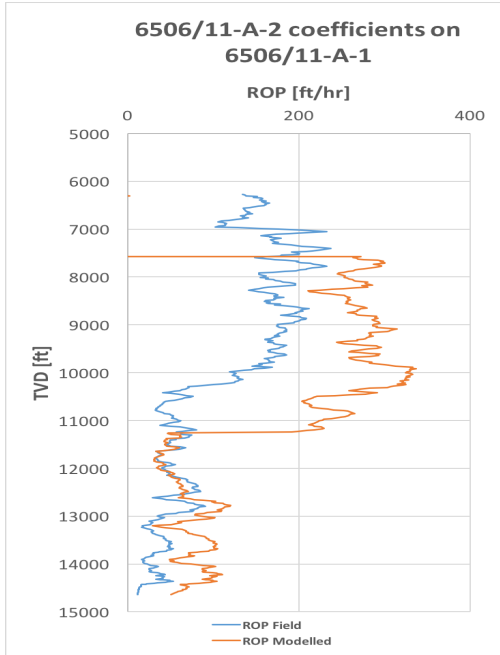
(a) using 6506/11-A-2 regression coeff. values
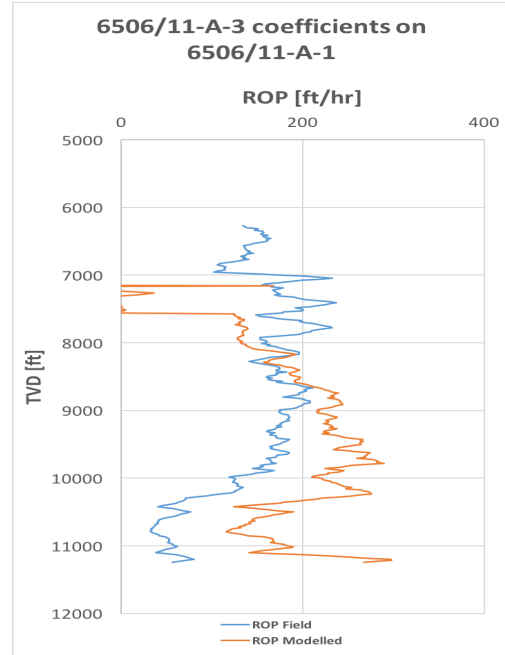
(b) using 6506/11-A-3 regression coeff. values
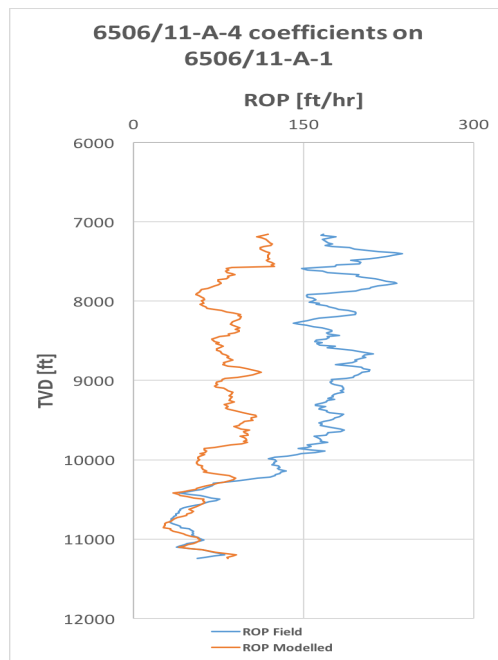
(c) using 6506/11-A-4 regression coeff. values

Figure 8.1: Warren Model - Nearby and far-away regression coeff. on 6506/11-A-1.
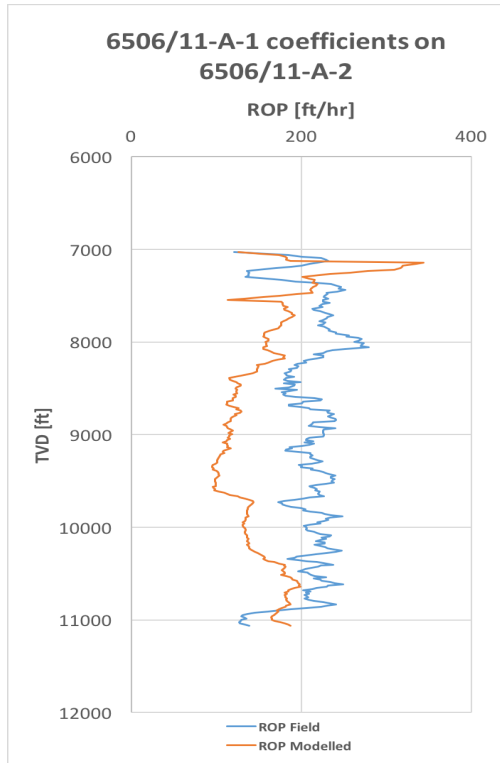
(a) using 6506/11-A-1 regression coeff. values
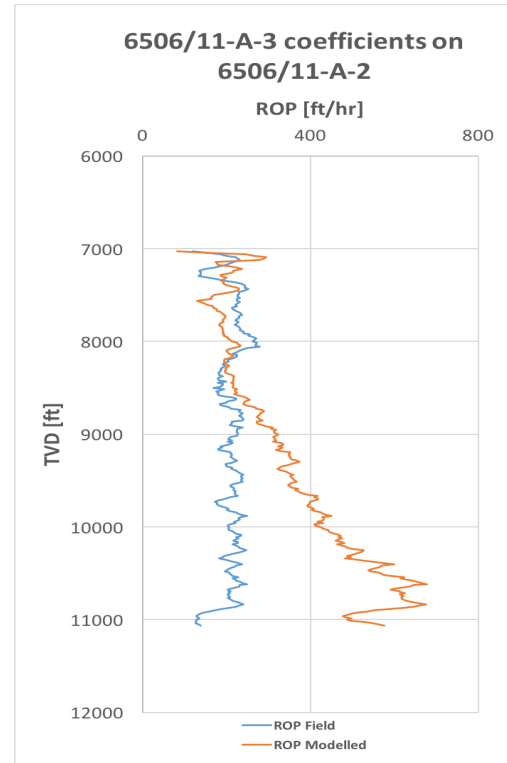
(b) using 6506/11-A-3 regression coeff. values
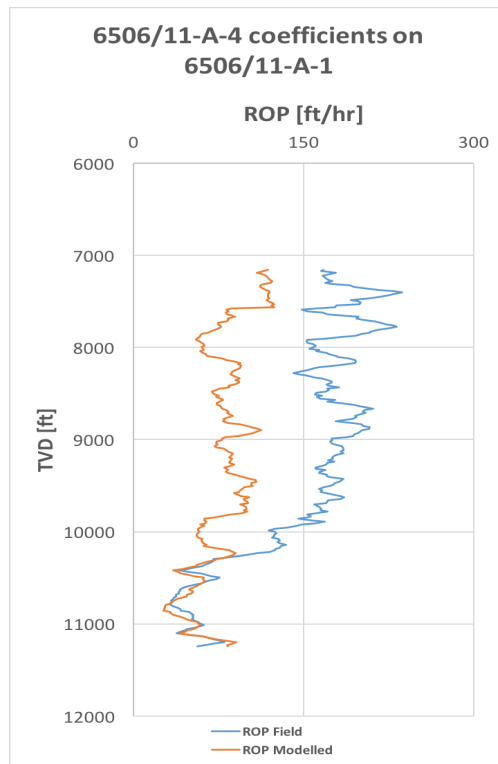
(c) using 6506/11-A-4 regression coeff. values

Figure 8.2: Warren Model - Nearby and far-away regression coeff. on 6506/11-A-2.
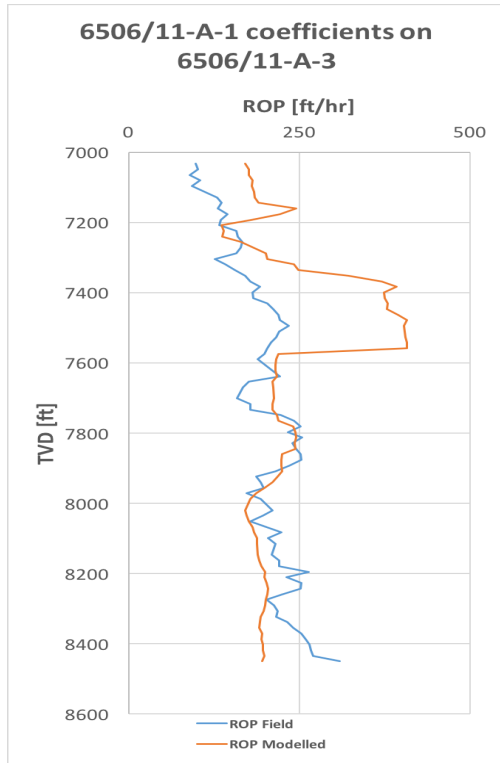
(a) using 6506/11-A-1 regression coeff. values
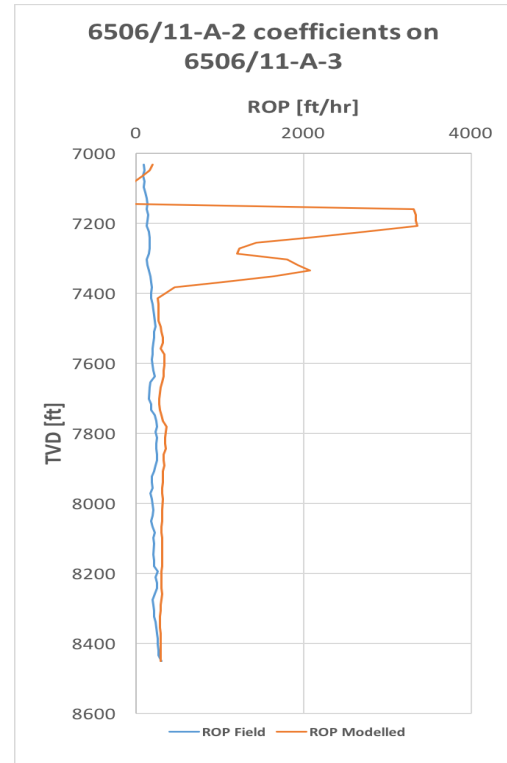
(b) using 6506/11-A-2 regression coeff. values
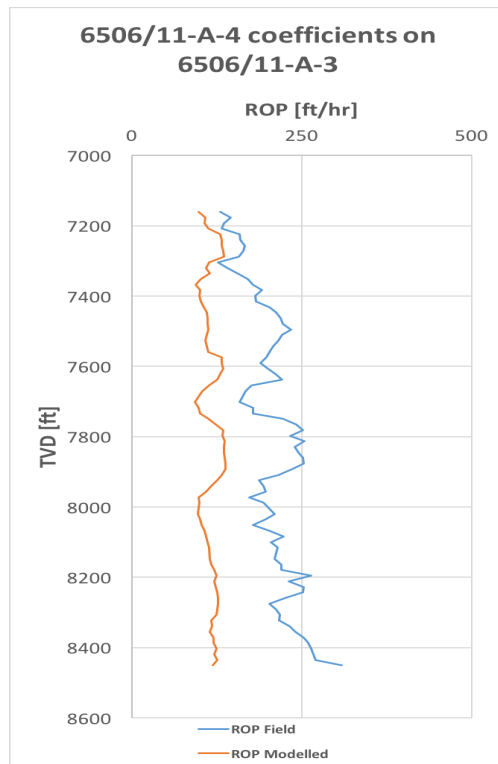
(c) using 6506/11-A-4 regression coeff. values

Figure 8.3: Warren Model - Nearby and far-away regression coeff. on 6506/11-A-3.
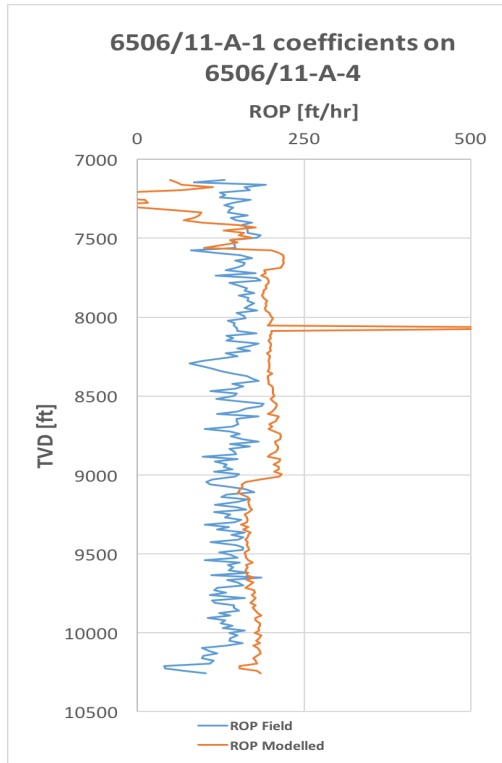
(a) using 6506/11-A-1 regression coeff. values
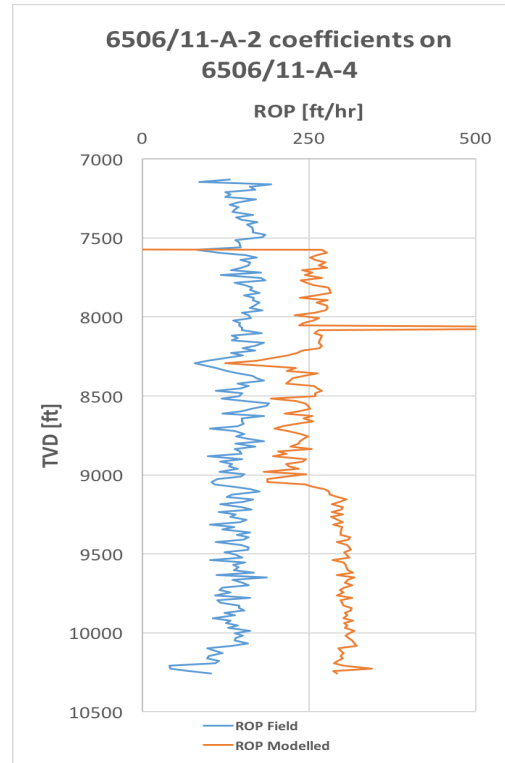
(b) using 6506/11-A-2 regression coeff. values
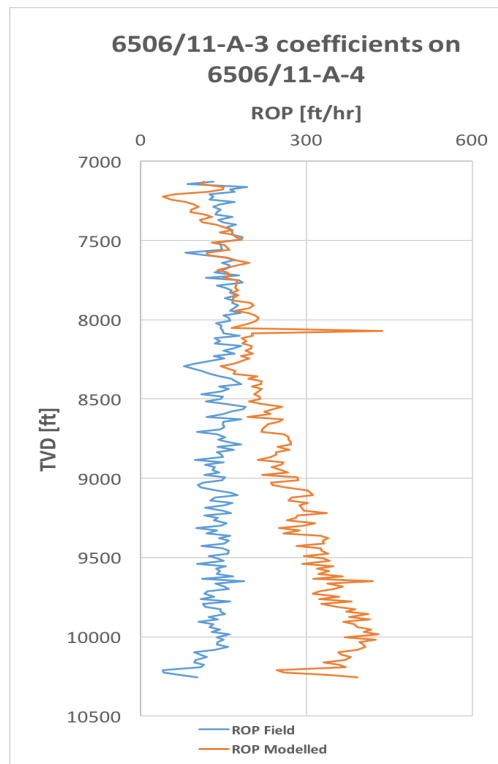
(c) using 6506/11-A-3 regression coeff. values

Figure 8.4: Warren Model - Nearby and far-away regression coeff. on 6506/11-A-4.

Warren Model - Modelling by Entire Well Data on Nearby and Far-Away Wells
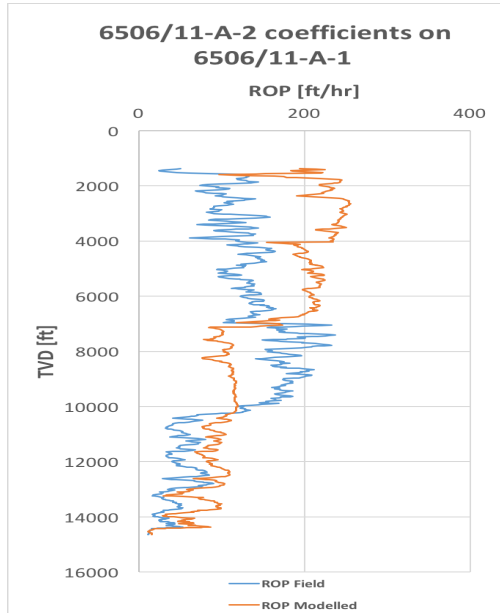
(a) using 6506/11-A-2 Warren constant values
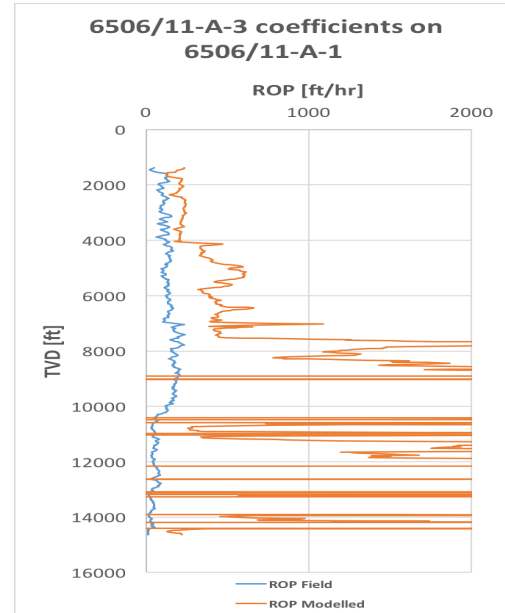
(b) using 6506/11-A-3 Warren constant values
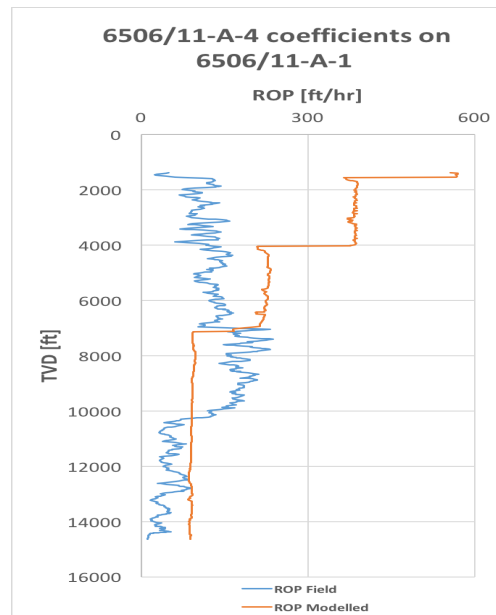
(c) using 6506/11-A-4 Warren constant values

Figure 8.5: Warren Model - Nearby and far-away Warren constants on 6506/11-A-1 for hole sections.
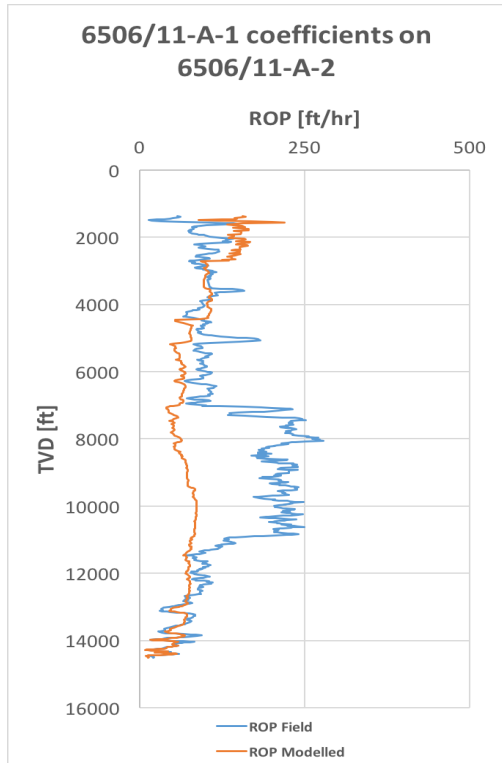
(a) using 6506/11-A-1 Warren constant values
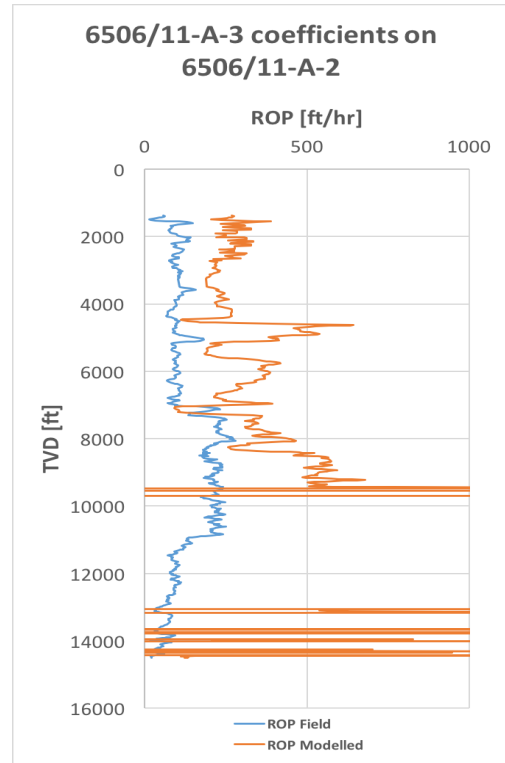
(b) using 6506/11-A-3 Warren constant values
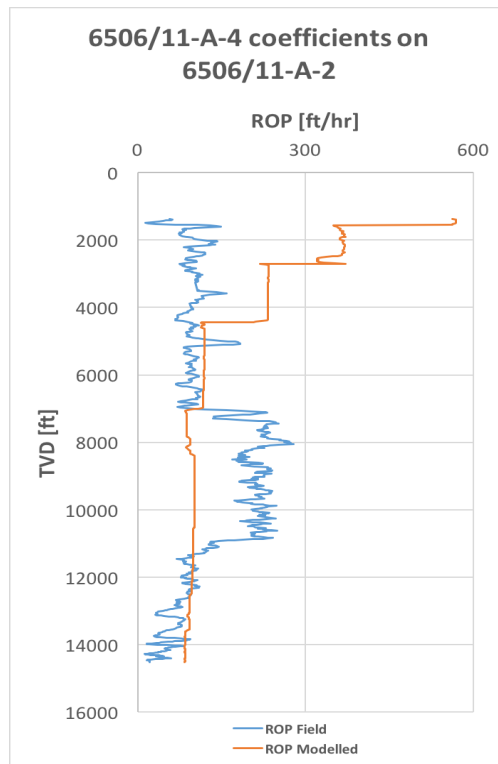
(c) using 6506/11-A-4 Warren constant values

Figure 8.6: Warren Model - Nearby and far-away Warren constants on 6506/11-A-2 for hole sections.
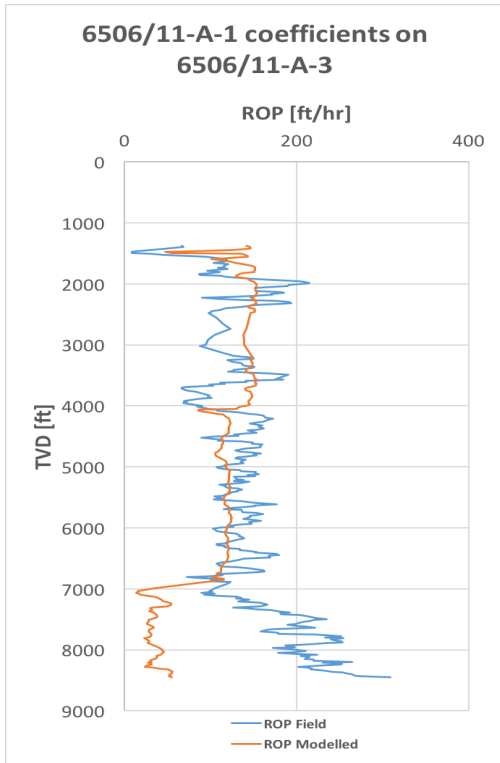
(a) using 6506/11-A-1 Warren constant values
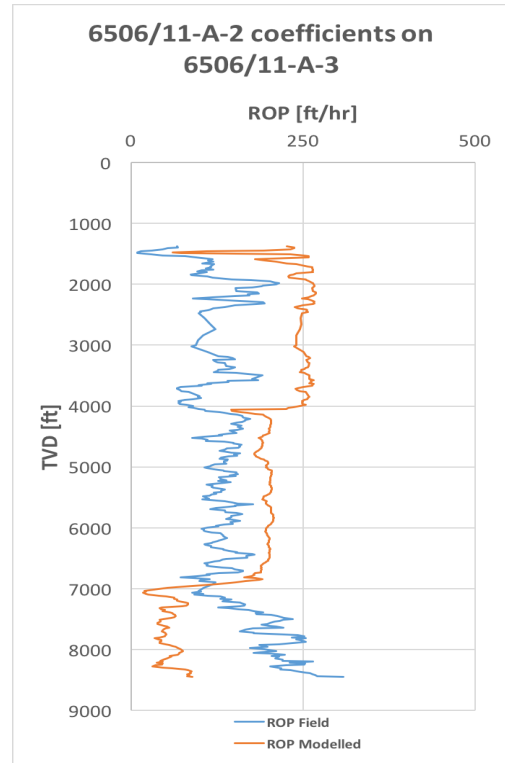
(b) using 6506/11-A-2 Warren constant values
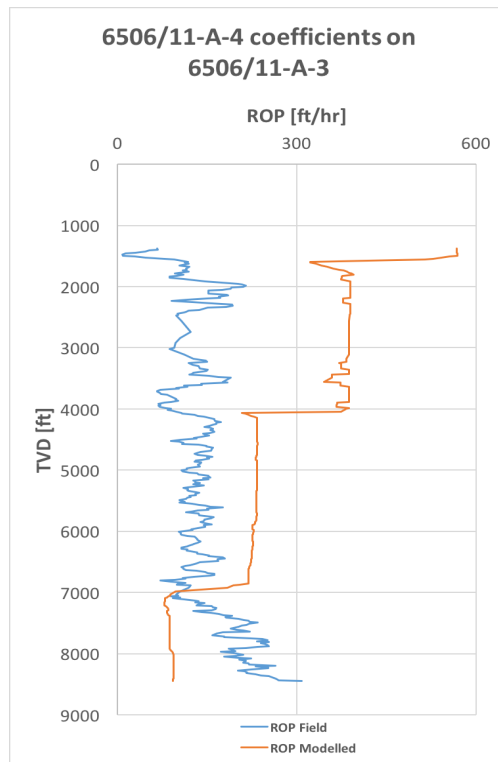
(c) using 6506/11-A-4 Warren constant values

Figure 8.7: Warren Model - Nearby and far-away Warren constants on 6506/11-A-3 for hole sections.
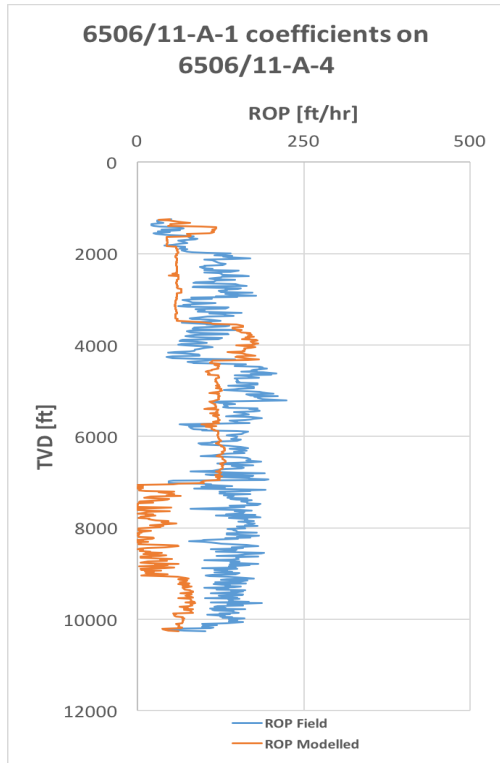
(a) using 6506/11-A-1 Warren constant values
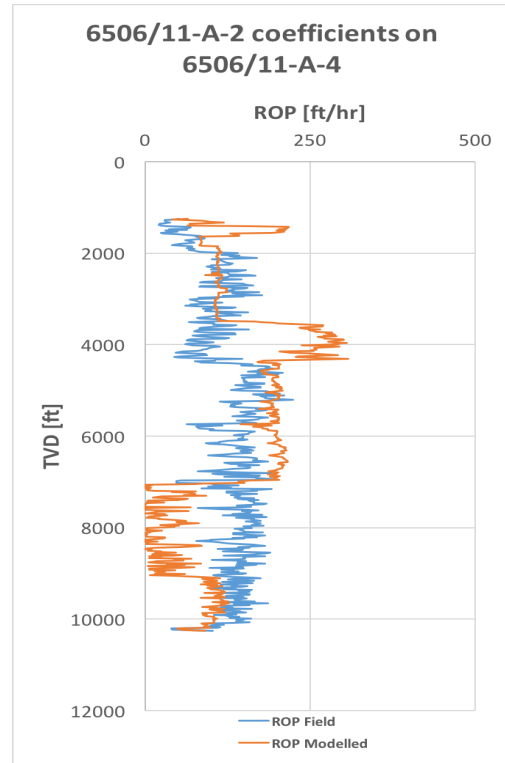
(b) using 6506/11-A-2 Warren constant values
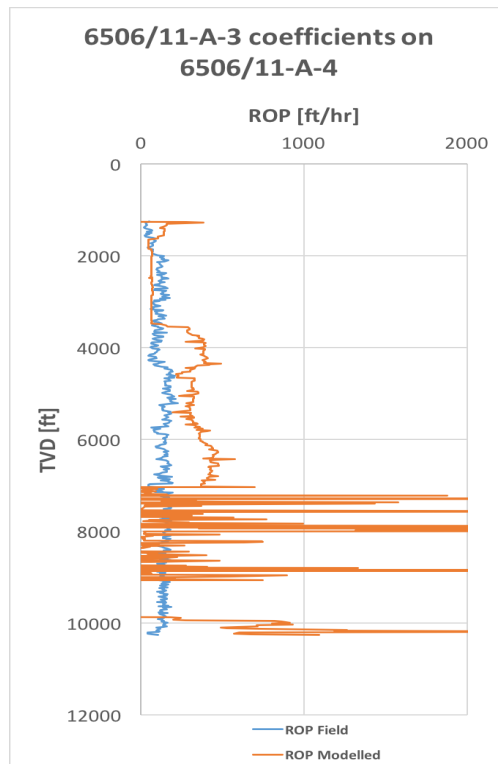
(c) using 6506/11-A-3 Warren constant values

Figure 8.8: Warren Model - Nearby and far-away Warren constants on 6506/11-A-4 for hole sections.

132

Warren Model - Modelling by Section by Sections on Nearby and Far-Away Wells

(a) using 6506/11-A-2 Warren constant values

(b) using 6506/11-A-3 Warren constant values

(c) using 6506/11-A-4 Warren constant values

Figure 8.9: Warren model - Nearby and far-away constants on 6506/11-A-1 for hole sections.
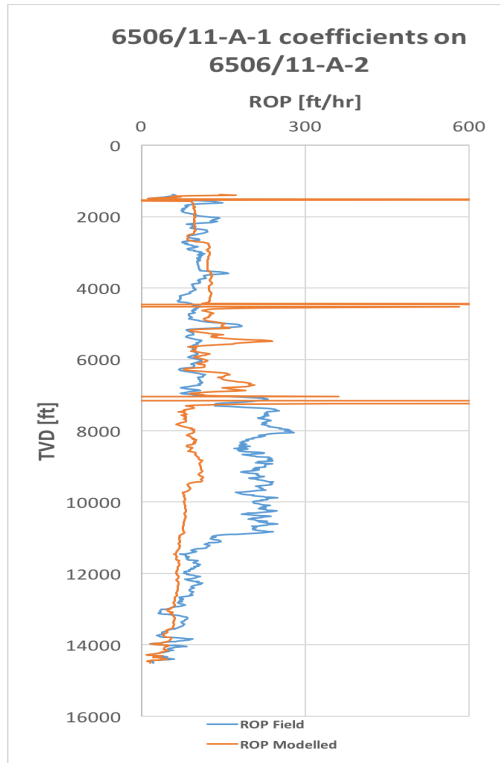
(a) using 6506/11-A-1 Warren constant values
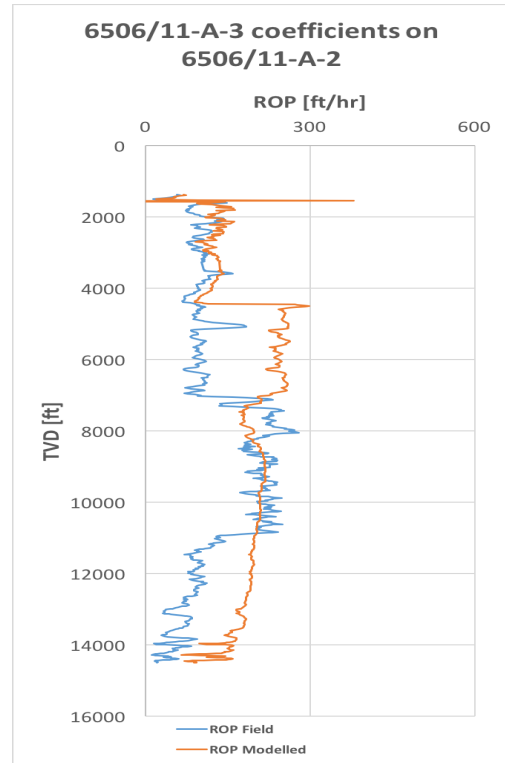
(b) using 6506/11-A-3 Warren constant values
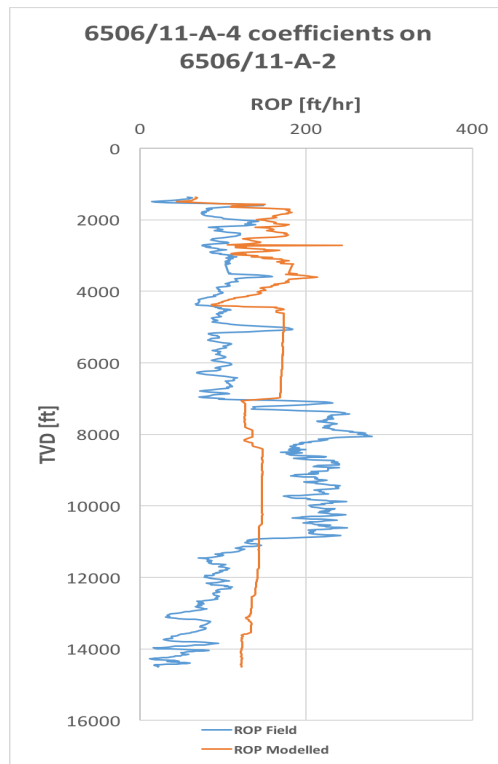
(c) using 6506/11-A-4 Warren constant values

Figure 8.10: Warren model - Nearby and far-away constants on 6506/11-A-2 for hole sections.
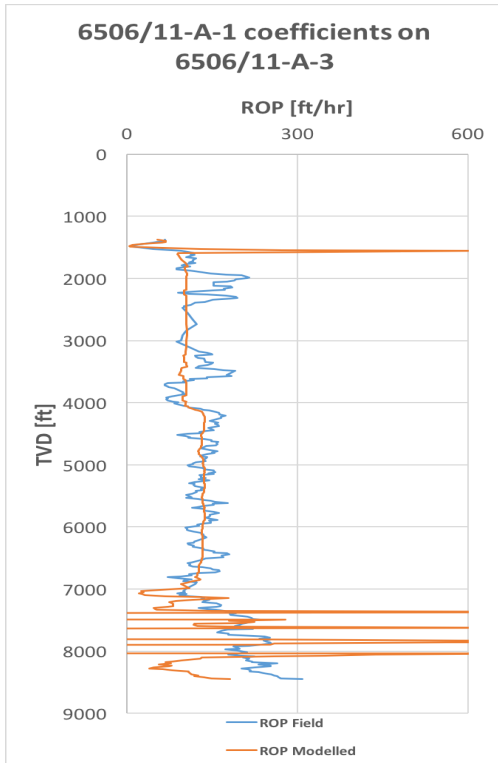
(a) using 6506/11-A-1 Warren constant values
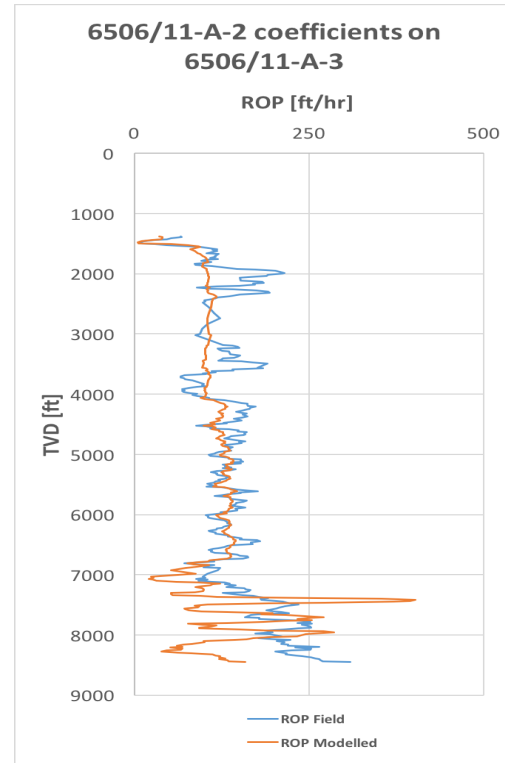
(b) using 6506/11-A-2 Warren constant values
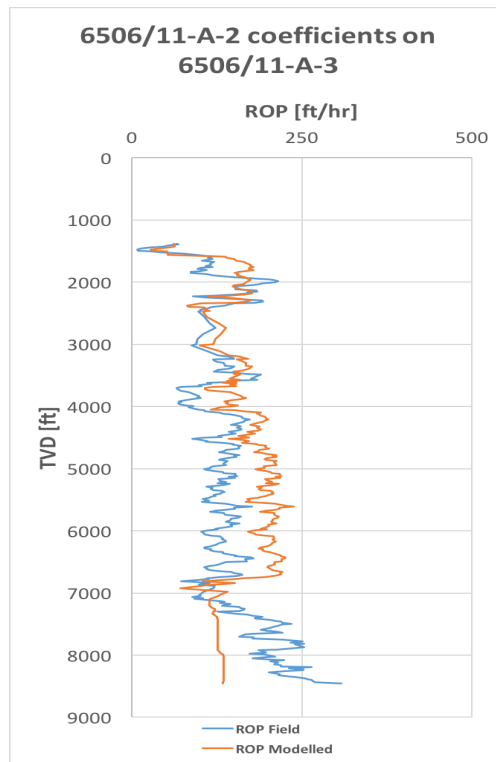
(c) using 6506/11-A-4 Warren constant values

Figure 8.11: Warren model - Nearby and far-away constants on 6506/11-A-3 for hole sections.
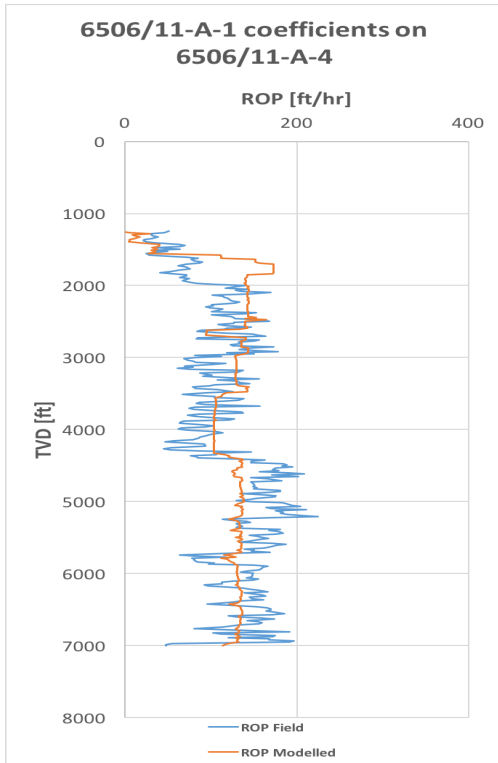
(a) using 6506/11-A-1 Warren constant values
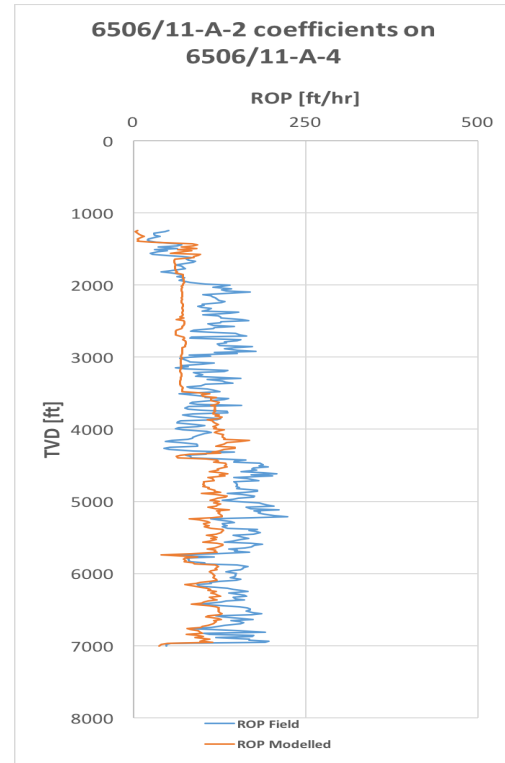
(b) using 6506/11-A-2 Warren constant values
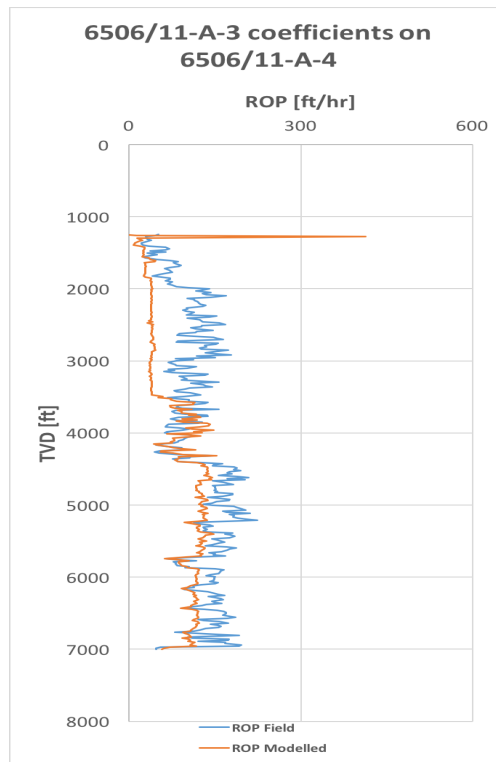
(c) using 6506/11-A-3 Warren constant values

Figure 8.12: Warren model - Nearby and far-away constants on 6506/11-A-4 for hole sections.

Warren Model - Modelling by Geological Groups on Nearby and Far-Away Wells
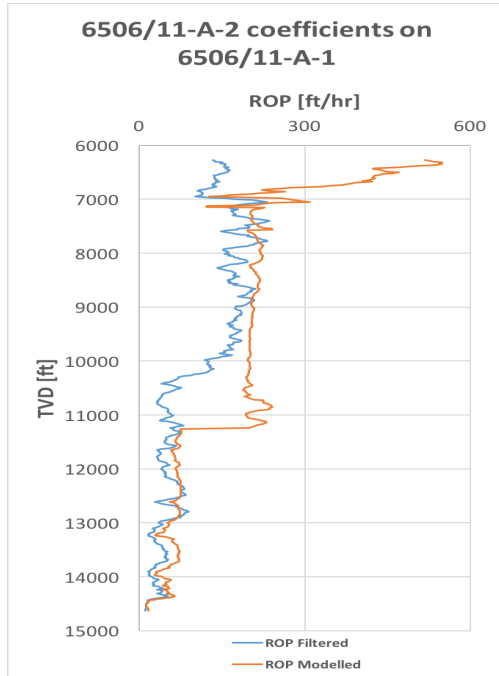
(a) using 6506/11-A-2 Warren constant values
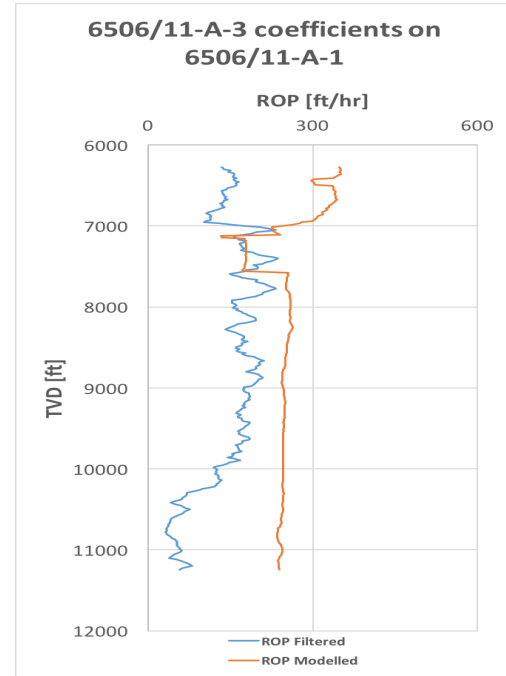
(b) using 6506/11-A-3 Warren constant values
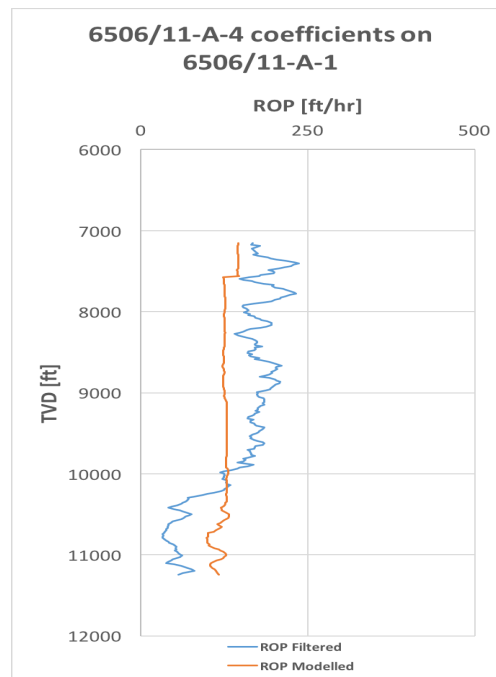
(c) using 6506/11-A-4 Warren constant values

Figure 8.13: Warren Model - Nearby and far-away Warren constants on 6506/11-A-1 for geological groups.
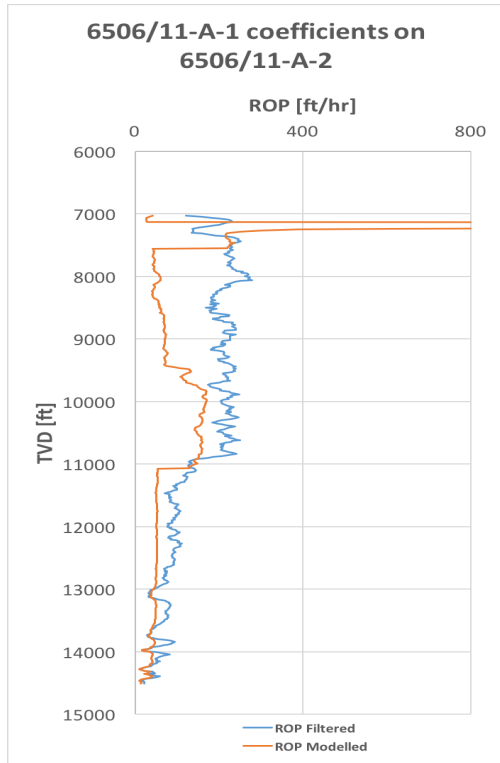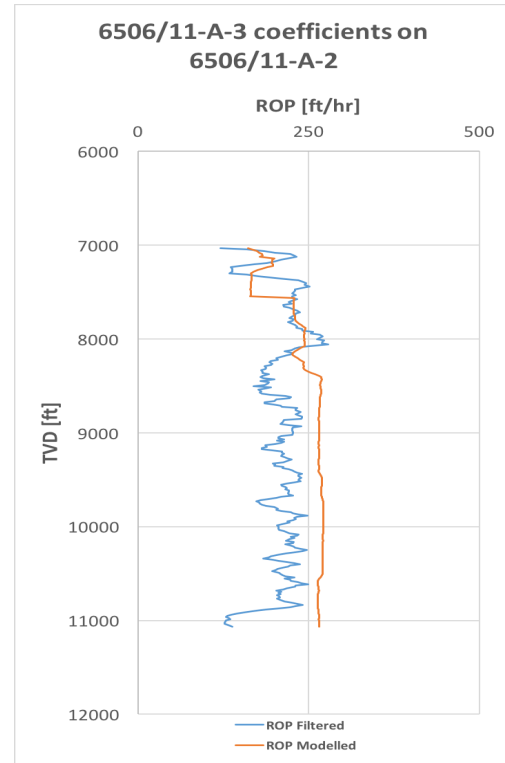
(a) using 6506/11-A-1 Warren constant values

(b) using 6506/11-A-3 Warren constant values
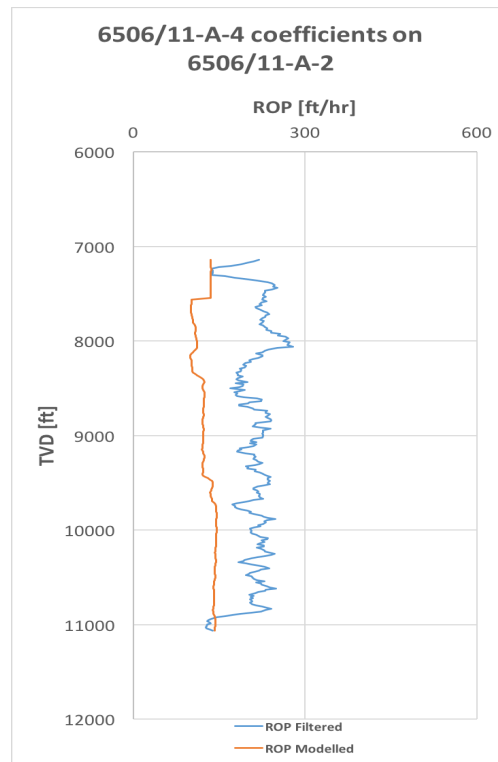
(c) using 6506/11-A-4 Warren constant values

Figure 8.14: Warren Model - Nearby and far-away Warren constants on 6506/11-A-2 for geological groups.
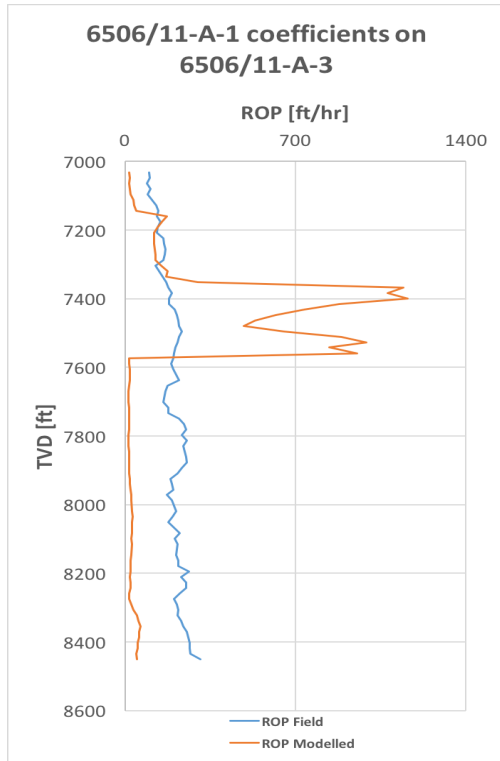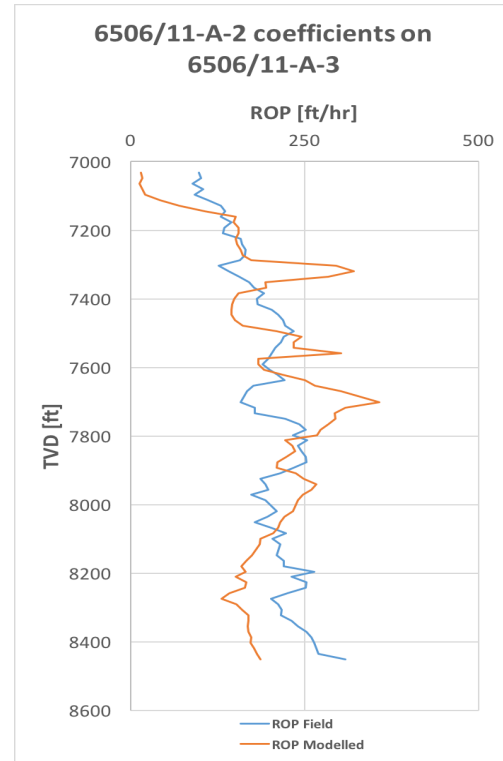
(a) using 6506/11-A-1 Warren constant values

(b) using 6506/11-A-2 Warren constant values
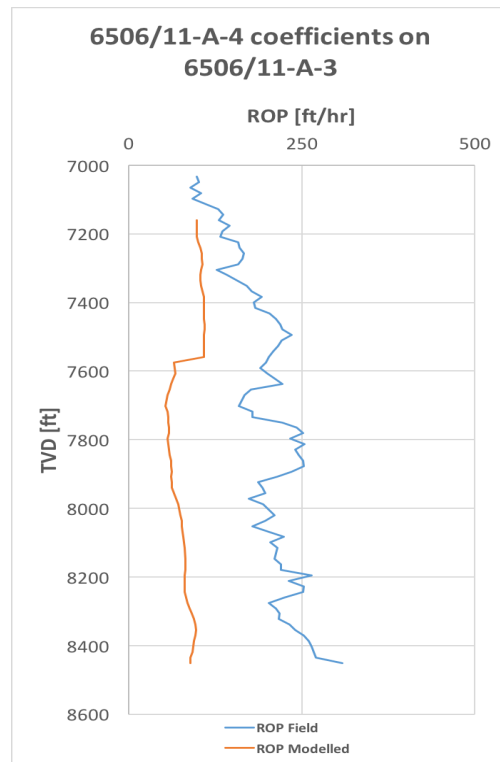
(c) using 6506/11-A-4 Warren constant values

Figure 8.15: Warren Model - Nearby and far-away Warren constants on 6506/11-A-3 for geological groups.
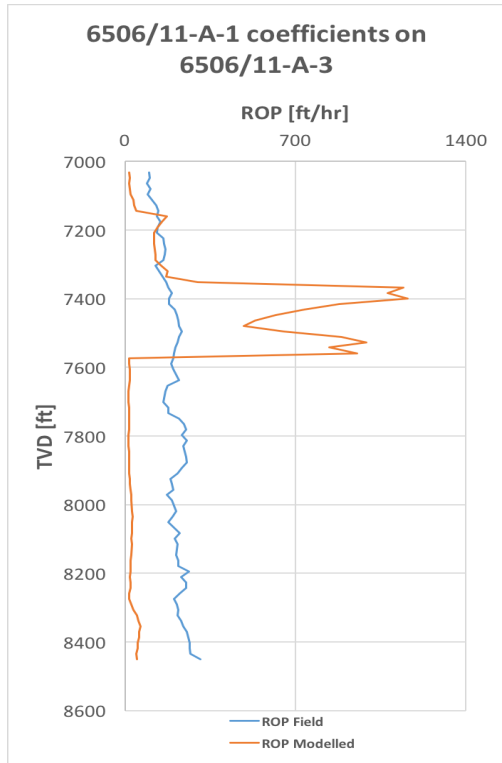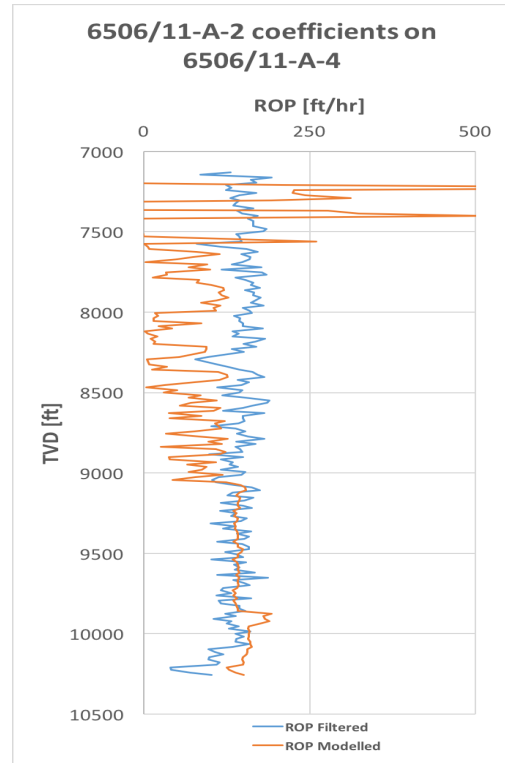
(a) using 6506/11-A-1 Warren constant values

(b) using 6506/11-A-2 Warren constant values
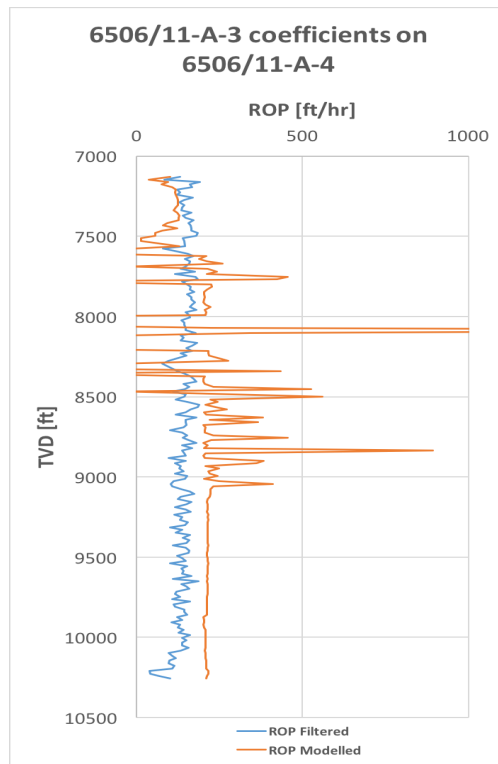
(c) using 6506/11-A-3 Warren constant values

Figure 8.16: Warren Model - Nearby and far-away Warren constants on 6506/11-A-4 for geological groups.

Bourgoyne & Young - Modelling by Entire Well Data on Nearby and Far-Away Wells
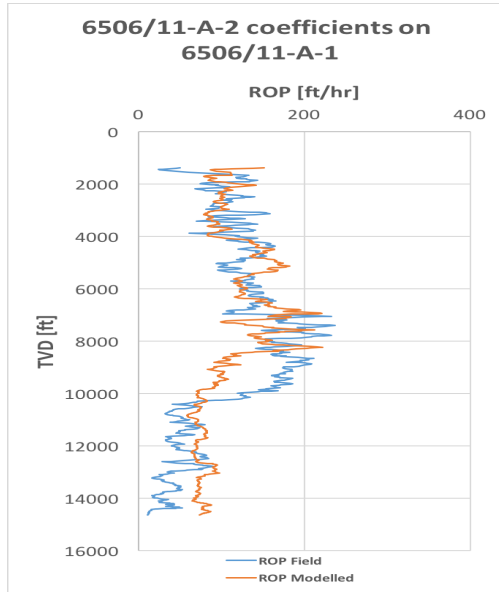
(a) using 6506/11-A-2 B&Y coefficient values
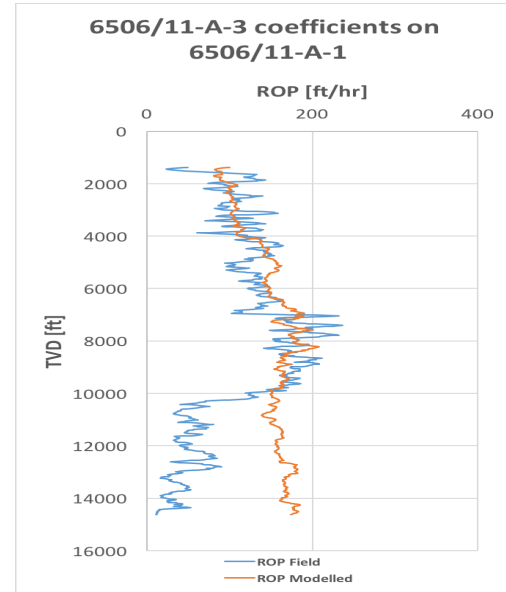
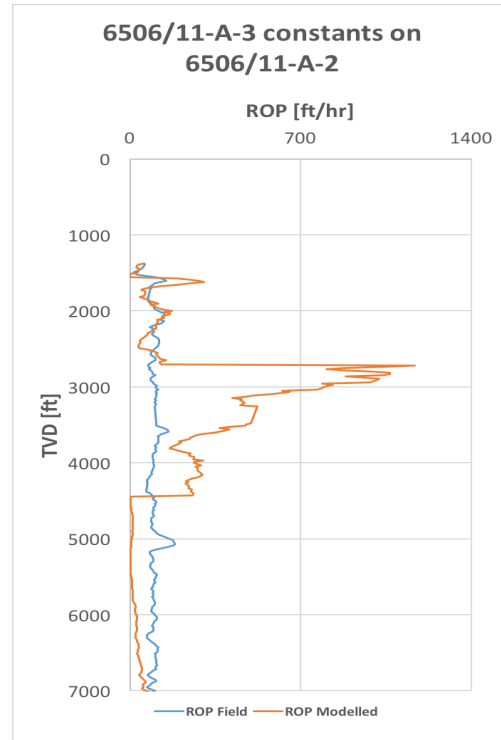**(b)** using 6506/11-A-3 B&Y coefficient values
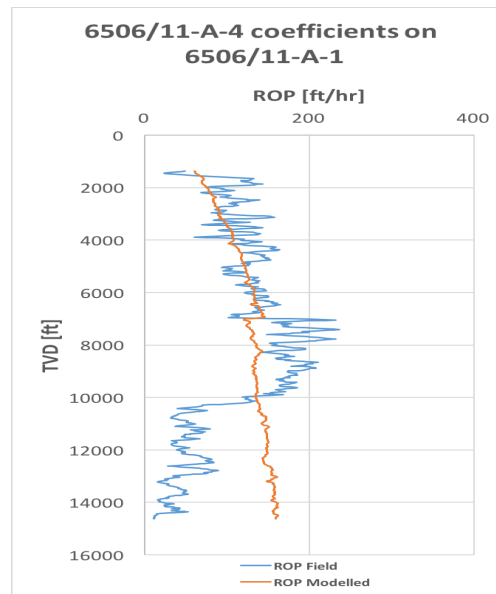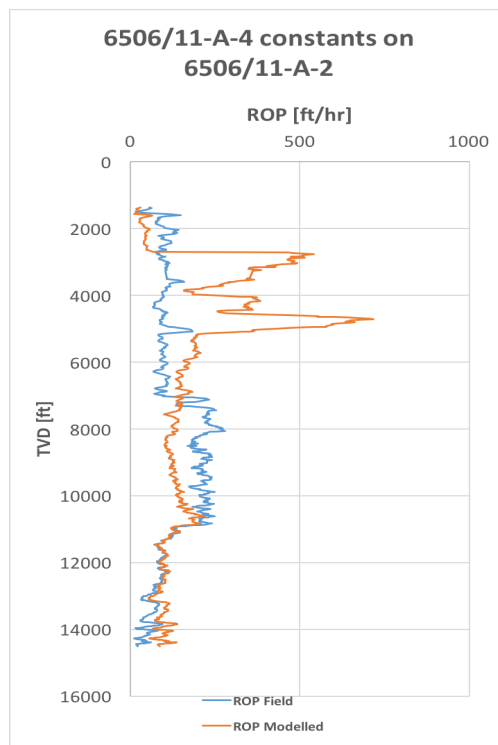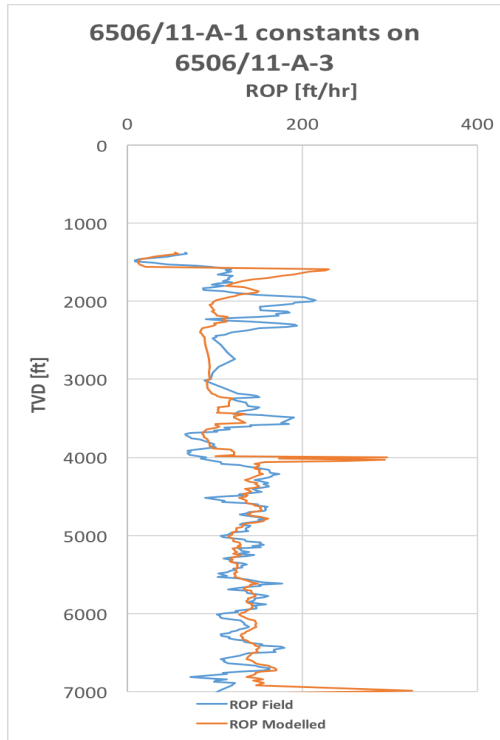
(c) using 6506/11-A-4 B&Y coefficient values

Figure 8.17: Bourgoyne & Young Model - Nearby and far-away B&Y coeff. on 6506/11-A-1 for entire well data.
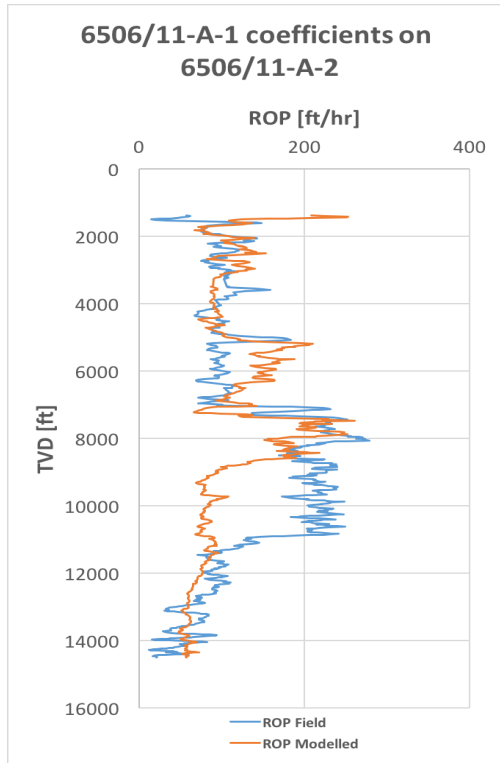
(a) using 6506/11-A-1 B&Y coefficient values
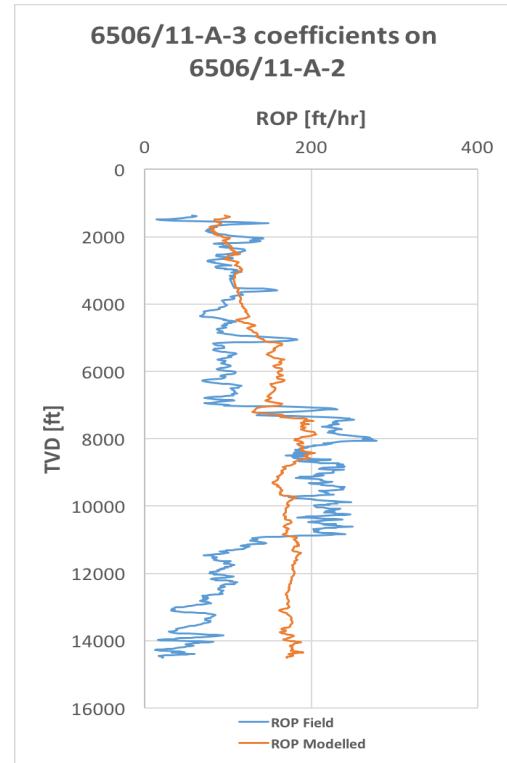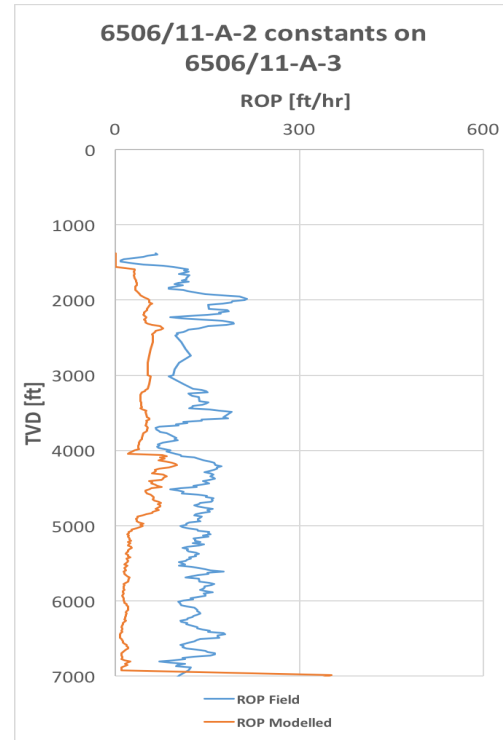
(b) using 6506/11-A-3 B&Y coefficient values
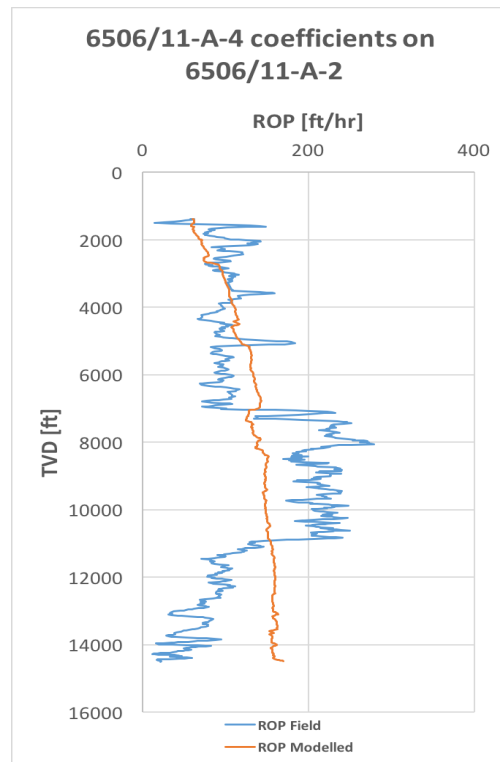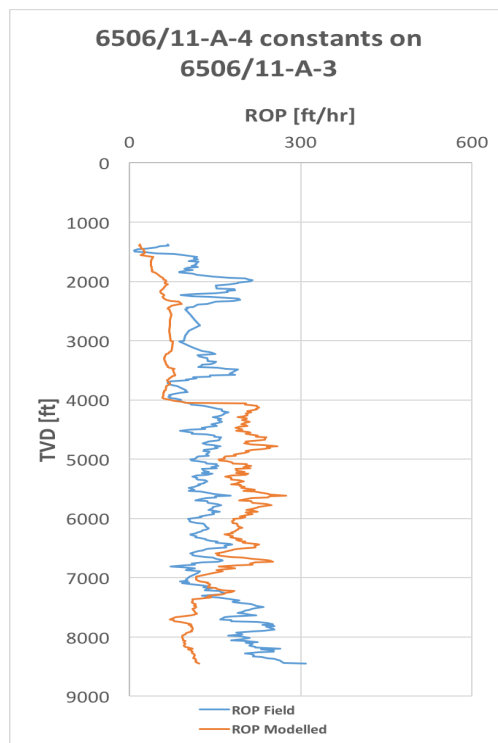
(c) using 6506/11-A-4 B&Y coefficient values

Figure 8.18: Bourgoyne & Young Model - Nearby and far-away B&Y coeff. on 6506/11-A-2 for entire well data.
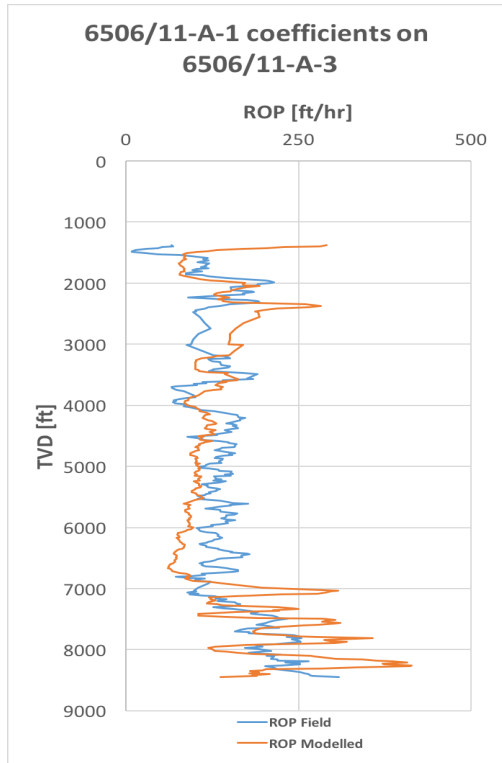
142

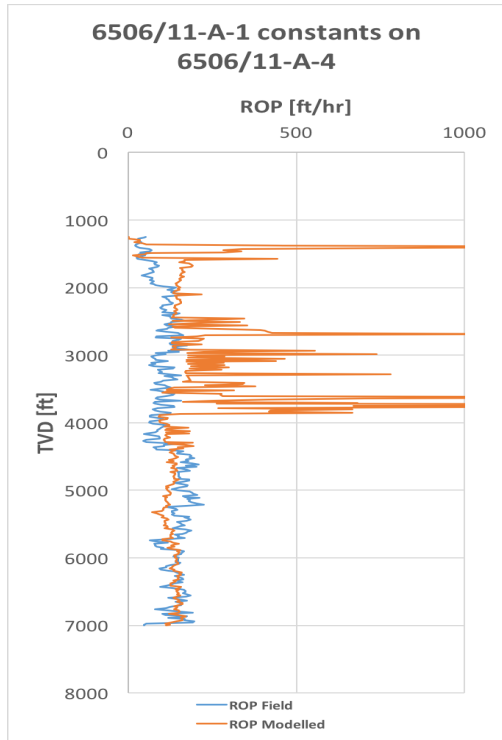**(a)** using 6506/11-A-1 B&Y coefficient values
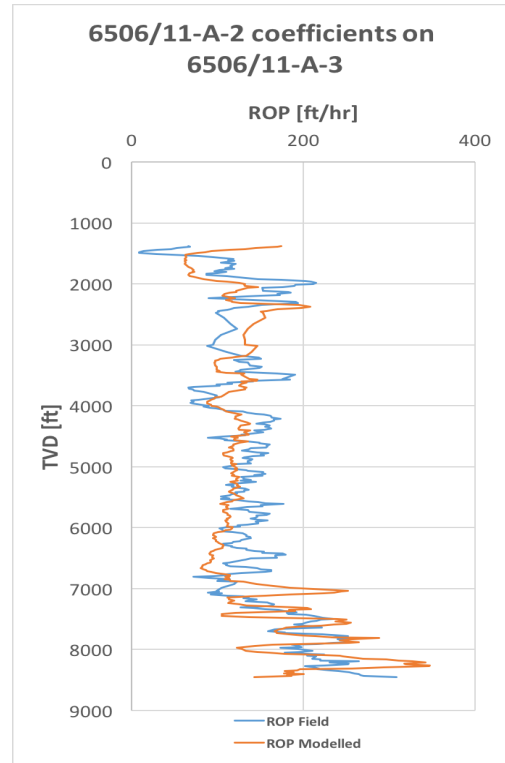
(b) using 6506/11-A-2 B&Y coefficient values
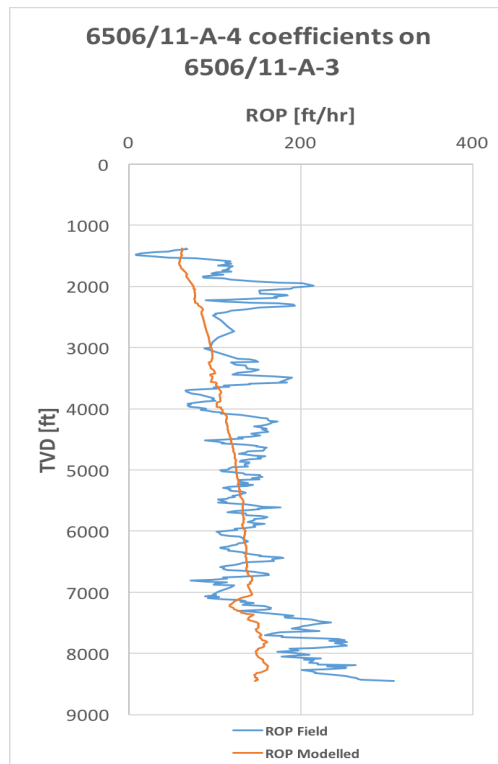
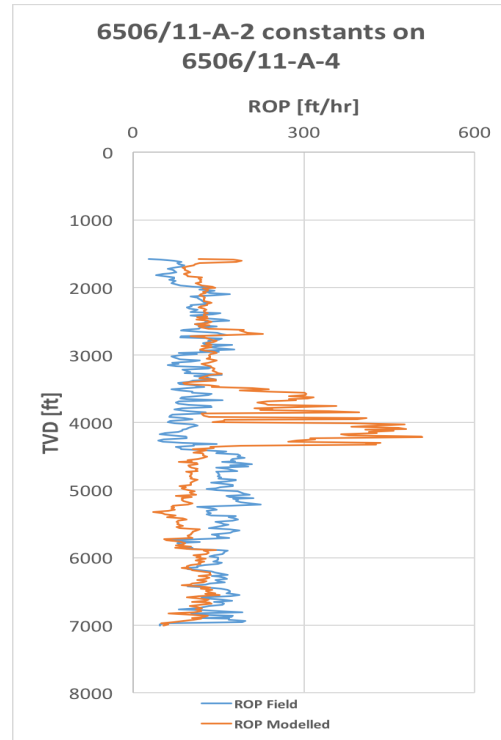**(c)** using 6506/11-A-4 B&Y coefficient values

Figure 8.19: Bourgoyne & Young Model - Nearby and far-away B&Y coeff. on 6506/11-A-3 for entire well data.
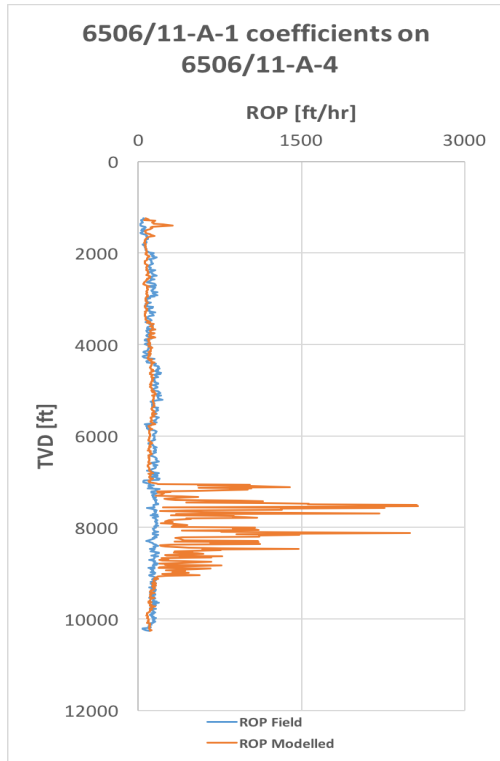
143

(a) using 6506/11-A-1 B&Y coefficient values
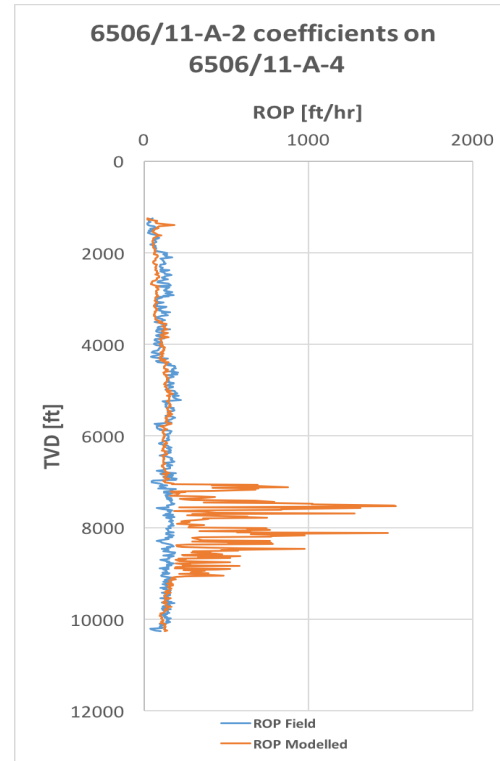
(b) using 6506/11-A-2 B&Y coefficient values
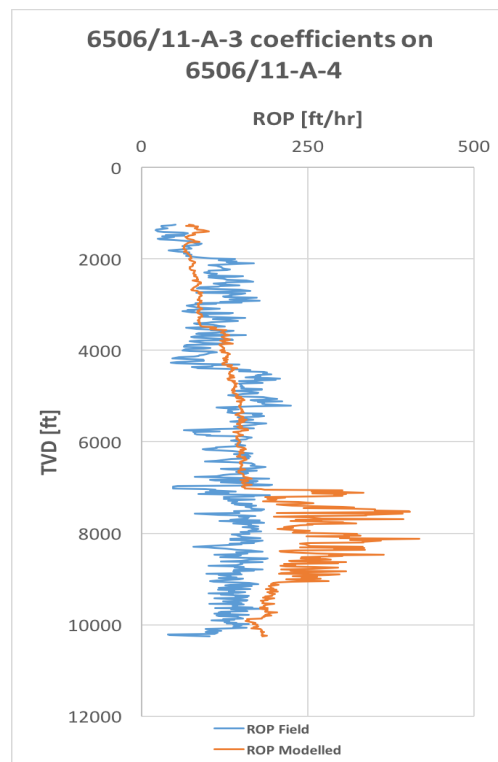
(c) using 6506/11-A-3 B&Y coefficient values

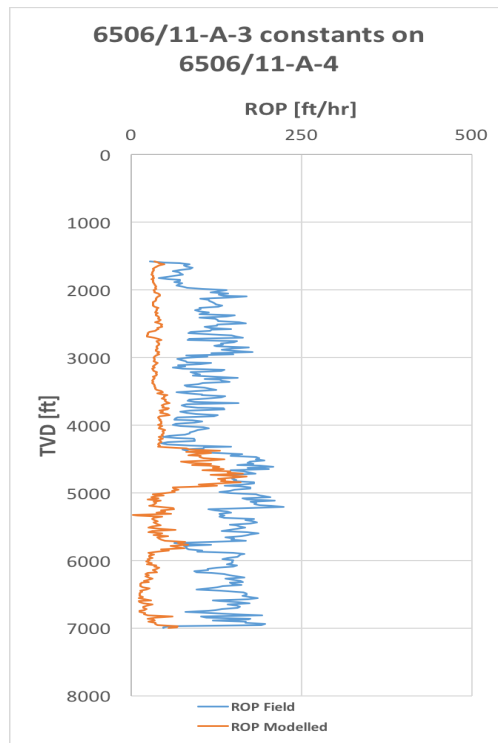**Figure 8.20:** Bourgoyne & Young Model - Nearby and far-away regression coeff. on 6506/11-A-4 for entire well data.

144

Modified Bourgoyne & Young - Modelling by Entire Well Data on Nearby and Far-Away Wells
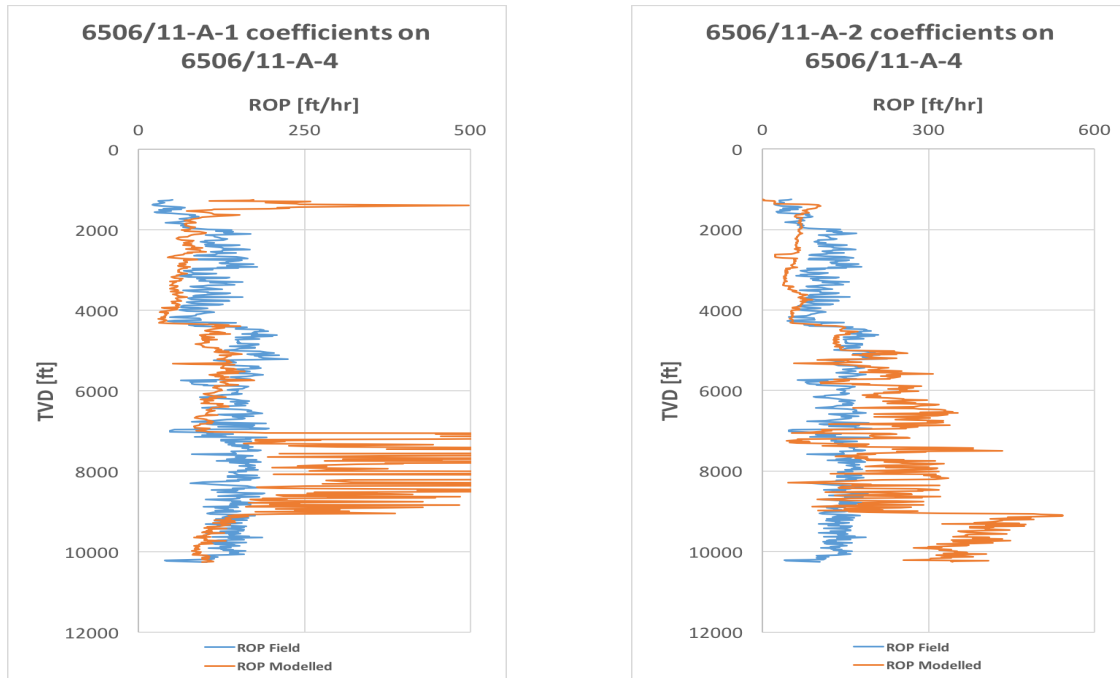
(a) using 6506/11-A-1 B&Y coefficient values

(b) using 6506/11-A-2 B&Y coefficient values
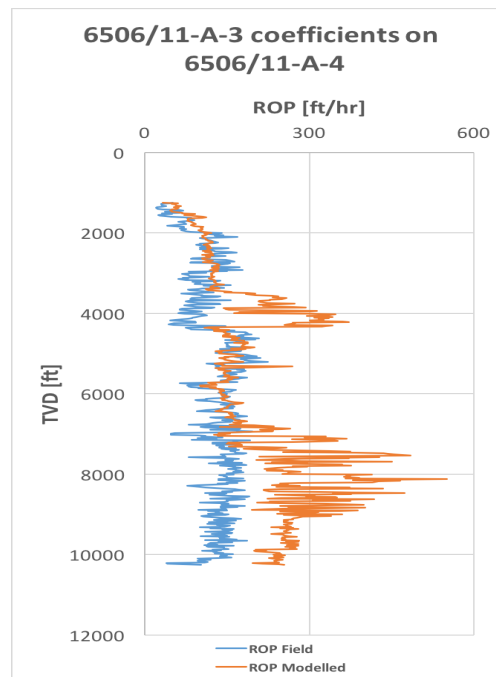
(c) using 6506/11-A-3 B&Y coefficient values

Figure 8.21: Modified Bourgoyne & Young Model - Nearby and far-away B&Y coeff. on 6506/11-A-1 for hole sections.

Modified Bourgoyne & Young - Modelling by Section by Section on Nearby and Far-away Wells
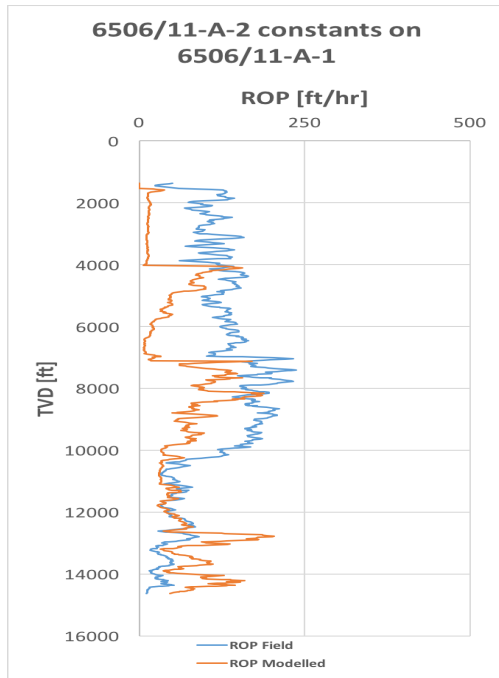
(a) using 6506/11-A-2 B&Y coefficient values
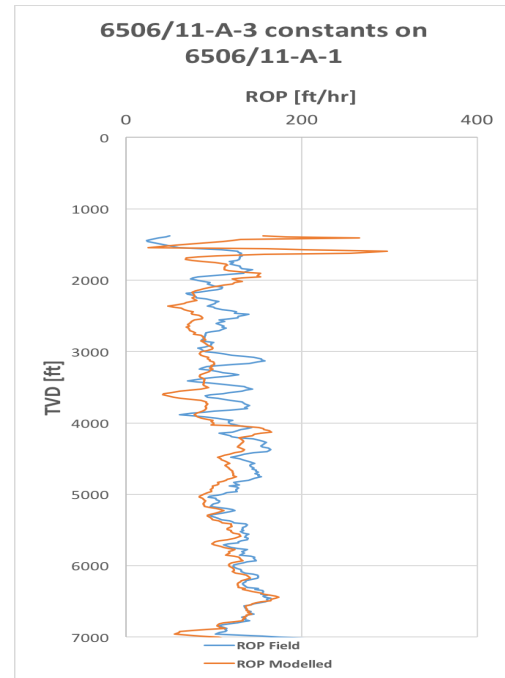
(b) using 6506/11-A-3 B&Y coefficient values
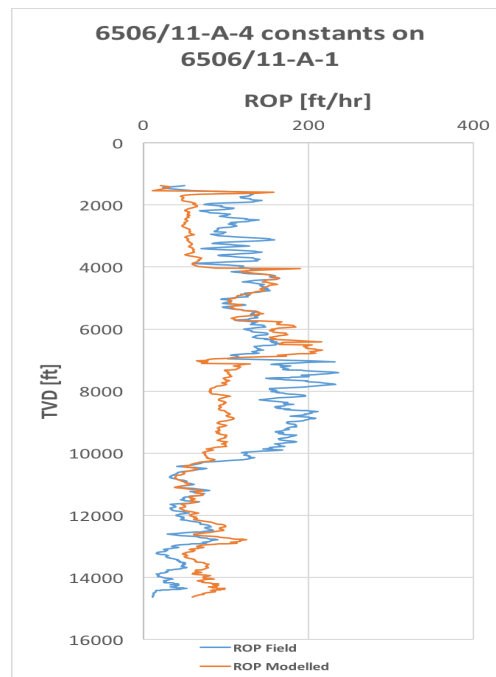
(c) using 6506/11-A-4 B&Y coefficient values

Figure 8.22: Modified Bourgoyne & Young Model - Nearby and far-away B&Y coeff. on 6506/11-A-1 for hole sections.
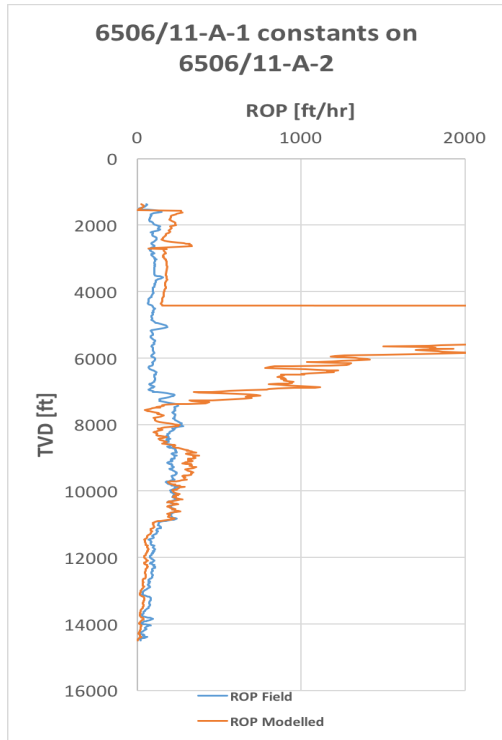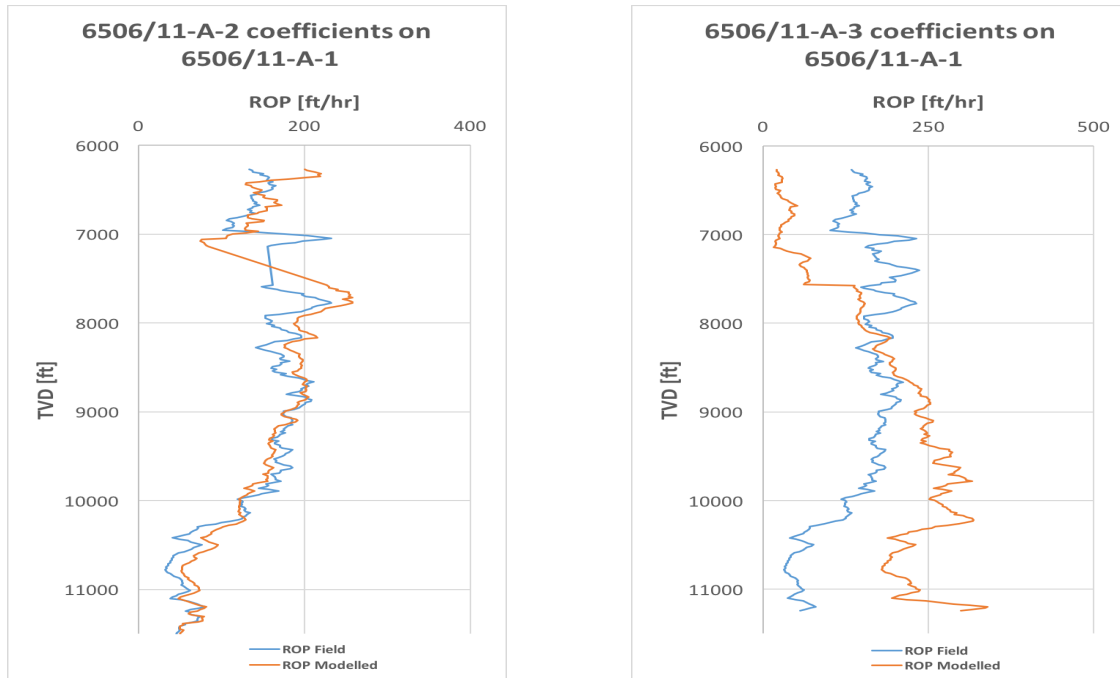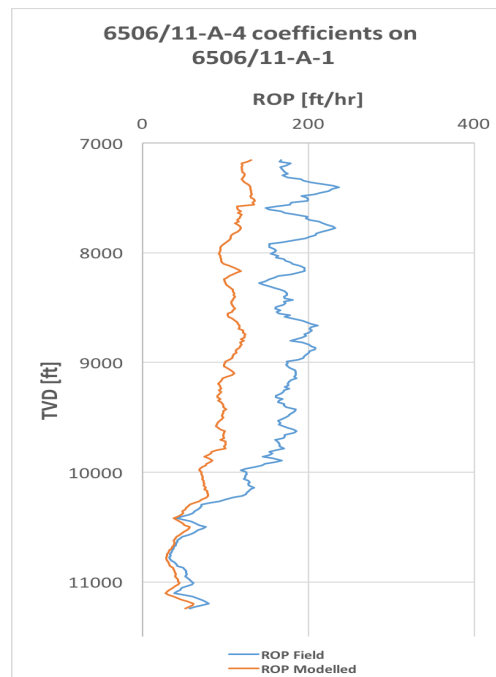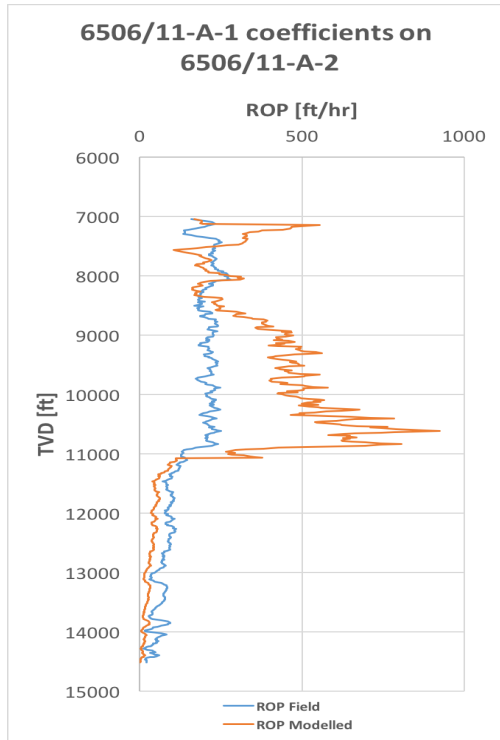
(a) using 6506/11-A-1 B&Y coefficient values

(b) using 6506/11-A-3 B&Y coefficient values

(c) using 6506/11-A-4 B&Y coefficient values

Figure 8.23: Modified Bourgoyne & Young Model - Nearby and far-away Warren constants on 6506/11-A-2 for hole sections.

(a) using 6506/11-A-1 B&Y coefficient values

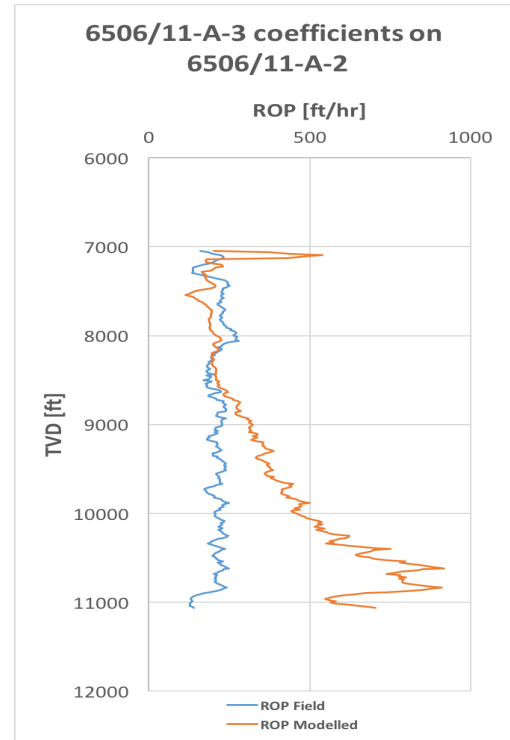

(b) using 6506/11-A-2 B&Y coefficient values
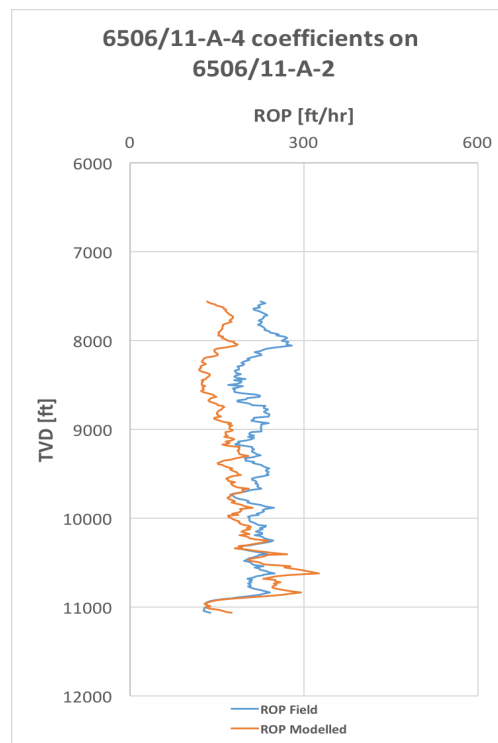

(c) using 6506/11-A-4 B&Y coefficient values

Figure 8.24: Modified Bourgoyne & Young Model - Nearby and far-away B&Y coeff. on 6506/11-A-3 for hole sections.

148

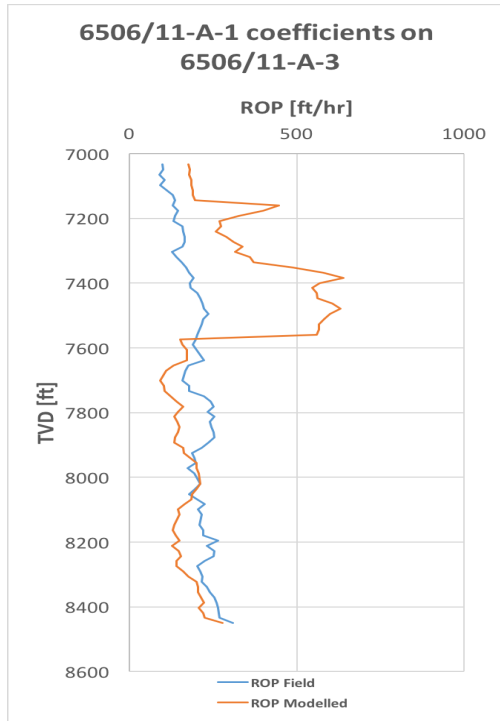(a) using 6506/11-A-1 B&Y coefficient values

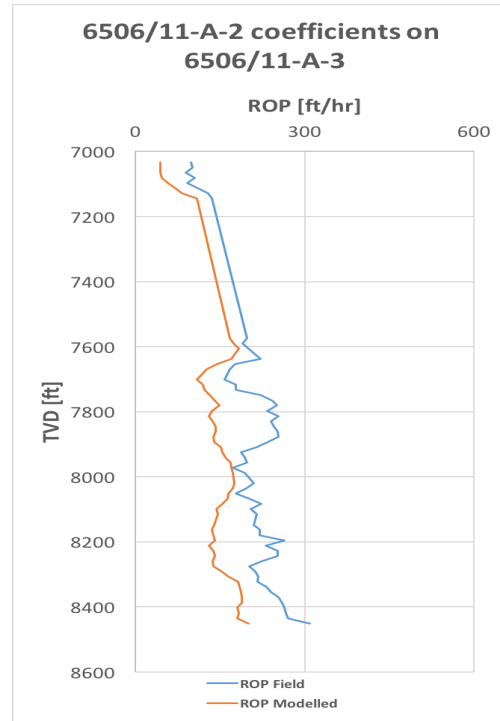(b) using 6506/11-A-2 B&Y coefficient values

(c) using 6506/11-A-3 B&Y coefficient values

Figure 8.25: Modified Bourgoyne & Young Model - Nearby and far-away B&Y coeff. on 6506/11-A-4 for hole sections.

149

Modified Bourgoyne & Young - Modelling by Geological Groups on Nearby and Far-Away Wells

(a) using 6506/11-A-2 B&Y coefficient values

(b) using 6506/11-A-3 B&Y coefficient values

(c) using 6506/11-A-4 B&Y coefficient values

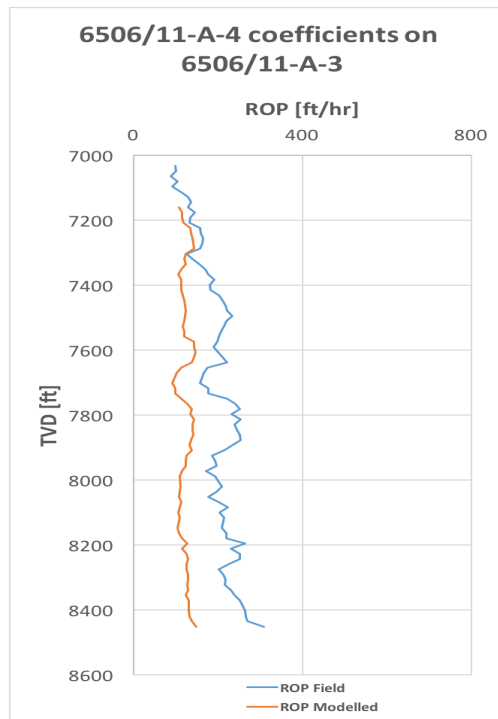**Figure 8.26:** Modified Bourgoyne & Young Model - Nearby and far-away B&Y coeff. on 6506/11-A-1 for geological groups.

150

(a) using 6506/11-A-1 B&Y coefficient values

(b) using 6506/11-A-3 B&Y coefficient values

(c) using 6506/11-A-4 B&Y coefficient values

Figure 8.27: Modified Bourgoyne & Young Model - Nearby and far-away B&Y coeff. on 6506/11-A-2 for geological groups.

151

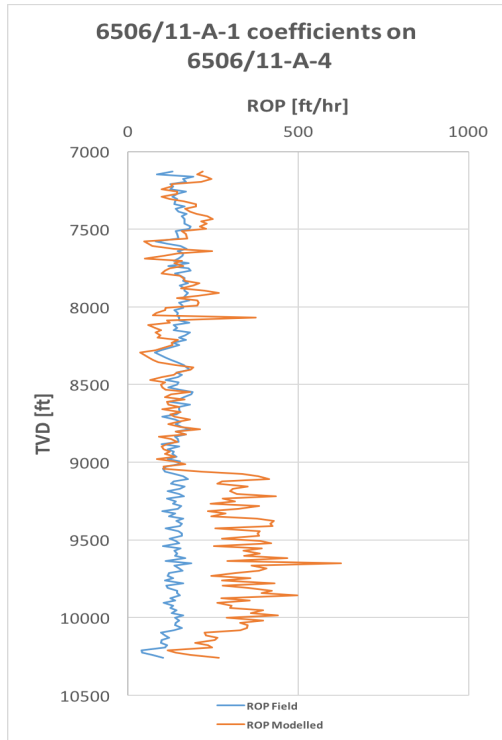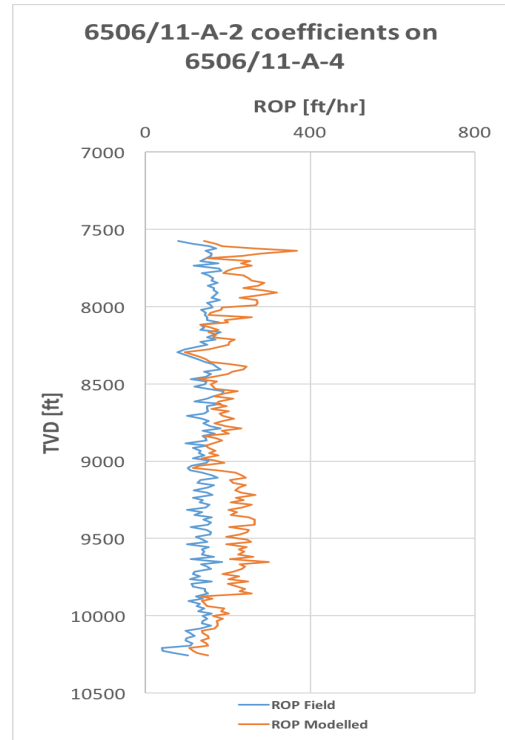**(a)** using 6506/11-A-1 B&Y coefficient values

(b) using 6506/11-A-2 B&Y coefficient values

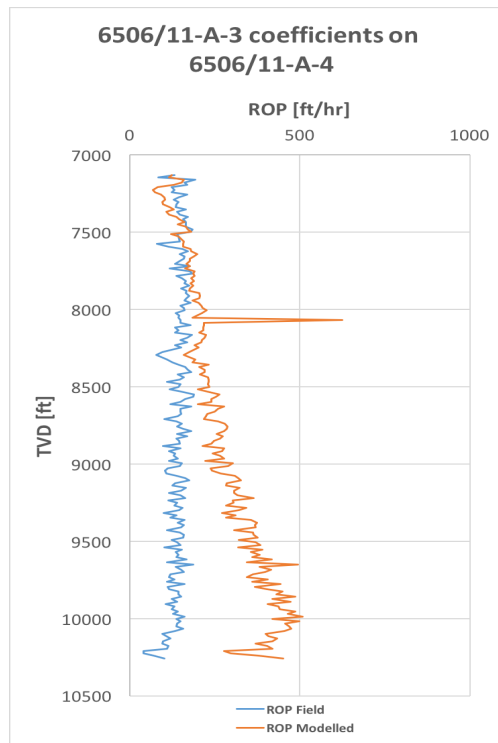**(c)** using 6506/11-A-4 B&Y coefficient values

Figure 8.28: Modified Bourgoyne & Young Model - Nearby and far-away B&Y coeff. on 6506/11-A-3 for geological groups.

(a) using 6506/11-A-1 B&Y coefficient values

(b) using 6506/11-A-2 B&Y coefficient values

(c) using 6506/11-A-3 B&Y coefficient values

Figure 8.29: Modified Bourgoyne & Young Model - Nearby and far-away B&Y coeff. on 6506/11-A-4 for geological groups.

8.2 APPENDIX B

Bingham Model

Bingham Model being described in Chapter 3.4 in page 19, which shows the relation between WOB, RMP, ROP and bit diameter. The model is viewed to be unique as it adds empirical exponent to the equation and therefore being applicable in large circumstances. However the Bingham model shows poor prediction of ROP in this thesis, due to it is limited drilling parameters input. In Figure 8.30 modelled ROP is illustrated.

When implementing Bingham model to predict ROP it is done in Microsoft Excel using regression analysis function. The steps for the equation is showed below:
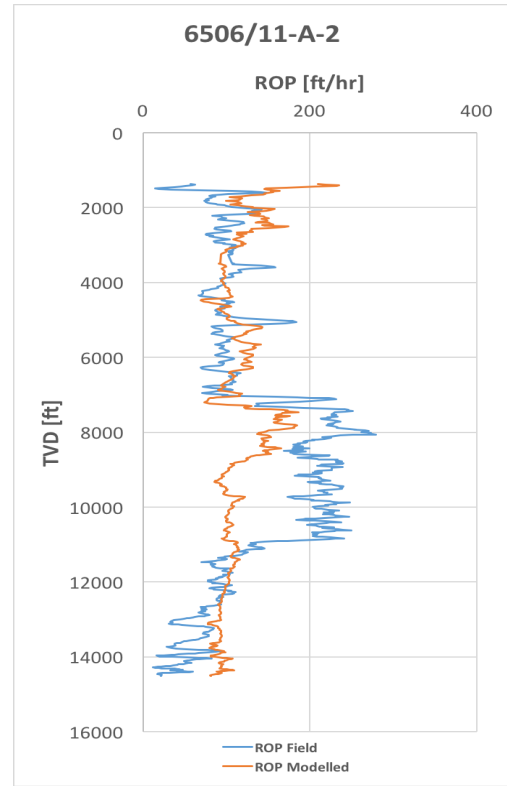
$$ROP = a \left(\frac{WOB}{D_b} \right)^b RPM^c$$

$$\log ROP = \log a + b \log \left(\frac{WOB}{D_b} \right) + c \log RPM$$
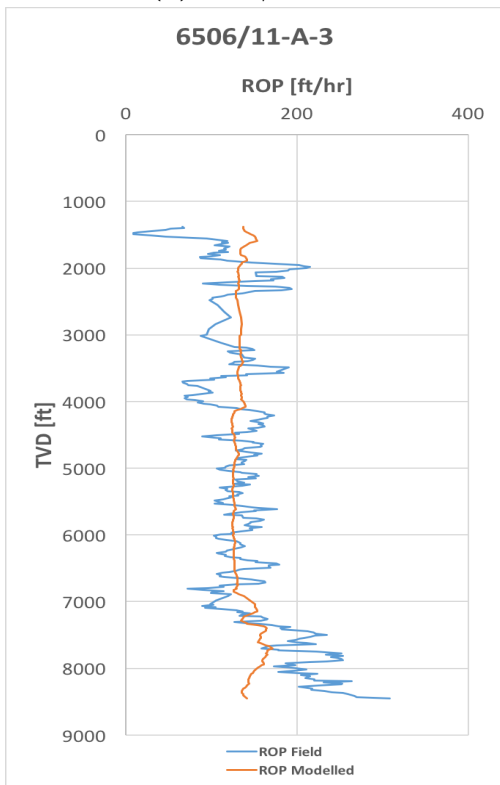
Furthermore, a, b and c coefficients are carried out using regression analysis function. This values are now implemented back into the Bingham model. This Bingham model is is modified as the original equation is without c-exponent, this exponent limits the deviations errors in RPM.
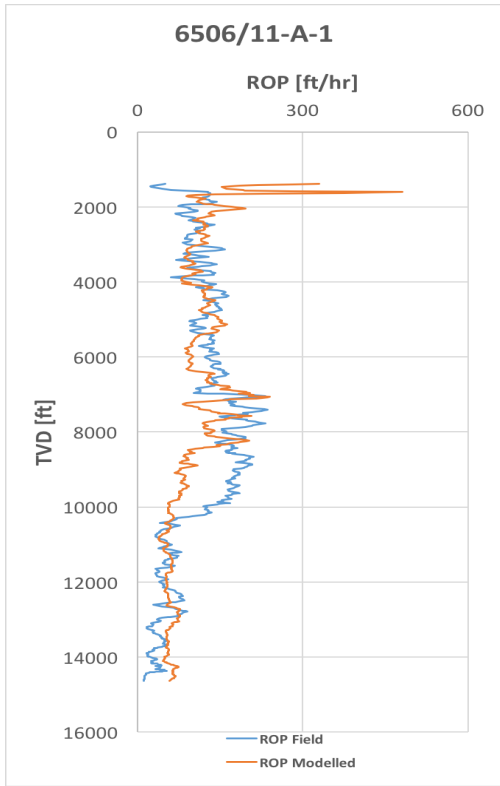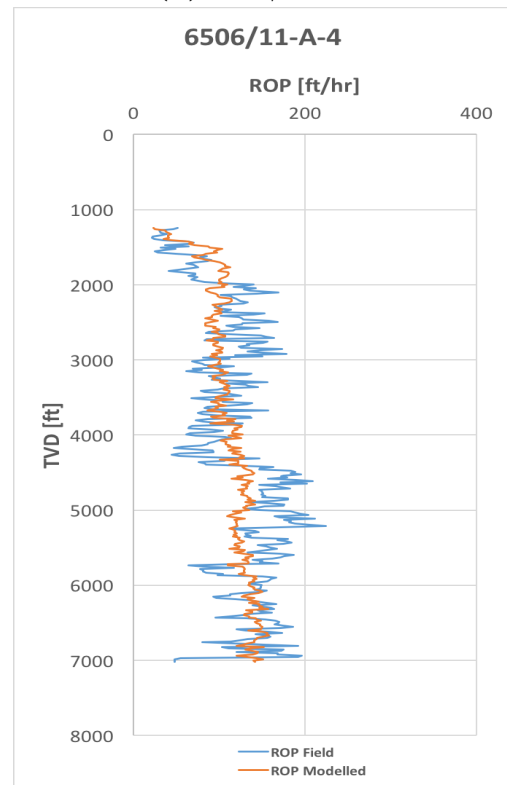
(a) 6506/11-A-1

(b) 6506/11-A-2

(c) 6506/11-A-3

(d) 6506/11-A-4

Figure 8.30: Bingham model - Using their own coefficient values.

The results generated in Figure 8.30 shows that the modelling is poor in throught almost all section of all wells, except for Nordaland and Hordaland groups for well 6506/11-A-1 and 6506/11-A-2.

The main reason for why the model struggles to correlate well with field ROP is due to few drilling parameters being accounted for in the model. The modelling confirms the research done in "Investigating ROP Dependent Variables" Chapter 5.1.1, the ROP prediction is limited to fewer drilling parameters.

Hareland & Rampersad Model

Hareland & Ramperstad (1994) made a description of the penetration of a single cutter acting on the formation where they applied conservation of mass. The model were built on the assumption that the volume of rock compressed and removed is proportional to contact area and WOB applied. Hareland & Rampersad model is expressed as [44]:

$$ROP = W_f \frac{a}{(RPM^b WOB^c)} \frac{14.14 N_c RPM}{D_b} cos\alpha \cdot sin\theta \cdot F \tag{8.1}$$

Where "F" is calculated as:

$$F = \left\{ \left[\frac{d_c}{2}\right]^2 cos^{-1}\left[1 - \frac{4W_{mech}}{\pi cos\theta d_c^2 \sigma_c}\right] - \sqrt{\left(\frac{2W_{mech}}{\pi cos\theta \sigma_c}\right) - \left(\frac{4W_{mech}}{\pi cos\theta d_c \sigma_c}\right)^2} \cdot \left[\frac{d_c}{2} - (\frac{W_{mech}^2}{\pi cos\theta d_c \sigma_c})\right] \right\}$$

Whereas "a", "b" and "c" are respectively correction factors for cutter geometry, W_f is a function of bit wear. W_{mech} is mechanical load of each cutter, N_c is number of PDC cutters, α and θ are the cutter and side- and back rake angle, d_c is the diameter of the cutter and finally the UCS is given as σ_c [44].

Hareland & Rampersad Model wasn't included in this thesis due to limitations with the input data.